

Copyright
by
Linsey Alison Yeager
2008

Host Response of Lung Cells to Virulent *Bacillus anthracis*

by

Linsey Alison Yeager

Dissertation

Presented to the Faculty of the Graduate School of

The University of Texas Medical Branch

in Partial Fulfillment

of the Requirements

for the Degree of

Doctor of Philosophy

The University of Texas Medical Branch

Galveston, Texas

December, 2008

For my loving family.

Acknowledgements

I would first like to thank my mentor, Dr. Johnny Peterson for allowing me the privilege to work in his laboratory and learn from such an excellent microbiologist. Dr. Peterson epitomizes the definition of a great mentor and gave me the guidance and knowledge necessary to become a successful young scientist at UTMB. Although he keeps a watchful eye on his graduate students, Dr. Peterson simultaneously gives us freedom in choosing our projects and encourages independent thinking and work, something I valued highly as a graduate student. He also dedicated much of his time to reading and editing my manuscripts to enhance their scientific content.

Dr. Ashok Chopra was also very instrumental in my graduate career. He spent countless hours discussing project ideas with me and editing my manuscripts. His knowledge of bacteriology and molecular biology was invaluable. I also had many meaningful discussions with Dr. Gary Klimpel, mainly concerning *Francisella tularensis*, a select agent I did research on in the beginning of my studies. His outstanding knowledge of immunology was very helpful to me and influenced my decision to perform certain experiments involving anthrax. Dr. Victor Reyes is also a terrific immunologist and provided many helpful critiques and suggestions which greatly helped improve my experiments. I would also like to thank my outside committee member, Dr. Louise Pitt, the Director of the Center for Aerobiological Sciences at USAMRIID. Dr. Pitt traveled all the way from Maryland to listen to my dissertation seminar and participate in the defense examination. She is well-known in the anthrax field and her help and support was pertinent to my dissertation work.

The life of a graduate student is difficult at times, but I had the support of several other graduate students in Dr. Peterson's lab and I am very grateful to them. We all had numerous scientific discussions and counseling sessions to encourage one another and keep each other focused. Finally, I would like to thank my family. My parents encouraged me to apply to graduate school and were extremely supportive the entire way. I also met the love of my life and husband, Zach Yeager, on the tiny island of Galveston. His love and support made my time here at UTMB some of the best years of my life.

Host Response of Lung Cells to Virulent *Bacillus anthracis*

Publication No. _____

Linsey Alison Yeager, Ph.D.

The University of Texas Medical Branch Graduate School of Biomedical Sciences, 2008

Supervisor: Dr. Johnny W. Peterson

Bacillus anthracis, the etiological agent of anthrax, is a Gram-positive, spore-forming bacterium that is classified as a Category A select agent. The current paradigm in anthrax literature labels the alveolar macrophage (MØ) as the primary cell utilized by spores as a safe site for germination and transport to host lymphatics. This study was the first to report that, unlike their murine counterparts, human alveolar MØs mediate the killing of the majority of internalized virulent *B. anthracis* spores/vegetative cells via a robust oxidative burst. However, ~23% of dormant spores remained viable at 24h post-infection. The “persistence” of some spores may allow them to hide long enough to avoid the first wave of the immune response and germinate later. Although the majority of MØs survived spore infection, a small percentage succumbed to infection via apoptosis.

B. anthracis produces edema toxin (EdTx), an adenylate cyclase that increases cAMP levels in host cells. EdTx significantly suppressed human alveolar MØ phagocytosis of Ames spores, accompanied by cytoskeletal changes such as decreased cell spreading and F-actin content. Further, EdTx altered protein levels/activity of cAMP-dependent PKA and exchange protein activated by cAMP (Epac). Including PKA- and Epac-selective cAMP analogs confirmed the involvement of both pathways in this inhibition. This suggests that EdTx-generated cAMP weakens the host immune response by impairing cytoskeletal functions essential for MØ phagocytosis via signaling by PKA and Epac.

Finally, the transcriptional response of murine lungs to inhalational infection with Ames spores was addressed using GeneChip analysis. Although few transcriptional alterations (15 genes) were detected in the lungs 8h post-infection, important inflammatory genes were both up- and down-regulated, indicating that the lung recognized microbial infection. After 48h, greater transcriptional changes (46 genes) occurred and many of the elevated genes serve protective roles, likely assisting the lungs in combating infection while shielding itself from inflammation-induced damage.

The research presented in this report provides new insight into the interaction between anthrax spores and human alveolar MØs, illustrates a novel suppressive role for EdTx, and identifies affected lung genes during *in vivo* anthrax infection, potentially yielding new opportunities to develop novel therapeutic strategies against this deadly disease.

Table of Contents

List of Tables	x
List of Figures.....	xi
CHAPTER 1: <i>Bacillus anthracis</i>.....	1
1.1 Introduction.....	1
1.2 Brief History of Disease.....	2
1.2.1 History.....	2
1.2 Use as a Biological Weapon	3
1.3 The microbe: <i>Bacillus anthracis</i>	5
1.3.1 Bacteriology.....	5
1.3.2 The Spore	7
1.3.3 The anthrax toxins.....	9
1.4 Human <i>B. anthracis</i> Infections	10
1.4.1 Epidemiology	10
1.4.2 Clinical Features of Inhalational Anthrax.....	11
1.4.3 Treatment	13
1.5 <i>B. anthracis</i> interaction with host immune cells.....	13
1.5.1 Alveolar Macrophages.....	13
1.5.2 Neutrophils.....	15
1.5.3 Dendritic Cells	15
1.5.4 T-Cells.....	16
1.6 The Anthrax Vaccine	17
CHAPTER 2: Interaction between <i>B. anthracis</i> spores and human macrophages	19
2.1 Introduction.....	19
2.2 Methods.....	20
2.2.1 Isolation of primary human macrophages.....	20

2.2.2	<i>Spore preparation</i>	21
2.2.3	<i>MTT assay</i>	22
2.2.4	<i>Spore phagocytosis and survival experiments</i>	22
2.2.5	<i>Germination assay</i>	23
2.2.6	<i>Oxidative burst assays</i>	24
2.2.7	<i>Chemotaxis assay</i>	24
2.2.8	<i>Immunofluorescence assay</i>	25
2.2.9	<i>Statistics</i>	26
2.3	Results	26
2.3.1	<i>Human MØs are efficient killers of virulent Ames spores</i>	26
2.3.2	<i>Survival kinetics of Ames-infected human MØs</i>	29
2.3.3	<i>Intracellular germination rates of Ames spores</i>	34
2.3.4	<i>Oxidative burst response of Ames-infected human MØs</i>	36
2.3.5	<i>Migration of spore-infected MØs</i>	38
2.4	Discussion	42
CHAPTER 3: Edema toxin suppresses human MØ phagocytosis and cytoskeletal remodeling		49
3.1	Introduction	49
3.2	Methods	50
3.2.1	<i>Cell line and reagents</i>	50
3.2.2	<i>Isolation and culture of primary human MØs</i>	51
3.2.3	<i>Spore preparation</i>	52
3.2.4	<i>cAMP ELISA</i>	53
3.2.5	<i>Phagocytosis assays</i>	53
3.2.6	<i>F-actin content</i>	54
3.2.7	<i>Immunofluorescence and cell spreading</i>	55
3.2.8	<i>PKA activity assay</i>	56
3.2.9	<i>Rap1 pulldown assay and Western blot analysis</i>	56
3.2.10	<i>MTT assay</i>	58

3.2.11	Statistics	58
3.3	Results.....	59
3.3.1	<i>EdTx increases cAMP levels in HL-60 MØs</i>	59
3.3.2	<i>EdTx reduces the phagocytic capacity of human MØs</i>	63
3.3.3	<i>Treatment with EdTx reduces MØ cytoskeletal spreading and F-actin levels</i>	67
3.3.4	<i>Macrophage PKA/Epac-1 protein levels and activity are altered following EdTx treatment</i>	71
3.4	Discussion	75
CHAPTER 4: Transcriptional profiling of murine lung genes in response to infection with <i>Bacillus anthracis</i>		82
4.1	Introduction.....	82
4.2	Methods.....	83
4.2.1	<i>Mouse nasal inoculation</i>	83
4.2.2	<i>Determining B. anthracis levels in mouse organs</i>	84
4.2.3	<i>Tissue fixation and slide preparation</i>	84
4.2.4	<i>Cytokine profiling</i>	85
4.2.5	<i>Affymetrix GeneChip analysis</i>	85
4.2.6	<i>Real-time reverse transcriptase-polymerase chain reaction (RT-PCR)</i>	87
4.3	Results.....	88
4.3.1	<i>Monitoring B. anthracis levels in the lungs during infection</i> ...	88
4.3.2	<i>Histopathological analysis of B. anthracis-infected lungs</i>	89
4.3.3	<i>B. anthracis infection elicits a biphasic pattern of cytokine secretion in the serum of mice</i>	91
4.3.4	<i>Inhalational anthrax alters the expression of numerous murine genes in the lung at both early and late time points</i>	93
4.3.5	<i>Confirmation of B. anthracis-induced gene expression alterations in mice</i>	93
4.4	Discussion	99

CHAPTER 5: Conclusions and future directions	104
References	112

List of Tables

Table 4.1 Custom-designed primers used for RT-PCR confirmation of gene alterations induced by anthrax infection.....	88
Table 4.2 Functional categories of genes up- or down-regulated in murine lungs post-intranasal infection with Ames spores.	94
Table 4.3 Significant genes up- or down-regulated in murine lungs 8 h post-infection with Ames spores, grouped by function.	95
Table 4.4 Significant genes up-regulated in murine lungs 48 h post-infection with Ames spores, grouped by function.	96
Table 4.5 Significant genes down-regulated in murine lungs 48 h post-infection with Ames spores, grouped by function.....	97
Table 4.6 Real-time RT-PCR confirmation of altered expression levels of selected genes from Ames-infected murine lungs.	98

List of Figures

Figure 1.1 Electron microscopic image of <i>B. anthracis</i> .	8
Figure 2.1 Tracking intracellular survival of Ames spores.	28
Figure 2.2 Determining the survival of <i>B. anthracis</i> in various stages of germination.	30
Figure 2.3 Effect of spore infection on MØ viability.	33
Figure 2.4 Immunofluorescence assay to identify the mechanism of death of spore-infected MØs.	34
Figure 2.5 Monitoring the intracellular germination rates of internalized Ames spores.	37
Figure 2.6 Effect of spore infection on the oxidative burst response of human MØ's.	39
Figure 2.7 Migration assay of Ames-spore infected MØs.	41
Figure 3.1. cAMP production by EdTx treated human MØs.	61
Figure 3.2. Effects of EdTx on human MØ viability.	62
Figure 3.3. Effects of EdTx on phagocytic activity of human MØs.	65
Figure 3.4. Phagocytosis of <i>E. coli</i> particles by EdTx-treated human MØs.	66
Figure 3.5. Assessment of morphological responses and spreading index of EdTx-treated MØs.	68
Figure 3.6. Effects of EdTx on the F-actin content of human MØs.	70
Figure 3.7 Western Blot analysis of PKA RII α and Epac levels post-EdTx treatment.	72
Figure 3.8 PKA activity assay of human MØs following exposure to EdTx.	73
Figure 3.9 Pull-down assay to evaluate Epac activation of Rap1 in EdTx-treated MØs.	74
Figure 4.1. <i>B. anthracis</i> infection in murine lungs at 8, 24, and 48 h post-infection.	90
Figure 4.2 Histopathological analysis of anthrax-infected lungs.	90
Figure 4.3 Cytokine array analysis of murine serum post-infection with Ames spores.	92

Chapter 1: *Bacillus anthracis*

1.1 INTRODUCTION

Bacillus anthracis is a Gram-positive bacterium that is the etiological agent of the disease anthrax. As a soil inhabiting organism, its ability to sporulate into dormant, metabolically inactive spores allows it to survive the harsh conditions endemic to the soil microenvironment, such as severe temperatures, UV light, and contact with water. Primarily a zoonotic disease, herbivorous animals, such as sheep and cattle, grazing in contaminated pastures may ingest spores and develop anthrax. However, humans may also contract anthrax by eating contaminated meat or handling infected carcasses. The disease progresses quickly and involves immense disruption of the host's immune response due to production of two powerful exotoxins. *B. anthracis* cells replicate extensively in the blood of infected hosts, and the majority of patients exhibit pulmonary edema, multi-organ failure, and meningitis in some cases.

Due to the hardy nature of *B. anthracis*, its relative ease of aerosolization, and potent virulence in humans, it is not surprising that this agent has been utilized as a biological weapon as recently as 2001. Now classified as a Category A select agent by the Centers for Disease Control, many laboratories world wide are working to further understand anthrax pathogenesis. Although there is a vaccine currently licensed by the FDA, the complex regimen and lack of information regarding its immunological

workings demands the advent of new vaccine strategies to protect against the release of weaponized spores.

1.2 BRIEF HISTORY OF DISEASE

1.2.1 History

Anthrax is an ancient disease, as documents written by Homer, Hippocrates, and Aristotle describe the infection (Turnbull, 2002). In fact, the word anthrax is derived from the Greek word for coal, *anthrakos*, referring to the black eschar characteristic to the cutaneous form of the disease (Dixon *et al.*, 1999). Historically and still today, naturally occurring anthrax infection in humans is acquired through contact with anthrax-infected animals or contaminated animal products. Anthrax gained notoriety in the nineteenth century when the microbiologist Robert Koch formulated his postulates that proved that the disease was caused by the microorganism *Bacillus anthracis*. Koch was also first to report that *B. anthracis* was a spore former. His groundbreaking investigations in 1875 not only helped create an understanding of the natural history of anthrax, but also laid the basis of medical bacteriology. Similarly, Pasteur focused on anthrax on which to develop his first vaccine. During the twentieth century, anthrax infection was prevalent among people working the wool industry through curing hides or handling infected animals. This prompted the development of an attenuated live spore vaccine in 1937 for livestock, and this, along with improved veterinary and public health controls, caused the disease to

decline in the developed world. However, there are still outbreaks of cutaneous anthrax in third world countries.

1.2 Use as a Biological Weapon

B. anthracis has a long track record of involvement in biological warfare, although its re-emergence as a biological threat in 2001 has renewed public and scientific interest in this organism (Inglesby *et al.*, 2002). An aerosol release of *B. anthracis* would have the potential to travel a great distance before dissipating. The World Health Organization (WHO) estimates that 50 kg of *B. anthracis* spores released over a population of 5 million would result in 100,000 deaths and incapacitation of 250,000 people (Inglesby *et al.*, 2002).

During the twentieth century, the Soviet Union, Britain, and the United States were participating in anthrax weapon production programs, mainly because the producers feared the other side was manufacturing anthrax weapons. The first documented attempts to use anthrax during wartime were by the Axis agents against Allied supply routes during World War I. Horses and mules were reportedly inoculated with anthrax before being sent to Europe to serve as draft animals to carry soldiers and supplies (Swiderski, 2004). In 1917, a German was intercepted near a major supply route with anthrax-laced sugar cubes, and it was speculated that he intended to insert the cubes into feed for horses and other animals (Swiderski, 2004).

As animals became less essential during wartime transport, the technology of anthrax was modified to have broader effects on agriculture and humans. The release of

gas bombs on the battlefield by German forces raised awareness of the possibility of “plague bombs”, weapons made of bacterial agents. In the 1940’s, investigators at Porton Down tested bombs and bullets filled with anthrax spores on sheep located on an island off the coast of Scotland (Swiderski, 2004). They found that the spores could survive the explosive dispersal in sufficient numbers to kill sheep downwind of the explosion. Eventually, the island became so saturated with spores that it was declared off-limits until it was treated with formaldehyde in the mid-1980s. It has also been confirmed that scientists in Japan were designing and testing anthrax bombs designed to release infectious aerosols. During the second World War, two facilities in the United States were opened in order to grow large quantities of anthrax spores for weapons, however, testing never proceeded beyond the use of *Bacillus globigi*, a non-virulent organism that sporulates under conditions similar to *B. anthracis*, before the factories were closed down (Swiderski, 2004).

It wasn’t until the Gulf War that American and British forces realized another potential method of germ attack, releasing an aerosol so that spores remained in the air for long periods of time for direct inhalation by humans rather than saturating the ground with spores and waiting for transmission from animal to human. High-speed milling and anti-electrostatic treatment techniques were refined to make the dried spores fine enough to remain airborne, while reducing clumping and keeping the spores viable (Swiderski, 2004).

In 2001, two waves of anthrax-laced letters traveled throughout the U.S. Postal system. The letters were sent to multiple news media offices and two U.S. Senators, and contained various ‘grades’ of anthrax spores. However, all spores were from the virulent Ames strain of *B. anthracis*. As a result, 22 people were inflicted with anthrax, 11 of

which developed severe cases of inhalational anthrax. The inhalational form of anthrax is the deadliest, and without treatment, it almost surely proceeds to fatal systemic infection (Dixon *et al.*, 1999; Friedlander *et al.*, 1999). Even with modern antibiotic treatment, almost half of the people who developed inhalational anthrax following exposure to the letters died (Jernigan *et al.*, 2002). Furthermore, a portion of those who recovered suffered from long-term disabilities (Reissman *et al.*, 2004).

1.3 THE MICROBE: *BACILLUS ANTHRACIS*

1.3.1 Bacteriology

B. anthracis is a large (1-2 μm by 4-10 μm), rod-shaped Gram-positive aerobe that is non-motile. *In vitro*, the organism typically grows in long chains of bacilli, but in the host it appears singly or perhaps short chains of 2-3 bacilli. On blood agar plates, gray-white colonies with a ground-glass appearance and fried egg morphology appear. *B. anthracis* does not exhibit hemolysis on blood agar plates.

The surface of vegetative cells of *B. anthracis* is unique because in addition to the cytoplasmic membrane and peptidoglycan, it possesses a surface layer (S-layer) and capsule. The S-layer consists of proteinaceous paracrystalline sheaths made of Sap (surface array protein) and EA1 (extractable antigen 1; Etienne-Toumelin *et al.*, 1995; Mesnage *et al.*, 1997). The capsule is comprised of poly-D glutamic acid and appears to have antiphagocytic properties. Although the exact role of the capsule during infection remains unknown, Drysdale *et al* (2005) demonstrated that a strain carrying both

plasmids but lacking the capsule biosynthetic operon (*capBCAD*) is highly attenuated in a mouse model of inhalation anthrax.

Fully virulent strains contain two large plasmids, pXO1 and pXO2. pXO1 is 182 kb and carries the structural toxin genes (*pagA*, *lef*, and *cya*), the regulatory elements (*atxA* and *pagR*), and the germination operon (*gerX*) among other genes. AtxA, anthrax toxin activator, is a global regulator of virulence gene expression (Hoffmaster *et al.*, 1999). Mutant strains with *atxA* deletions do not produce anthrax toxin components and, interestingly, also exhibit reduced capsule synthesis encoded on the other plasmid, pXO2. pXO2 is 96 kb and encodes genes essential for capsule synthesis and degradation, such as *capA*, *capB*, *capC*, and *dep*.

The existence of anthrax toxin was first suspected when plasma from *B. anthracis*-infected animals produced lethality in normal animals (Smith *et al.*, 1954). Today, we know that *B. anthracis* secretes two powerful A-B type toxins, lethal toxin (LeTx) and edema toxin (EdTx). There are three components of the anthrax toxins: lethal factor (LF, 90 kDa), edema factor (EF, 89 kDa), and protective antigen (PA 83 kDa). PA binds the cell surface receptors ANT XR1 (TEM8) and ANT XR2 (CMG2; Bradley *et al.*, 2001; Scobie *et al.*, 2003). After PA heptamerizes on the cell surface, pores in the lipid bilayer are formed (Abrami *et al.*, 2000), and LF and EF enzyme moieties are delivered to the mammalian cytosol, where they exert their toxic activities. The majority of information regarding *B. anthracis* lethality has been gained from work with LeTx, which is comprised of LF and PA. LF is a zinc-dependent protease whose major function is proteolytic cleavage of mitogen-activated protein kinase kinase (MAPKK) family members (Vitale *et al.*, 2000). EdTx is formed by EF and PA, and has intrinsic adenylate

cyclase activity that increase cAMP levels in numerous host cell types (Leppä *et al.*, 1982).

1.3.2 The Spore

When faced with adverse conditions, such as nutrient deprivation or extreme temperatures, vegetative cells transition into dormant spores (1-9 μm in size) that can survive for decades. Spores are highly resistant to desiccation, boiling for 10 min, radiation, heat, cold, and many disinfectants. Because vegetative *B. anthracis* does not survive long outside of the host (Titball *et al.*, 1991), spores are considered the infectious particles for initiating an anthrax infection.

The structure of the *B. anthracis* spore is relatively homologous to spores of *Bacillus subtilis*. Spores are composed of a set of layers that are arranged in a series of concentric shells, and each shell contributes to spore durability. The innermost portion is the core, which houses the chromosome. The core is surrounded by an inner membrane and beyond that are two peptidoglycan layers. The first is a highly cross-linked germinal cell wall and the outer is a thicker cortex. The cortex has a structure resembling a woven fabric and forms a tight girdle with the core to keep the DNA dry, which helps preserve the DNA during spore dormancy. Beyond the cortex is the spore coat, a biochemically complex bilayer made of about 60 unique proteins that is the foremost contributing factor to the resistant properties belonging to spores. A significant gap exists between the coat and the outermost layer of the spore, the exosporium. The exosporium is a loose fitting multilayered glycoprotein sac-like structure. Diverse proteins are found on the

exosporium, including arginase, superoxide dismutase, and the major structural glycoprotein, *Bacillus* collagen-like protein of *anthracis* (BclA). BclA proteins form a hair-like nap layer that surrounds the spore surface. Recent studies indicated that the presence of the exosporium might influence spore germination within the MØ (Baillie *et al.*, 2005).

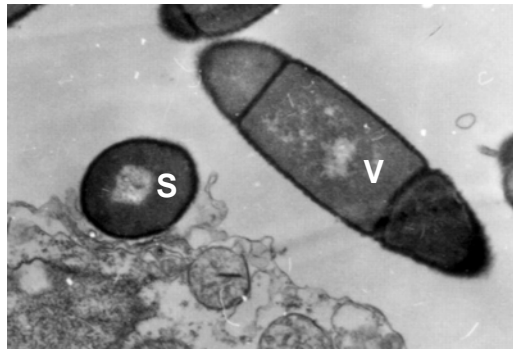


Figure 1.1 Electron microscopic image of *B. anthracis*. Electron photomicrograph (EM) showing vegetative cells (V) and spores (S) at 19,000x. EM courtesy of Vsevolod Popov, Ph.D., Department of Pathology, University of Texas Medical Branch, Galveston, TX

Upon exposure to favorable conditions, such as the warm, moist environment of the human lung, spores germinate forming vegetative cells capable of replication. There appears to be at least two germination systems, named *gerH* and *gerX*, that function to transition dormant spores into vegetative cells. Each system recognizes germinant molecules (certain amino acids, nucleosides, glucose) and triggers the germination event. For instance, *gerH* responds to a purine plus an aromatic amino acid, especially histidine (Hu *et al.*, 2007). Once in contact with germinants, the process is irreversible even if the germinants are removed.

1.3.3 The anthrax toxins

LeTx is a zinc-dependent metalloprotease which cleaves six of the seven MAPKK isoforms close to their N-terminus (Vitale *et al.*, 2000). MAPKKs belong to a major signaling pathway linking the activation of membrane receptors to the transcription of several genes, including those encoding pro-inflammatory cytokines. LeTx results in the apoptotic death of macrophages (Kim *et al.*, 2003; Friedlander *et al.*, 1993; Lin *et al.*, 1996), endothelial cells (Kirby *et al.*, 2004), human peripheral blood mononuclear cells (Popov *et al.*, 2002), and dendritic cells (Alileche *et al.*, 2005). LeTx also modulates cytokine production by several immune cell types. For instance, LeTx impairs secretion of TNF α , IL-1 β , IL-6, and IL-8 by nonhuman primate alveolar M ϕ s (Ribot *et al.*, 2006). When LeTx is administered to rats, it decreases blood pressure and heart rate several hours before lethality (Sherer *et al.*, 2007), which are parameters indicative of shock. Although the mediators and mechanisms underlying LeTx-induced shock remains unclear, growing evidence implies that direct action of LeTx on endothelial cells is a likely contributing factor.

EF is a calcium- and calmodulin-dependent adenylate cyclase that causes a prolonged increase in intracellular cAMP within numerous target cells types (Leppla *et al.*, 1982). EF is at least 1000-fold more active in cAMP production than are host adenylyl cyclases (Drum *et al.*, 2002; Leppla, 1984; Tang *et al.*, 1991). This is also a strategy utilized by several other successful pathogens, such as *Yersenia pestis* and *Pseudomonas aeruginosa*. Interestingly, EdTx elicits death at lower doses and more rapidly than LeTx in a mouse model (Firoved *et al.*, 2005). Extensive tissue lesions were observed and death was likely due to multi-organ failure. Studies examining the effect of

EdTx on human neutrophils have shown that the phagocytic capacity and oxidative burst of these cells is reduced (O'Brien *et al.*, 1985; Wright *et al.*, 1986). EdTx-treated human monocytes showed increased levels of IL-6 secretion with concomitant impairment of the TNF- α response, suggesting a disruption of cytokine networks (Hoover *et al.*, 1994). Recent Microarray data published from our laboratory revealed murine MØ gene changes related to inflammatory responses, regulation of apoptosis, immune cell activation, and transcription regulation as early as 3 h post-toxin treatment, emphasizing the powerful activity of this toxin (Comer *et al.*, 2006). However, the downstream effects of EdTx activity have not been studied extensively and it is still unclear how EdTx subverts host defenses.

1.4 HUMAN *B. ANTHRACIS* INFECTIONS

1.4.1 Epidemiology

Anthrax most commonly occurs in herbivores, which are infected after ingesting spores in the soil. Animal vaccination programs have reduced the animal mortality from disease, however, *B. anthracis* spores continue to reside in soil throughout the world and anthrax cases among herbivores emerge annually (Inglesby *et al.*, 2002). Anthrax remains a risk for humans in most countries of sub-Saharan Africa and Asia, the Americas, several European countries, and certain areas of Australia. There are three forms of the disease (cutaneous, gastrointestinal, and inhalational), but cutaneous anthrax is the most common in humans (95% of cases; Inglesby *et al.*, 2002). The largest reported epidemic

of cutaneous anthrax occurred between 1979 and 1985 in Zimbabwe, when over 10,000 humans became infected. In the United States, 224 cases of cutaneous anthrax were reported between 1944 and 1994 (Inglesby *et al.*, 2002).

Naturally occurring inhalational anthrax is now a rare cause of human disease (5%; Dixon 1999). In the past, woolsorters at industrial mills were at highest risk of inhalational anthrax. Only 18 cases of inhalational anthrax were reported in the United States from 1900 to 1978, with the majority occurring in special-risk groups, such as wool or tannery workers. There is no evidence of human-to-human transmission. In 1979, there was an accidental aerosolized release of anthrax spores from a military microbiology facility in Sverdlovsk, of the former Soviet Union, resulting in at least 79 cases of pulmonary anthrax infection and 64 deaths (Abramova *et al.*, 1993; Meselson *et al.*, 1994). This event demonstrated the fatal effects of an aerosol anthrax release.

1.4.2 Clinical Features of Inhalational Anthrax

The LD₅₀ of *B. anthracis* for humans is estimated to be approximately 10,000 spores (Franz *et al.*, 2001). Meticulous examination of the 11 patients who developed inhalational anthrax, as a result of contact with the anthrax-laced letters in 2001, provided much detail regarding the clinical disease, as reported by Jernigan *et al.* (2002). The average incubation from known exposure to symptoms was 4 days. Non-specific symptoms exhibited by most of the patients included fever, chills, drenching sweats, fatigue, a cough, and chest discomfort. Chest X-rays at the initial examination of the 11 patients showed mediastinal widening, paratracheal and hilar fullness, and pleural

effusions or infiltrates or both, although some of the findings were subtle in some patients. Six of the 11 patients sought treatment when they were in this stage of infection and were immediately placed on a combinational antibiotic therapy. Consequently, all six of these patients survived.

Disease can then progress to the second, fulminant stage anywhere from a few hours to days after the first phase. This stage is characterized by respiratory distress, dyspnea, diaphoresis, and shock, and death generally occurs within 24 hours of reaching this stage (Jernigan *et al.*, 2002). Four of the patients exposed in 2001 were not admitted to the hospital until they were in the fulminant stage of the disease, and all four died. Autopsy findings in all four of these patients showed hemorrhagic mediastinal lymphadenitis and evidence of disseminated *B. anthracis* infection (Jernigan *et al.*, 2002).

During the initial phase of bioterrorism-related inhalational anthrax, most patients had a normal or only slightly elevated total white blood cell (WBC) count, but did show neutrophilia. However, during the course of illness, WBC counts dramatically increased in most patients. Pleural effusions were also present in all cases, often small initially, but in the surviving patients effusions were characterized by progressive enlargement and persistence. The pleural fluid in all patients was hemorrhagic, with a high protein concentration and relatively few WBCs. Further, there were large quantities of *B. anthracis* capsule and cell-wall antigens in the pleural tissue.

Meningitis is a complication of inhalational anthrax and is characteristically hemorrhagic. Over half of the patients at Sverdlovsk who died of inhalational anthrax showed evidence of meningeal involvement, while only one patient presented with meningitis as a result of bioterrorism-related exposure in 2001.

1.4.3 Treatment

Because inhalational anthrax progresses rapidly, early antibiotic administration is essential. Most naturally occurring *B. anthracis* strains are susceptible to many antibiotics, such as penicillin, doxycycline, and ciprofloxacin. All three of these antibiotics are approved by the FDA for the treatment of inhalational anthrax, yet the latter two are preferred due to proven efficacy in monkey and other animal studies (Franz *et al.*, 1997; Friedlander *et al.*, 1993; Kelly *et al.*, 1992). Following the 2001 anthrax attacks, the CDC has recommended that two or three antibiotics be administered in combination and that treatment should continue for 60 days. Because anthrax is not transmissible from human-to-human, there is no need to treat or vaccinate people that come into contact with infected patients.

1.5 *B. ANTHRACIS* INTERACTION WITH HOST IMMUNE CELLS

1.5.1 Alveolar Macrophages

The innate immune system is very well developed in the deeper parts of the lung. Although there is a multitude of antimicrobial molecules, such as lysozyme, surfactant proteins, and defensins, the major defender of the alveoli space is the alveolar MØ. The pool of alveolar MØs can handle up to 10^9 intratracheally administered bacteria before there is a “spillover” of bacteria to dendritic cells present in the underlying epithelium (MacLean *et al.*, 1996). In an uninfected lung, alveolar MØs are under tight self-control

to prevent unwarranted activation. However, stimulation of MØ Toll-like receptors (TLRs) releases the brakes on MØ activation and they become primed to secrete proinflammatory cytokines and phagocytose particulates. However, *B. anthracis* and other important pathogens, such as *Francisella tularensis*, *Leishmania* spp., *Legionella pneumophila*, and *Yersenia pestis*, have evolved to manipulate MØs to their own advantage.

To date, only a single host cell receptor that binds anthrax spores has been identified. The spore BclA protein binds to the Mac-1 (CR3) receptor on the surface of phagocytic cells, which facilitates attachment and subsequent uptake of spores (Oliva *et al.*, 2008). RAW 264.7, J774A.1, and murine primary MØs have all been shown to phagocytose virulent and avirulent *B. anthracis* spores and quickly traffic the spores to acidic lysosomes (Guidi-Rontani *et al.*, 1999; Guidi-Rontani *et al.*, 2001). A portion of the phagocytosed spores successfully germinate within the phagolysosome of MØs and are capable of elongating and replicating by 5-6 h post-infection (Ruthel *et al.*, 2004). Human alveolar MØs also ingest Sterne spores and respond with the production of inflammatory cytokines such as IL-1, IL-6 and TNF- α (Chakrabarty *et al.*, 2006). The exosporium appears to mask epitopes otherwise recognized by MØs, as exosporium-deficient Sterne spores induced significantly higher concentrations of cytokines in murine MØs than normal spores (Basu *et al.*, 2007). However, the sequence of events that occurs next is contradictory in the literature and the exact role that MØs play during anthrax infection remains controversial in the anthrax field.

1.5.2 Neutrophils

Neutrophils are quick responders of the innate immune system and play a vital role in resolving many microbial infections. *B. anthracis* spores are engulfed by neutrophils and germinate intracellularly. However, EdTx has been shown to suppress the phagocytic activity of neutrophils (O'Brien *et al.*, 1985). Neutrophils kill spores and the vegetative cells quite efficiently (Mayer-Scholl *et al.*, 2005), independent of toxin or capsule expression. Interestingly, the killing occurs through a ROS-independent mechanism (Mayer-Scholl *et al.*, 2005). In fact, LeTx and EdTx are capable of blocking NADPH oxidase assembly and/or activation in human neutrophils (Crawford *et al.*, 2006). Instead, neutrophil granules called α -defensins are responsible for killing *B. anthracis*. In untreated cutaneous anthrax cases, a high influx of neutrophils surround the bacteria-laden tissue (Lebowich *et al.*, 1943). Perhaps this is why cutaneous anthrax typically resolves spontaneously. However, neutrophil infiltration is rarely seen in the lungs of patients with pulmonary anthrax (Albrink *et al.*, 1960), possibly explaining why the infection is able to rapidly progress and leads to sepsis and death.

1.5.3 Dendritic Cells

Human dendritic cells (DCs) are an additional cell type capable of endocytosing *B. anthracis* wild-type spores and display a mature phenotype with enhanced co-stimulatory activity (Brittingham *et al.*, 2005). Additionally, spore infection elicits a down-regulation of tissue retaining chemokine receptors, while up-regulating lymph node

homing receptors (Brittingham *et al.*, 2005). DCs also appear to play a role in dissemination (Cleret *et al.*, 2007). DCs are susceptible to the action of LeTx and are effectively killed by apoptosis (Alileche *et al.*, 2005). Further, LeTx has been shown to inhibit cytokine secretion by DCs, such as TNF- α , IL-10, and IL-6 (Agrawal *et al.*, 2003; Cleret *et al.*, 2007), and prevent up-regulation of co-stimulatory molecules (Agrawal *et al.*, 2003). As a result, DCs can no longer prime naïve T-cells, thus impairing the adaptive immune response.

1.5.4 T-Cells

Similar to the interaction with other immune cells, the anthrax toxins negatively impact T-cell function in several ways. Injecting mice with sub-lethal doses of LeTx or EdTx inhibited subsequent activation of T lymphocytes by T-cell receptor-mediated stimulation (Comer *et al.*, 2005). Additionally, both *in vivo* and *in vitro*, T-cell proliferation is impaired, as well as cytokine secretion by stimulated T-cells (Comer *et al.*, 2005; Paccani *et al.*, 2005). As expected, treatment with LeTx blocked multiple kinase signaling pathways of murine T-cells (Comer *et al.*, 2005; Paccani *et al.*, 2005). Recently, it has been shown that both EdTx and LeTx subvert signaling by CXC and CC chemokine receptors of T-cells, thus inhibiting T-cell chemotaxis (Paccani *et al.*, 2007).

1.6 THE ANTHRAX VACCINE

The U.S. anthrax vaccine, named anthrax vaccine adsorbed (AVA) or Biothrax[®], was licensed in 1970 and initially administered to veterinarians and workers processing animal hides to protect against *B. anthracis* infection. However, administration of AVA was expanded during the 1990s when the Department of Defense (DoD) vaccinated some of the military deployed during the Gulf War due to concerns of bioterrorism. Following establishment of the Anthrax Vaccine Immunization Program (AVIP) in 1998, roughly 2.1 million doses of AVA had been given by the year 2001 (Joellenbeck *et al.*, 2002).

AVA is made from the cell-free culture filtrate of a nonencapsulated attenuated strain of *B. anthracis*, adsorbed to aluminum hydroxide, and contains the toxin receptor binding moiety, PA, as the principle immunogen. It is not surprising that this immunogen has been successful for protection, as several studies have demonstrated a relationship between levels of circulating anti-PA antibody and protection from spore challenge in multiple animal models (Barnard *et al.*, 1999; Little *et al.*, 1997; Pitt *et al.*, 2001).

It is administered in six subcutaneous injections of 0.5 mL each. The first three doses are given every two weeks, while the remaining doses are given 6, 12, and 18 months after administration of the first. Further, annual booster shots are required. Local events, such as redness, swelling, or nodules at the injection site are associated with receipt of AVA, and less commonly fever and malaise (Joellenbeck *et al.*, 2002).

Although the current anthrax vaccine appears to be sufficiently safe and effective for use, there are areas that need improvement. For instance, the vaccine is relatively reactogenic and the dose schedule is long and demanding. In addition, AVA is not

completely characterized and current efforts are underway to understand correlates of immunity in animals, the components necessary to stimulate protective immunity, and the best way to administer the vaccine (Joellenbeck *et al.*, 2002).

Research on new anthrax vaccine strategies is being carried out by the DoD, the National Institutes of Health (NIH), and at many other laboratories world-wide. Importantly, research topics pertaining to anthrax disease and the organism itself, *B. anthracis*, is also a hot field of study in order to provide novel vaccines and treatments against inhalational anthrax.

Chapter 2: Interaction between *B. anthracis* spores and human macrophages

2.1 INTRODUCTION

It is well documented that both human and murine MØs rapidly engulf *B. anthracis* spores. However, there are contradictions in the literature concerning the fate of the spores once they are inside the MØ. In some experimental systems, murine cell lines and primary peritoneal MØs kill spores and vegetative cells of the Sterne strain (Guidi-Rontani *et al.*, 1999; Welkos *et al.*, 1989) and Ames strain (Welkos *et al.*, 2002). However, others describe Sterne spores surviving within murine MØs (Dixon *et al.*, 2000, Guidi-Rontani *et al.*, 2001). This discrepancy has been attributed to such factors as varying MØ types and sources, the strain of *B. anthracis* spore, different MOI's and diverse growth conditions. Yet, there is also evidence that a race between the MØ and the spore transpires. Will MØs be more beneficial to the spore (i.e. as a site of germination and protection) or more beneficial to the host (i.e., successfully kill spores)?

Importantly, because most prior studies describing interactions between spores and MØs have involved murine cells, there is very limited data regarding spore infection in human MØs. Certain attenuated strains of *B. anthracis* spores do not kill murine MØs, but do kill human MØs (Gold *et al.*, 2004), demonstrating the likelihood of interspecies differences in response to *B. anthracis*. Thus, it is imperative to examine spore interaction with human MØs in detail.

MØ-generated reactive oxygen species are an important component of microbial killing, however, the involvement of this component is not fully understood regarding *B. anthracis* pathogenesis. It is known that *B. anthracis* enhances its ability to survive within the phagolysosome by regulating nitric oxide (NO) levels (Raines *et al.*, 2006). Other vital molecules of the oxidative burst (OB), such as hydrogen peroxide (H₂O₂) and peroxynitrite (ONOO⁻) were not assessed.

In order to characterize the early response of an important sentinel of the human innate immune system, several parameters were measured with regard to human MØ-spore interaction. This chapter describes human MØ phagocytosis of and intracellular survival kinetics of Ames spores, as well as MØ viability and oxidative burst response, and tests the hypothesis that MØs are efficient sporicidal cells and resistant to spore-induced cytotoxicity.

2.2 METHODS

2.2.1 Isolation of primary human macrophages

First, monocytes were purified from buffy coats as described previously (Ben Nasr *et al.*, 2006). Briefly, human PBMC were collected following Ficoll-Paque Plus (GE Healthcare, Piscataway, NJ) density centrifugation. Monocytes were isolated by negative selection using a magnetic column separation system (StemCell Technologies, Vancouver, Canada). Monocytes were then differentiated into alveolar-like MØs as previously described (Akagawa, *et al.*, 2002; Komura *et al.*, 2001). Monocytes were

resuspended in RPMI 1640 at a concentration of 2.5×10^5 per ml in 6-well tissue culture plates and cultured with GM-CSF (500 units/ml; PeproTech, Rocky Hill, NJ) and 10% heat-inactivated FBS for 7 days at 37°C in a CO₂ incubator.

2.2.2 Spore preparation

Spores were prepared as previously described (Peterson *et al.*, 2007). Briefly, *B. anthracis* Ames strain was inoculated in Schaeffer's sporulation medium (pH 7.0), consisting of 16 g Difco Nutrient Broth, 0.5 g MgSO₄·7H₂O, 2.0 g KCl, and 16.7 g MOPS (morpholinepropanesulfonic acid) per liter. Before inoculation, the following supplements were added to the medium: 0.1% glucose, 1 mM Ca(NO₃)₂, 0.1 mM MnSO₄, and 1 μM FeSO₄. Cultures were grown at 37°C with gentle shaking (180 rpm) for 48 h, after which sterile distilled water was added to dilute the medium and promote sporulation. After 10 to 11 days of continuous shaking, sporulation was confirmed at >99% via phase-contrast microscopy and a modified Wirtz-Conklin spore stain, and the spores were centrifuged at $630 \times g$ at 4°C for 15 min. The spore pellets were then washed four times in Cellgro sterile water (Mediatech, Herndon, VA) and resuspended in sterile water. Subsequently, the spore suspension was layered onto a cushion of 58% Hypaque-76 (GE Healthcare, Piscataway, NJ) at a ratio of 1:2.5 by volume. Without mixing, the tubes were centrifuged at $8,270 \times g$ for 45 min at 4°C. The spore pellet was washed twice with sterile water and finally resuspended in PBS. Aliquots of the stock spore suspension were stored at -70°C and freshly diluted in PBS to the desired number of colony forming units (CFU) immediately before each experiment. The spore suspensions were

homogeneous and the spores were highly refractile when examined by phase-contrast microscopy.

2.2.3 *MTT assay*

Primary MØs were seeded in 96-well plates (2.5×10^5 /well) and infected with the various spore types, at the MOI indicated, for 6, 18, and 24h. Media contained 25 µg/ml gentamicin at all times. As the time points expired, 10 µl of the MTT reagent (3-(4, 5-dimethylthiazoyl-2)-2, 5-diphenyltetrazolium bromide, included in the MTT Cell Proliferation Assay (ATCC, Manassas, VA), was added to each well and the plate was incubated for 2 h at 37°C. During this incubation, the yellow tetrazolium MTT salt is reduced by living cells and forms an intracellular purple formazan. Subsequently, 100 µl of the detergent reagent was added per well and the plate incubated at room temperature overnight in the dark. Finally, the absorbance was read at 570 nm. Internal controls included wells with no cells (only media plus MTT reagent and detergent) to detect background absorbance levels. A decrease in absorbance indicated a decrease in cell viability, and the experiment was performed independently three times. Absorbance levels were converted to percent viability, and the graph shows combined results of all experiments.

2.2.4 *Spore phagocytosis and survival experiments*

MØs were seeded in triplicate at a density of 5×10^5 per well in 24-well plates and

infected with Ames spores at various MOI's for 1 h at 37°C with 5% CO₂. Cells in Figure 2.2 were pretreated with chloramphenicol (50 µg/ml), or D-Alanine (2 mM; Acros Organics, Belgium) plus D-Histidine (2 mM; Acros Organics) for 1 h before the addition of spores. Cells were then treated with 100 µg/ml gentamicin for 30 minutes to kill extracellular bacteria. Next, five PBS washes were performed to remove extracellular spores. To determine the phagocytosis efficiency, some wells were immediately lysed with 1% Triton X-100. Lysates were serially diluted with PBS and plated on blood agar plates. For quantification of dormant spores in each lysate, half of the sample was heated at 65°C for 30 minutes before plating on 5% sheep blood agar plates. To evaluate *B. anthracis* intracellular survival over a time course, parallel wells were replenished with fresh media (with 10 µg/ml gentamicin) and returned to the incubator. At later time points, these cells were lysed and plated as described above. The graph shows combined results of three independent experiments.

2.2.5 Germination assay

MØs (5×10^5 in triplicate) were infected with Ames spores (MOI 5) for 15, 30, 45, and 60 minutes at 37°C with 5% CO₂. The medium contained 25 µg/ml gentamicin during infection. As time points expired, five PBS washes were performed to remove extracellular spores. Cells were then lysed with 1% Triton X-100, serially diluted with PBS and plated on blood agar plates. For quantification of dormant spores in each lysate, half of the sample was heated at 65°C for 30 minutes before plating on 5% sheep blood agar plates. The graph shows combined results of two independent experiments.

2.2.6 Oxidative burst assays

This assay was performed similarly to what has been previously described (Teufelhofer *et al.*, 2003). Primary cells (1.5×10^5 per well) were seeded in 96-well plates, with quadruplicate wells seeded per each condition. Spores were then added to experimental wells, and each plate was centrifuged at 2000 rpm for 5 minutes to synchronize phagocytosis. Immediately after centrifugation, 10 μ M DHR 123 was added to detect the reactive oxygen species that were produced. As a positive control, some wells were not infected with spores, but were instead treated with 16 μ M PMA to initiate a robust oxidative burst. Other internal controls for the assay included uninfected cells not receiving PMA, and wells without cells that only received DHR 123 in order to detect background levels of fluorescence. The plate was read immediately on a plate reader (485 nm excitation and 535 nm emission) for a time zero recording, and then incubated at 37°C with 5% CO₂. The fluorescence was measured every 10 min for 40 min. This experiment was repeated three times and the graph depicts one representative experiment.

2.2.7 Chemotaxis assay

Primary human MØs were allowed to phagocytose Ames spores for 1 h at 37°C before multiple washes were performed to remove uninternalized spores. Cells (125,000 per well) were then collected and added to the top chamber of an 8- μ M transwell filter resting in a 96-well plate (Chemicon, Billerica, MA). Uninfected cells were collected

separately as a control. The bottom chamber either contained 100 μ L medium alone or medium with 10 ng/ml recombinant human MIP-1 α (R&D Systems, Minneapolis, MN) to stimulate alveolar M ϕ chemotaxis (Opalek *et al.*, 2007). Cells were incubated for 2 h at 37°C to allow M ϕ s to migrate into the lower chamber of the transwell system. Samples from the lower chamber were saved, while the filters were transferred to a new 96-well plate containing warmed Cell Detachment Solution (Chemicon) for 30 minutes at 37°C. This was to dislodge any M ϕ s that had migrated through the filter and “stuck” to the underside. These samples were then combined with the saved samples from the lower chamber and mixed with a combination of lysis buffer and Cyquant GR dye (Chemicon) for 15 min to label migrated cells. Finally, the fluorescence of these samples was measured at 485 nm excitation and 528 nm emission. This assay was performed three times and the graph shown is one representative experiment.

2.2.8 Immunofluorescence assay

M ϕ s were seeded (1×10^6 cells) on glass coverslips. Various types of spores were added to wells and incubated at 37°C for the indicated time points. Negative control cells were left untreated, and positive control cells were treated with 5 μ M camptothecin (Sigma, St. Louis, MO). Coverslips were then washed with PBS and fixed for 30 minutes with 3.7% paraformaldehyde. Following another set of washes, coverslips were incubated for 15 minutes at 37°C in the dark with a mixture of Syto 13 (20 μ M; Molecular Probes, Eugene, OR) and propidium iodide (7.5 μ g/ml; Molecular Probes) made in PBS. Finally, cells were washed and mounted onto glass slides with SlowFade Gold (Molecular

Probes) mounting media. Samples were immediately viewed with a Nikon Eclipse 50i fluorescence microscope. The number of viable, necrotic, early apoptotic, and late apoptotic cells were scored in at least five fields of view per slide (averaging to approx. 400 cells total examined per slide). The experiment was repeated three times and the graph shows the combined results of all three experiments.

2.2.9 Statistics

Experimental conditions were performed in triplicate and repeated two to three times to ensure reproducibility. Data was expressed as mean \pm SD of the replicates. Differences were considered statistically significant when the *p* value was <0.05 as determined by one-way analysis of variance (ANOVA), followed by either the Dunnett's or Tukey test using SigmaStat software.

2.3 RESULTS

2.3.1 Human MØs are efficient killers of virulent Ames spores

There is no preexisting data tracking the survival of virulent Ames spores within human MØs, as the single other study only involved avirulent Sterne spores (Chakrabarty *et al.*, 2006). Thus, to determine whether human MØs were capable of killing virulent *B. anthracis*, primary MØ cultures were infected with Ames spores at an MOI of 5 or 100 for 1 h to allow optimal phagocytosis. Next, cultures were treated with gentamicin and

extracellular spores were washed away. Some wells were lysed immediately and plated on blood agar plates to determine how many organisms were phagocytosed. To determine how many intracellular organisms survived over time, parallel cultures were given fresh media, returned to the incubator, and lysed at later time points of 4, 10, and 24 h. To determine which form of *B. anthracis* was being killed, the spore or the vegetative cell, MØ lysates were heated at 65°C for 30 minutes to kill surviving vegetative cells. The heat-resistance property of spores allowed dormant spores to survive the treatment. Therefore, quantifying the number of surviving organisms after heating and comparing this to plate counts performed before heating allowed calculation of the number of spores verses the number of vegetative cells. As **Figure 2.1** shows, both the number of dormant spores and the number of vegetative cells inside the MØs became reduced over time. For instance, the percent of viable vegetative cells decreased 43% (MOI 5; **Figure 2.1A**) and 49% (MOI 100; **Figure 2.1B**) at 10 h post-infection, compared to the initial organisms phagocytosed at time zero. The percent of dormant spores at 10 h post-infection was also reduced to approximately 50% of the original number at both MOI's. By 24 h, the percent of recovered vegetative cells decreased to 62% (MOI 5) and 46% (MOI 100) of the original concentration. However, the majority of dormant spores were killed by 24 h, with only 23% surviving in the MOI 5 group (**Figure 2.1A**) and 34% surviving in the MOI 100 group (**Figure 2.1B**).

To confirm that primary human MØs were indeed capable of killing the dormant spore form of *B. anthracis*, compounds with differing effects on spore germination were tested next. Chloramphenicol allows spore germination, but prevents outgrowth of the newly germinated cell into replicating bacilli (Hu *et al.*, 2007). On the contrary, D-Alanine in combination with D-Histidine blocks 95% Ames spore germination (Hu *et al.*,

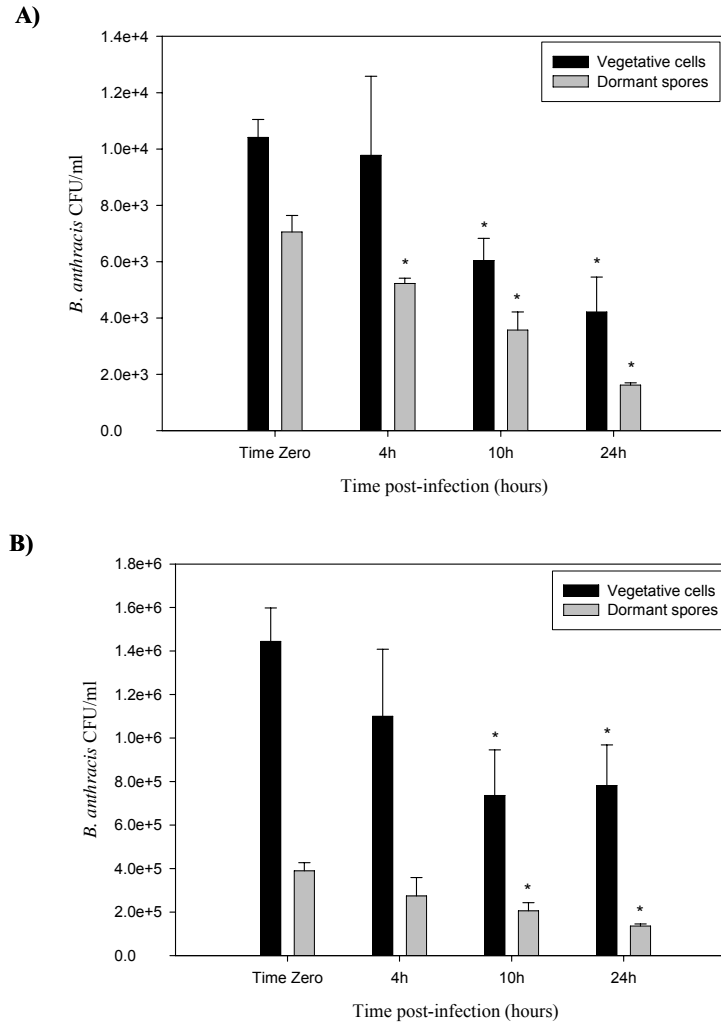


Figure 2.1 Tracking intracellular survival of Ames spores. Human MØs (5×10^5 per well) were infected with Ames spores at MOI of 5 (**A**) or 100 (**B**) for 1h at 37°C. Some wells were exposed to cytochalasin B (10 µg/ml) for 1 h before the addition of spores. Cells were then treated with gentamicin and washed to remove extracellular spores. Time zero wells were immediately lysed and plated on blood agar plates. For later time points, wells were replenished with fresh media (with 10 µg/ml gentamicin) and lysed as each time point expired. For quantification of dormant spores in each lysate, half of the sample was heated at 65°C for 30 min before plating. * indicates statistical significance ($p < 0.05$) versus respective group values at time zero as determined by ANOVA and Tukey test.

2007). Thus, MØs were either incubated in media alone, or pre-treated for 1 h with chloramphenicol or D-Alanine with D-Histidine. Spores were added to cultures and the uptake and survival experiment was followed as performed in **Figure 2.1**. Chloramphenicol pre-treated wells showed a similar pattern of Ames killing as that of untreated cells, suggesting that human MØs destroy newly germinated spores as efficiently as outgrown vegetative cells (**Figure 2.2**). For instance, untreated wells displayed a survival index of 0.48 at 24 h, while chloramphenicol-treated cells resulted in an index of 0.51, relative to the time zero time point. MØs were also capable of killing dormant spores because wells containing D-Alanine and D-Histidine displayed a similar killing trend as media control wells (indexes of 0.38 and 0.48, respectively). This supports the data from the heated lysates (**Figure 2.1**), verifying that human MØs are powerful killers of *B. anthracis* at all life stages. Interestingly, a higher percentage of *B. anthracis* organisms from D-Alanine + D-Histidine treated wells survived at 48 h compared to untreated wells (0.24 versus 0.04, respectively; **Figure 2.2**).

To verify that the observed killing of Ames spores was not simply due to the removal of an appropriate site of germination, i.e., by death of the MØ, the effect of spore infection on MØ viability was next investigated.

2.3.2 *Survival kinetics of Ames-infected human MØs*

Murine MØs are sensitive to killing by Sterne spores, with some reports of 80% MØ death observed as early as 3 h post-infection (Guidi-Rontani *et al.*, 2001). However, the death rate of Ames-infected human MØs remains unknown. Therefore, primary

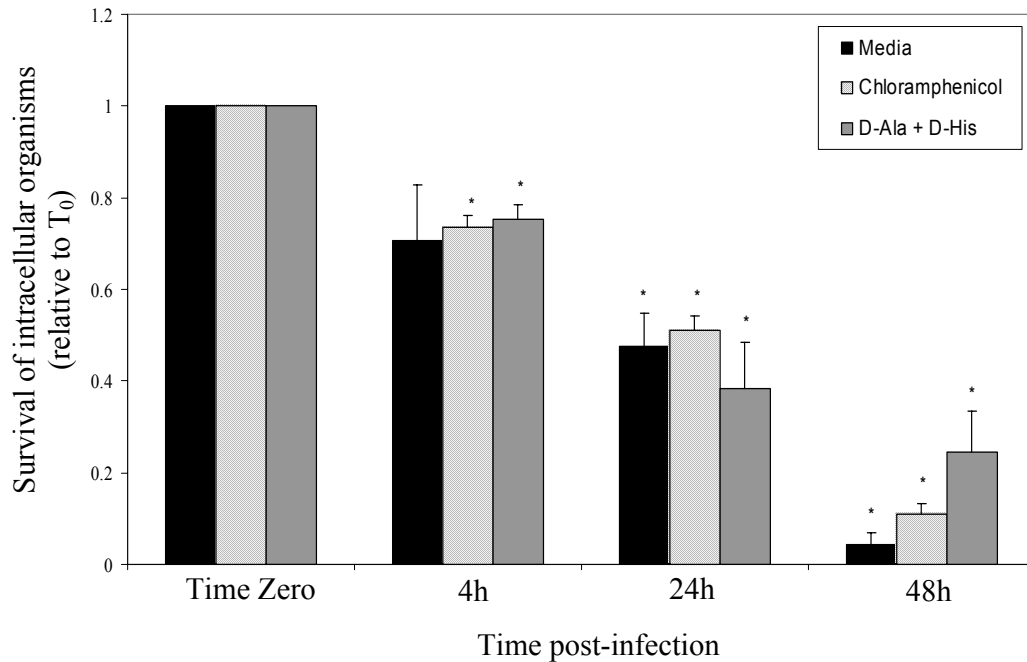


Figure 2.2 Determining the survival of *B. anthracis* in various stages of germination. MØs (5×10^5 per well) were left untreated or pre-treated with chloramphenicol (50 µg/ml) or D-Alanine (2 mM) plus D-Histidine (2 mM) for 1 h. Cells were then infected with Ames spores at MOI of 5 (A) or 100 (B) for 1h at 37°C. Next, cultures were treated with 100 µg/ml gentamicin for 30 min and washed five times to remove extracellular spores. Time zero wells were immediately lysed, serially diluted, and plated on blood agar plates. For later time points, parallel wells were replenished with fresh media (with 10 µg/ml gentamicin) and lysed as each time point expired. The graph shows combined results of three independent experiments. * indicates $p < 0.05$ versus respective group values at time zero (determined by ANOVA and Tukey test).

human MØs were infected with Ames spores at a MOI of either 5 or 100. Gentamicin remained in the media at all times to prevent outgrowth of extracellular spores and subsequent replication of extracellular bacilli. The MTT assay was used to assess MØ viability at time points of 6, 18, and 24 h. As **Figure 2.3A** shows, human MØs did not exhibit high rates of death due to spore infection at an MOI of 5. At 24 h post-infection, 82% of cells infected with wild-type spores remained viable. However, when the MOI was increased to 100, the percent survival dropped slightly to 71% at 24 h (**Figure 2.3B**). When gentamicin was not added to MØ cultures, long chains of bacilli were observed in wells as early as 4 h post-infection, and 100% killing was observed by 12 h (data not shown).

It was hypothesized that the death observed was due to LeTx being produced by intracellular, newly germinated bacilli. It is not known how much LF, EF, and PA are produced by bacteria while still in the MØ, however it is known that human MØs are sensitive to extracellular applications of purified LeTx in vitro (Kassam *et al.*, 2005). To test this, spores derived from an Ames strain deficient in the pXO1 plasmid (pXO1⁻), thus unable to produce toxins, was included in the experiment. It was hypothesized that the pXO1⁻ spores would not induce any cytotoxicity, yet the MOI 5 treatment did elicit a slight level of killing, as 85% of infected cells remained viable at 24 h (**Figure 2.3A**). When the MOI was increased to 100, the percent survival at 24 h dropped even further to 76%, but was not as low as that induced by wild-type spores (71%; **Figure 2.3B**). This suggested that LeTx is not the only means by which the small percent of MØs are dying. To determine if a spore surface-located molecule was perhaps responsible for the killing, paraformaldehyde-killed Ames spores were included as a group in this experiment. MØs were not killed as a result of exposure to paraformaldehyde-killed spores (**Figure 2.3**),

suggesting that the death that is elicited by spores is dependent on the viability of *B. anthracis* spores.

Although the level of MØ killing achieved by *B. anthracis* infection was not strikingly high, low levels of death may still play an important role during infection. Therefore, the mechanism of death was next investigated. Primary MØs seeded on glass coverslips were infected at an MOI of 100 with wild-type Ames spores, pXO1⁻ spores, or paraformaldehyde-killed spores for 6, 18, and 24 h. After staining cells with two fluorescent dyes, Syto 13 and propidium iodide (PI), the physiological state of infected cells was scored using a fluorescent microscope (Kassam *et al.*, 2005). Positive control cells were treated with camptothecin, a topoisomerase inhibitor that induces apoptosis (King *et al.*, 2002). **Figure 2.4A** depicts the distinct staining patterns that can be observed in cells at various stages of death. Viable cells stained a bright, uniformly green color, due to Syto 13 staining, and the chromatin had an organized structure. Necrotic cells stained a bright, uniform red color due to the PI being able to cross the compromised membrane. Early apoptotic cells have a largely intact membrane with nuclear DNA that has begun to condense and many exhibited membrane blebbing and apoptotic body formation. Thus, these cells stained punctate green and had highly condensed or fragmented chromatin. Finally, late apoptotic cells stained bright, punctate red due to PI diffusing across the compromised membrane and labeling fragmented chromatin.

Figure 2.4B shows camptothecin-treated cells undergoing both early and late apoptosis as early as 6 h. Cells in the early stage of apoptosis were observed at 6 h in wild-type spore-infected groups and comprised 20% of the total population of cells by 24 h. Cells in the late stage of apoptosis were first observed at 18 h and accounted for

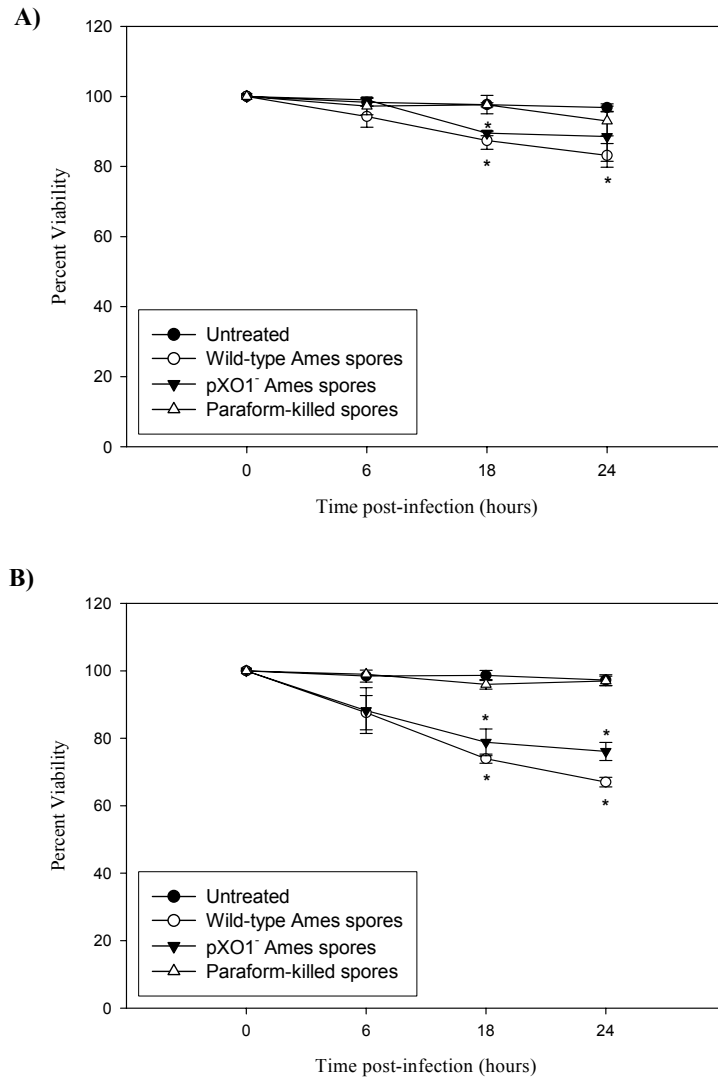


Figure 2.3 Effect of spore infection on MØ viability. Primary MØs were seeded in 96-well plates (2.5×10^5 /well) and infected with the various spore types, at the MOI of 5 (A) or 100 (B) for 6, 18, and 24h. Media contained 25 μ g/ml gentamicin at all times. As the time points expired, 10 μ l of the MTT reagent was added to each well and incubated for 2 h at 37°C. Subsequently, 100 μ l of the detergent reagent was added per well and the plate incubated at room temperature overnight. The absorbance was read at 570 nm. Absorbance levels were converted to percent viability. * indicates $p < 0.05$ versus untreated cells (ANOVA and Dunnett test).

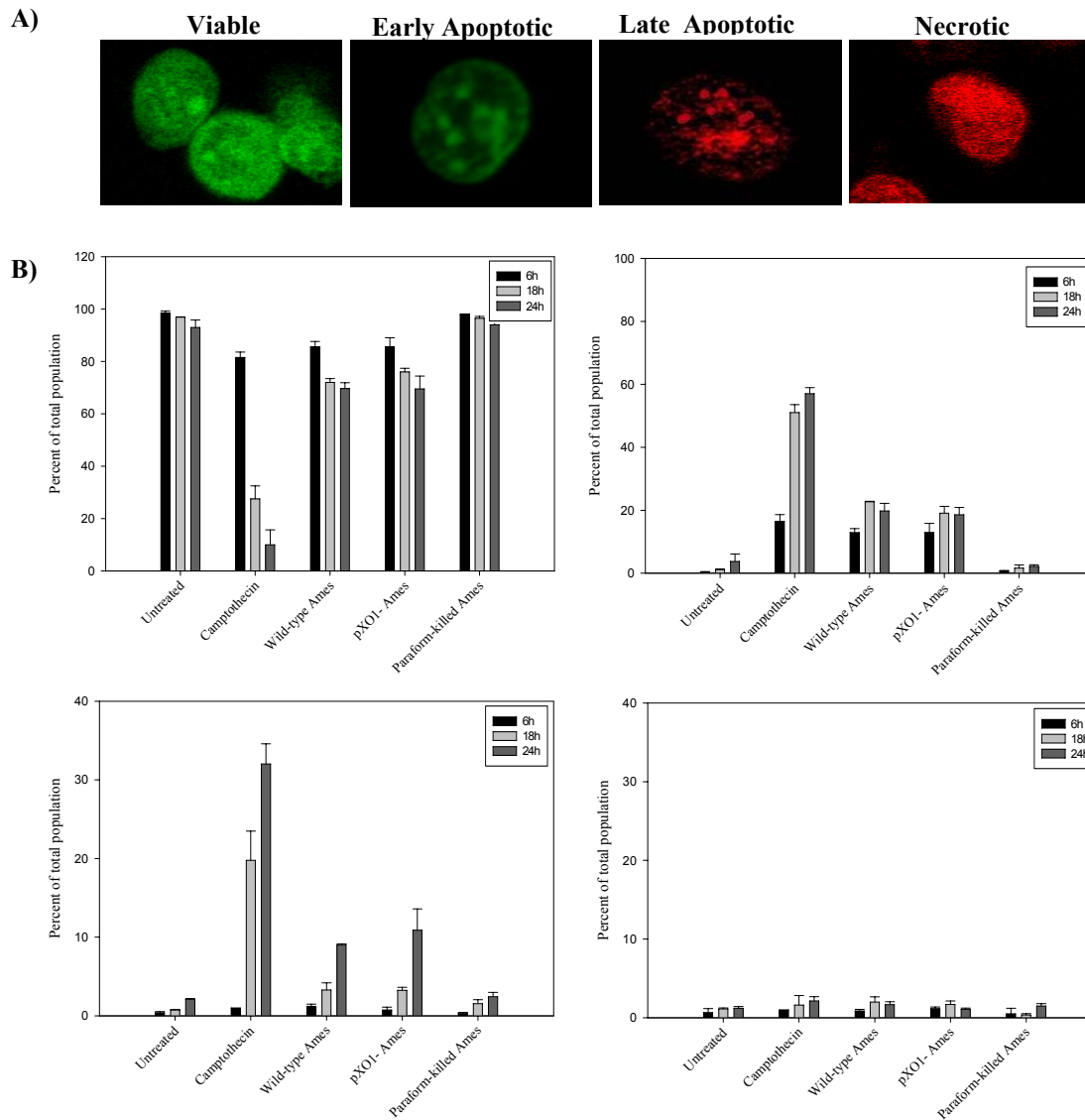


Figure 2.4 Immunofluorescence assay to identify the mechanism of death of spore-infected MØs. MØs (1×10^6 cells) were exposed to the indicated types of spores and incubated at 37°C for 6, 18, or 24 h. Negative control cells were left untreated, and positive control cells were treated with $5 \mu\text{M}$ camptothecin to induce apoptosis. Coverslips were then washed, fixed, and incubated with a mixture of Syto 13 ($20 \mu\text{M}$) and propidium iodide ($7.5 \mu\text{g/ml}$). Samples were then immediately viewed with a fluorescence microscope. The number of viable, necrotic, early apoptotic, and late apoptotic cells were scored in at least five fields of view per slide. **Panel A** depicts representative images of the staining pattern of cells in all stages examined and **Panel B** shows the quantitative results of three combined experiments.

approximately 9% of the population of wild-type spore-treated groups by 24 h. Cells infected with pXO1⁻ spores displayed a similar apoptotic pattern as those infected with wild-type spores, with evidence of cells in both early and late apoptosis (**Figure 2.4B**). Paraformaldehyde-killed spores did not elicit significant cytotoxicity compared to uninfected cells, which is in agreement with **Figure 2.3**. The percentage of necrotic cells remained constant (2%) throughout all conditions, representing a basal level of necrotic death.

2.3.3 Intracellular germination rates of Ames spores

Sterne spores germinate very quickly within murine RAW 264.7 cells and human alveolar MØs (Chakrabarty *et al.*, 2006; Dixon *et al.*, 2000). To determine the germination kinetics of Ames spores, primary human MØs were infected (MOI 5) and lysed at time points of 15, 30, 45, and 60 minutes. Gentamicin was added to the medium to prevent the germination and replication of extracellular organisms. Half of each lysate was plated immediately to quantify total organisms, while the other half was heated at 65°C for 30 minutes to measure the number of dormant spores. The results are graphed in **Figure 2.5**. Similar to the profile of Sterne spores, approximately 85% of Ames spores had germinated into vegetative cells as early as 15 minutes post-infection. After 60 minutes of infection, approximately 90% of intracellular organisms had germinated (**Figure 2.5**). Although this was a similar experimental set-up as the uptake and killing assay (**Figure 2.1**), one important difference was that spores remained in the wells throughout the duration of this experiment instead of being washed away. Therefore,

continuous uptake of spores was possible and likely explains why the number of dormant spores remained about the same over time despite the obvious germination. Additionally, the number of vegetative cells increases over the 60 minute time period likely because of increased germination of intracellular spores and perhaps even slight replication of bacilli.

2.3.4 Oxidative burst response of Ames-infected human MØs

To explain how the human MØ is capable of killing the large majority of *B. anthracis* organisms, the oxidative burst response was considered to be a likely player. Dihydrorhodamine 123 (DHR 123) was chosen to measure the intensity of the oxidative burst response of Ames-infected MØs for several reasons. DHR 123 is a dye that is practically non-fluorescent until oxidized intracellularly to the bright red fluorescent rhodamine 123 product. DHR detects both extracellular and intracellular levels of H₂O₂, hypochlorous acid (HOCl), and peroxynitrite anion (ONOO⁻). Also, there is minimal sample manipulation, as DHR 123 is added directly to the culture medium and fluorescence is measured immediately from the wells. An increase in fluorescence is indicative of enhanced oxidative burst activity.

Ames spores were added to MØ cultures, followed by the immediate addition of 10 µM DHR 123 to all wells. Fluorescence was measured every 10 minutes for up to 120 minutes. As a positive control for a robust oxidative burst response, one group included uninfected cells treated with 16 µM PMA. As **Figure 2.6** shows, these cells started exhibiting an increase in fluorescence at 20 minutes after PMA treatment. On the contrary, uninfected cells that did not receive PMA never showed a substantial increase

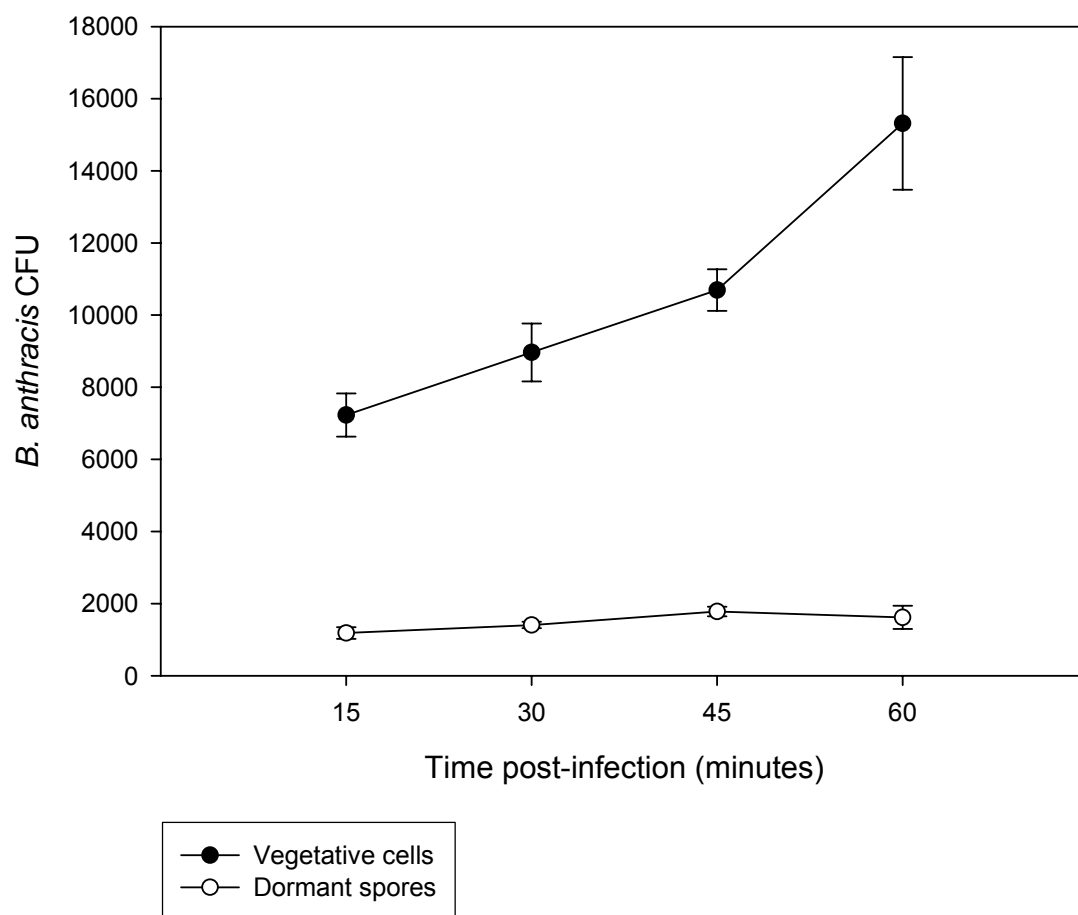


Figure 2.5 Monitoring the intracellular germination rates of internalized Ames spores. MØs (5×10^5 in triplicate) were infected with Ames spores (MOI 5) for 15, 30, 45, and 60 min at 37°C. The medium contained 25 µg/ml gentamicin during infection. As time points expired, five PBS washes were performed to remove extracellular spores. Cells were then lysed with 1% Triton X-100, serially diluted with PBS and plated on blood agar plates. For quantification of dormant spores in each lysate, half of the sample was heated at 65°C for 30 minutes before plating on 5% sheep blood agar plates. The graph shows combined results of two independent experiments.

in fluorescence. As shown in **Figure 2.6**, wild-type spores elicited a significantly higher oxidative burst than untreated cells at 20 minutes and this response remained significantly higher throughout the remaining time points. The oxidative burst of spore-infected cells became significantly higher than even the positive control cells after 60-120 minutes post-infection.

To glean more information, pXO1⁻ and paraformaldehyde-killed spores were also included in this assay. Paraformaldehyde-killed spores were unable to germinate, thus the oxidative burst against the spore itself could be assessed without interference by bacilli-associated products. Both of these groups elicited a significantly higher oxidative burst than untreated cells, however, it started 20 minutes later than that caused by wild-type spores, and the response never equaled the level elicited from PMA treatment (**Figure 2.6**). Additionally, cytochalasin B pre-treatment before the addition of Ames spores was performed on some wells to determine if spore phagocytosis was required in order for initiation of an oxidative burst. As **Figure 2.6** shows, the oxidative burst response did slightly increase over time, suggesting that surface contact with spores triggers a minor response by the MØs. However, phagocytosis does appear to be required to achieve a maximum oxidative burst.

2.3.5 Migration of spore-infected MØs

The current paradigm in anthrax literature dictates that MØs are responsible for transporting *B. anthracis* spores from the alveolar space to the lymphatics, upon which they escape by an unknown mechanism. To assess the effects of spore infection on the

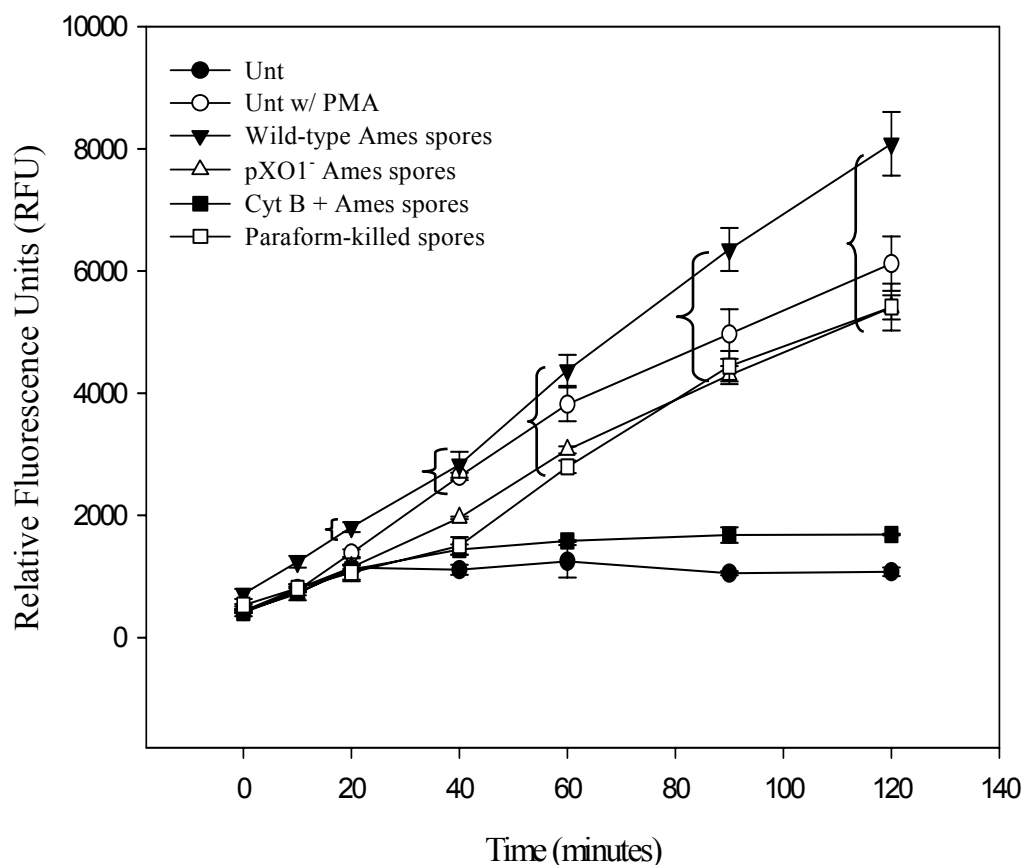


Figure 2.6 Effect of spore infection on the oxidative burst response of human MØs. Primary cells (1.5×10^5 cells in quadruplicate) were seeded in 96-well plates. Spores were then added to experimental wells, and each plate was centrifuged to synchronize phagocytosis. 10 μ M DHR 123 was added to detect the reactive oxygen species that were produced. Positive control wells received 16 μ M PMA (unt w/ PMA). Negative control wells included uninfected cells not receiving PMA (unt). Fluorescence was measured at 485/535 nm every 10 min for 40 min. — marks the groups statistically significant ($p < 0.05$) versus untreated control cells determined by ANOVA and Dunnett's test.

migration of alveolar MØs, a fluorescence-based migration assay was performed. Primary human MØs were allowed to phagocytose Ames spores for 1 h at 37°C. Cells were then collected and added to the top chamber of an 8-µM transwell filter resting in a 96-well plate. Uninfected cells were collected separately as a control. The bottom chamber either contained medium alone or medium with 10 ng/ml recombinant human MIP-1α to stimulate alveolar MØ chemotaxis (Opalek *et al.*, 2007). Cells were incubated for 2 h at 37°C to allow MØs to migrate into the lower chamber of the transwell system. Samples from the lower chamber of each well were collected and pooled with MØs adhered to the underside of their respective filters. Migrated cells were then fluorescently labeled with Cyquant GR dye for 15 minutes. Finally, the fluorescence of these samples was measured at 485/528 nm. Uninfected primary MØs exhibited a low level of basal migration that became significantly increased when exposed to the chemoattractant (**Figure 2.7**). However, the basal migration of Ames spore-infected MØs was significantly lower than the basal level of uninfected MØs. In the presence of MIP-1α, infected MØs reached a similar level of chemotaxis as their uninfected counterparts (**Figure 2.7**). These results indicated that Ames-spore infection reduced undirected alveolar-like MØ migration, but did not influence directed migration toward a chemoattractant.

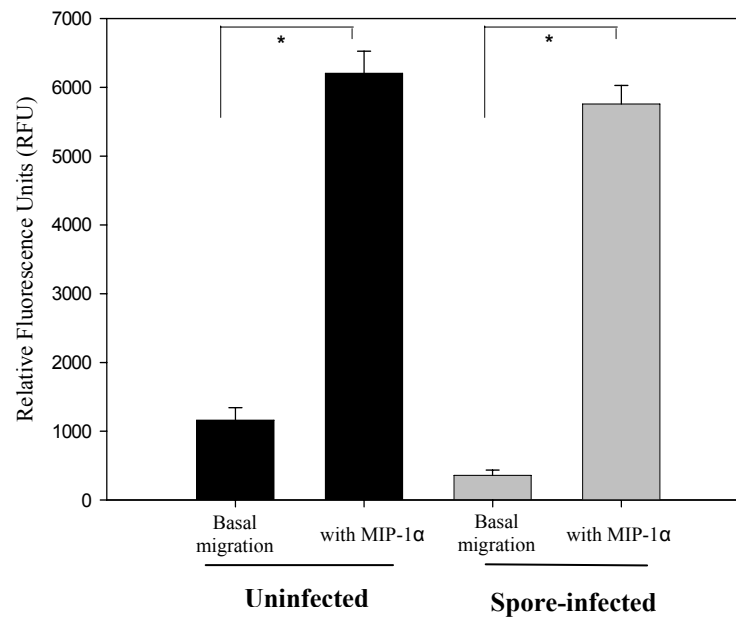


Figure 2.7 Migration assay of Ames-spore infected MØs. Primary MØs phagocytosed Ames spores for 1 h before cells were collected and given 2 h to migrate through an 8- μ M transwell filter. Uninfected cells were collected separately as a control. The bottom chamber either contained medium alone or medium with 10 ng/ml human MIP-1 α to stimulate alveolar MØ chemotaxis. Migratory cells were fluorescently labeled and samples measured at 485/528 nm. * denotes $p < 0.05$ between groups as indicated (ANOVA and Tukey test).

2.4 DISCUSSION

Because *B. anthracis* is a spore-former, it is one of the most resilient microbes yet identified. This is evidenced by the spores' ability to persist despite extreme temperatures, UV exposure, and bombardment with a multitude of disinfectants. The presence of two distinct types of infectious particles during anthrax infection (the spore versus the bacilli) makes anthrax pathogenesis a complex phenomenon in both the human and animal host. To simplify matters, infection can be categorized into two phases: (1) the primary interaction between spores and host cells, and (2) the later interaction between host cells and toxin-secreting vegetative cells. The purpose of this work was to focus on the earliest phase, involving *B. anthracis* spores and one of the first responding cell types following inhalational exposure, the human alveolar MØ.

Ames spores germinated within primary human MØs at an astonishing speed. After 15 minutes of infection, 85% of the spores had germinated into vegetative cells. This rate is very similar to that previously published when human alveolar MØs (Chakrabarty *et al.*, 2006) were exposed to Sterne spores. Thus, it is apparent that both virulent and avirulent *B. anthracis* spores adapt well within the MØ, regardless of the host type. The indiscrimination towards utilizing molecules/nutrients of multiple species likely contributes to the successful pathogenicity rates of *B. anthracis*.

MØs have long been implicated as a safe site of germination for anthrax spores. However, mice depleted of MØs before challenge with Ames spores succumbed to anthrax infection more rapidly than PBS control mice (Cote *et al.*, 2006). This led to the hypothesis that MØs have the potential to play a protective role during anthrax infection in the human host. Indeed, this work demonstrates that human MØs are potent killers of

B. anthracis Ames organisms. It seems the MØ is not a fastidious destroyer, as both dormant spores, newly germinated spores, and vegetative cells were targeted and effectively inactivated. Differential plating of heated versus unheated MØ lysates, as well as compounds that modulate the progression of the germination stage of *B. anthracis* confirmed this hypothesis. As mentioned previously, *in vitro* data from different laboratories suggest that MØs are capable of both clearing infection by *B. anthracis* spores and facilitating intracellular survival and release of germinated organisms (Cote *et al.*, 2004, 2006; Dixon *et al.*, 2000; Guidi-Rontani *et al.*, 1999, 2001; Welkos *et al.*, 2002). Microscopic data from guinea pig infection suggest that both situations are possible *in vivo*. In that model, a portion of inhaled spores phagocytosed by alveolar MØs were killed, while others were transported by MØs to the regional lymphatics where they germinated into vegetative bacilli (Ross, 1957). Thus, there is likely a sequence of events that is unique to each individual case of anthrax exposure, including the virulence and size of spore challenge, route of exposure, and resistance of the host. Re-examination of human specimens from autopsies of the victims of the epidemic of inhalational anthrax in Sverdlovsk, Russia in 1979 revealed that observation of a large number of mononuclear cells, including MØs, correlated with increased survival time of the patients (Grinberg *et al.*, 2001).

Interestingly, although the majority of *B. anthracis* organisms were killed, approximately 20% of dormant spores survived even at 48 h post-infection. The presence of survivors has also been reported during murine MØ infections (Hu *et al.*, 2006). Perhaps these survivors remain in the spore state until they reach a favorable environment, such as the nutrient-rich lymphatics, upon when they germinate and escape

from the MØ. *In vivo*, dormant spores have been recovered from the lungs of infected non-human primates as late as 100 days post-infection (Henderson, 1956).

MØs have traditionally been considered to be the primary cell type responsible for transporting *B. anthracis* spores from the alveolar space to the lymphatics. On the contrary, recent evidence is reshaping this model and suggests that the DC is the true ‘Trojan Horse’ of anthrax (Cleret *et al.*, 2007). The fact that human MØs in this work exhibited reduced basal migration following infection with Ames spores, but responded with normal levels of chemotaxis toward MIP-1 α indicates that spore infection alone is not enough to elicit MØ migration *in vitro*. However, the MØ is still capable of migrating when the appropriate extracellular stimuli are present, *i.e.*, MIP-1 α , therefore ruling out potential modulatory effects of the spore itself on directed MØ chemotaxis. Although the *in vivo* situation is certainly more complex than this *in vitro* experiment, the results imply that the spore infection in the MØ may differ from what occurs in DCs. For instance, spore infection encourages DCs to migrate by increasing lymph node homing receptors (Brittingham *et al.*, 2005) and they were identified as the primary cell type transporting spores to the thoracic lymph nodes in a mouse model (Cleret *et al.*, 2007). Data from this report support the new model in which alveolar MØs are responsible for quick phagocytosis and killing of inhaled spores, while DCs are responsible for transporting any remaining spores to the lymph nodes.

Human MØs were not particularly sensitive to cytotoxicity due to anthrax spore infection, although the MØ death rate does appear to be dependent on the concentration of spores. Including gentamicin in the culture medium allowed the investigation of MØ death solely due to intracellular spore infection. Cellular death began at 6 h post-infection and the rate increased over time. The maximum percent death observed was 29% at 24 h

with the MOI of 100. High rates of MØ death were not achieved likely because MØs are such efficient killers of anthrax organisms, thus not leaving substantial opportunity for death. Exposure to paraformaldehyde-killed Ames spores, which cannot germinate, did not elicit significant death, suggesting that bacilli-associated factors are indeed required for MØ cytotoxicity. Data from this work, along with previous reports, indicate that MØs demonstrate differential susceptibility to spore infection. Murine RAW 264.7 and J774.1 MØs exhibited 100% killing in response to infection with spores of the virulent Vollum 1B strain, while murine IC-21 MØs remained 98% viable (Gutting *et al.*, 2005).

Cote *et al* have recently shown that *B. anthracis* produces LeTx while inside the phagosome, which subsequently targets and kills murine MØs from the inside (Cote *et al.*, 2008). Thus, it was hypothesized that pXO1⁻ Ames spores, which are deficient in their ability to produce LeTx, would not be able to kill human MØs to the same extent as wild-type spores. Although MØ death rates were not as high as that caused by wild-type spore infection, MØs infected with pXO1⁻ spores did exhibit some killing. This suggested that other virulence factors, perhaps presently unidentified, produced by *B. anthracis* were capable of inducing the observed MØ death. For example, anthrolysin O is a pore-forming cytolysin produced by *B. anthracis* that has been shown to kill MØs, monocytes and neutrophils, and may be responsible (Mosser *et al.*, 2006).

Apoptosis was determined to be the mechanism of MØ killing elicited by wild-type Ames spores. LeTx itself kills human MØs via apoptosis (Kassam *et al.*, 2005) and likely contributed to the apoptotic pattern displayed by MØs infected by wild-type spores. Additionally, pXO1⁻ spores that did not secrete LeTx elicited a pattern of early and late apoptosis similar to that of wild-type spores. This confirmed earlier results from the MTT assays which indicated that LeTx is not the sole contributor to spore-infected

MØ toxicity. Future work is imperative to identifying the specific reason for a portion of spore-infected MØs to undergo apoptosis.

MØs have an extensive arsenal of weapons designed to eliminate microbial invaders. This includes (i) production of superoxide ($O_2^{\cdot-}$) by NADPH oxidase (ii) generation of nitric oxide (NO), $O_2^{\cdot-}$, peroxynitrite ($ONOO^-$), and H_2O_2 by inducible nitric oxide synthase (NOS 2), (iii) activation of cationic proteins, and (iv) production of defensins. Not surprisingly, recent evidence shows that *B. anthracis* has evolved a method of decreasing production of NO by producing arginase, a molecule that effectively competes with NOS 2 for L-arginine (Raines *et al.*, 2006). However, other components of the oxidative burst have not been evaluated with regards to anthrax spore infection. It was determined in this work that wild-type Ames spores elicited a robust oxidative burst response of primary human MØs, at least that specifically involving H_2O_2 , HOCl, and $ONOO^-$. Surface contact between the spores and the MØ did trigger a slight oxidative burst, but it appears that complete phagocytosis of spores is necessary for a maximal response in human MØs. Ames pXO1⁻ spores also prompted an oxidative burst, though not as vigorous as that generated by wild-type spores. These data suggested that the bacterial products associated with newly emerged vegetative cells, such as LeTx and EdTx, likely influences the respiratory burst to a certain extent. Therefore, although the NO component of the respiratory burst may be impaired by *B. anthracis*, the other components remain unaffected and function to aid human MØs in destroying anthrax spores and vegetative cells.

From an immunological point of view, spores were once thought to be relatively inert particles. On the contrary, because it is considered the infectious form of *B. anthracis*, the spore is the first form of the organism that will interact with the host.

Therefore, it is not unreasonable to hypothesize that the spore will elicit the earliest host defense responses. Indeed, two recent reports have shown that the spore particle itself is capable of eliciting robust cytokine responses from both murine splenocytes (Glomski *et al.*, 2007) and primary murine MØs (Basu *et al.*, 2007). Both studies concluded that spores are recognized by pattern-recognition receptors, which triggered the subsequent secretion of cytokines such as IL-12, IFN- γ , IL-1 β , TNF- α and IL-6 (Basu *et al.*, 2007; Glomski *et al.*, 2007). The spore exosporium does not contain any known TLR ligands, thus it is likely that upon phagocytosis, spores may be degraded within the phagolysosome, leading to release of spore-associated molecular patterns (SAMP). Interestingly, none of the individual TLRs were necessary for inducing cytokine secretion by the splenocytes (Glomski *et al.*, 2007), which suggests there is likely spore recognition through multiple pattern recognition receptors or an unidentified MyD88-dependent mechanism. Additionally, this work has confirmed the notion that spores are immunologically active because human MØs were able to recognize Ames spores and respond with a significant oxidative burst. The use of paraformaldehyde-killed spores that are unable to germinate allowed the assessment of the oxidative burst to the spore particle itself without interference of newly germinated cells.

In conclusion, human MØs are more efficient killers of *B. anthracis* spores and vegetative cells than their murine counterparts. Phagocytosis of anthrax spores generates a powerful oxidative burst response that functions to eliminate the pathogen and prevent the organism from killing the majority of the MØ population. These data support a protective role for MØs during anthrax pathogenesis. Finally, despite the powerful level of killing demonstrated by human MØs, a small portion of spores did survive, perhaps providing a narrow window of opportunity for the infection to become established after

the first wave of the host immune response has subsided. Perhaps therapeutics designed toward eliminating the few persistent spores will be more effective rather than targeting the second phase of the disease (i.e., toxins).

Chapter 3: Edema toxin suppresses human MØ phagocytosis and cytoskeletal remodeling

3.1 INTRODUCTION

As an intrinsic adenylate cyclase, EdTx causes prolonged production of cAMP in multiple cell types, including MØs. Other agents that elevate cAMP concentrations within MØs result in inhibition of an array of MØ functions such as phagocytosis, migration, spreading, adhesion, superoxide production, and bacterial killing (Cantarow *et al.*, 1978; Razin *et al.*, 1978; Takei *et al.*, 1998). Indeed, studies examining the effect of EdTx on human neutrophils have shown that the phagocytic capacity and oxidative burst of these cells is reduced (O'Brien *et al.*, 1985; Wright *et al.*, 1986). Additionally, EdTx treatment impairs human MØ migration. Rossi *et al* attributed this phenomenon to a reduction in chemokine receptor signaling following toxin treatment (Rossi *et al.*, 2007). However, we hypothesized that a second mechanism potentially responsible for reduced motility is impairment of the MØ cytoskeleton by EdTx.

EdTx treatment of the murine MØ cell line RAW 264.7 cells elicited significant alterations of multiple genes whose products are vital for proper actin structure and rearrangement, including an important signaling molecule that binds cAMP and modulates the actin cytoskeleton. There was a 2.6-fold up-regulation of the regulatory subunit of protein kinase A (PKA; Comer *et al.*, 2006) in toxin-treated MØs. cAMP-dependent PKA is involved in nearly every family of the cytoskeletal network, including microtubules, intermediate filaments, and actin microfilaments. PKA plays a

dichotomous role as some hallmarks of cell migration and cytoskeletal assembly require PKA activity (activation of Rac, Cdc42, and microfilament assembly), while others are inhibited by it (activation of Rho, actin polymerization; reviewed in Howe *et al.*, 1994).

Although the effects of cAMP were once thought to be solely transduced by PKA, exchange protein activated by cAMP (Epac) has recently been implicated as a member of the cAMP signaling cascade that acts independently of PKA (de Rooij *et al.*, 1998; Kawasaki *et al.*, 1998). Epac belongs to a family of guanine exchange factors (GEFs) that directly activates the small GTPase Rap1 and participates in versatile pathways, among which include modulation of integrins associated with the actin cytoskeleton and regulation of actin dynamics. It was recently shown that human endothelial cells treated with EdTx underwent cytoskeletal changes and exhibited impaired chemotaxis due to activation of the Epac pathway (Hong *et al.*, 2007).

Thus, in order to further examine the role of EdTx during anthrax pathogenesis in the human host, we explored the hypothesis that EdTx-treatment leads to deregulation of the cAMP-dependent PKA and/or Epac system, resulting in impaired cytoskeletal functions of host MØ's that are essential for their migration and phagocytosis.

3.2 METHODS

3.2.1 Cell line and reagents

Human HL-60 cells (ATCC, Manassas, VA) were maintained in Iscove's Modified Dulbecco's Medium with 20% fetal bovine serum (FBS) and

penicillin/streptomycin. To differentiate these cells into MØs, 200 nM phorbol 12-myristate 13-acetate (PMA; Sigma, St. Louis, MO) was added where indicated for 24 h. Differentiation was confirmed by adherence, morphological changes, increased expression of CD11b, and phagocytosis of *Escherichia coli*-conjugated particles (data not shown). Before each experiment, the PMA-containing media was removed and cells were washed with phosphate buffered saline (PBS). Purified *B. anthracis* EF and PA were provided by the Biodefense and Emerging Infections Research Resources Repository (BEI Resources, Manassas, VA) and reconstituted with molecular grade water. Aliquots were stored at -80°C. Concentrations used were 1.25 µg/ml EF and 5 µg/ml PA in all cases, except where noted. DHR 123 and Alexa Fluor 594 phalloidin were purchased from Molecular Probes (Eugene, OR). PMA, lipopolysaccharide (LPS), Cytochalasin B, phosphatase inhibitor cocktail 1, and protease inhibitor cocktail were purchased from Sigma. Horseradish peroxidase (HRP)-conjugated GAPDH antibody, and rabbit anti-Epac were purchased from Santa Cruz (Santa Cruz, CA). Mouse anti-PKA RIIα was from BD Biosciences (San Jose, CA). 8-(4-chlorophenylthio)-2'-O-methyladenosine-3',5'-cAMP (8-CPT-2Me), N6-benzoyladenine-3',5'-cAMP (6-Bnz-cAMP), and myristoylated PKI (mPKI), each purchased from BIOLOG Life Sciences Institute (Bremen, Germany), were reconstituted with molecular grade water and aliquots stored at -20°C.

3.2.2 Isolation and culture of primary human MØs

First, monocytes were purified from buffy coats as described previously (Ben Nasr *et al.*, 2007). Briefly, human peripheral blood mononuclear cells (PBMC) were

collected following Ficoll-Paque Plus (GE Healthcare, Piscataway, NJ) density centrifugation. Monocytes were isolated by negative selection using a magnetic column separation system (StemCell Technologies, Vancouver, Canada). Monocytes were then differentiated into alveolar-like MØs as previously described (Akagawa *et al.*, 2002; Komuro *et al.*, 2001). Monocytes were resuspended in RPMI 1640 at a concentration of 2.5×10^5 per ml in 6-well tissue culture plates and cultured with granulocyte-macrophage colony-stimulating factor (GM-CSF) (500 units/ml; PeproTech, Rocky Hill, NJ) and 10% heat-inactivated FBS for 7 days at 37°C in a CO₂ incubator.

3.2.3 Spore preparation

Spores were prepared as previously described (Peterson *et al.*, 2007). Briefly, *B. anthracis* Ames strain was inoculated in Schaeffer's sporulation medium (pH 7.0), consisting of 16 g Difco Nutrient Broth, 0.5 g MgSO₄·7H₂O, 2.0 g KCl, and 16.7 g MOPS (morpholinepropanesulfonic acid) per liter. Before inoculation, the following supplements were added to the medium: 0.1% glucose, 1 mM Ca(NO₃)₂, 0.1 mM MnSO₄, and 1 µM FeSO₄. Cultures were grown at 37°C with gentle shaking (180 rpm) for 48 h, after which sterile distilled water was added to dilute the medium and promote sporulation. After 10 to 11 days of continuous shaking, sporulation was confirmed at >99% via phase-contrast microscopy and a modified Wirtz-Conklin spore stain, and the spores were centrifuged at $630 \times g$ at 4°C for 15 min. The spore pellets were then washed in sterile water and resuspended in sterile water. Subsequently, the spore suspension was layered onto a cushion of 58% Hypaque-76 (GE Healthcare) at a ratio of 1:2.5 by volume. Without mixing, the tubes were centrifuged at $8,270 \times g$ for 45 min at 4°C. The

spore pellet was washed twice with sterile water and finally resuspended in PBS. Aliquots of the stock spore suspension were stored at -80°C and freshly diluted in PBS to the desired number of colony forming units (CFU) immediately before each experiment. The spore suspensions were homogeneous when examined by phase-contrast microscopy.

3.2.4 *cAMP ELISA*

MØs (5×10^5 /well) were seeded in triplicate wells per condition and exposed to two concentrations of EdTx, either 0.625 µg/ml EF + 2.5 µg/ml PA or 1.25 µg/ml EF + 5 µg/ml PA. Some wells were left untreated, while others received 1 ng/ml LPS to account for the low levels of LPS in the toxin preparations, or EF or PA alone. A portion of the culture supernatant in each well was saved at time points of 2, 6, and 24 h, followed by lysing the MØs in the well with 0.1M HCl and saving a portion of each intracellular lysate. Samples were stored at -80°C until the cAMP ELISA kit (Assay Designs, Ann Arbor, MI) was used to measure cAMP levels of combined intracellular lysates and extracellular supernatants. This experiment was performed independently three times.

3.2.5 *Phagocytosis assays*

MØs (5×10^5 /well) were seeded in triplicate using 24-well plates and exposed to EdTx for the indicated times. Simultaneously, cells were infected with Ames spores (MOI of 5) for 1 h at 37°C with 5% CO₂. Cells were subsequently treated with 100 µg/ml gentamicin for 30 min to kill extracellular bacteria. All wells then underwent multiple

washes with PBS to remove extracellular spores. Lysates were serially diluted with PBS, immediately plated on blood agar plates, and incubated at 37°C. Colonies were counted the next day and phagocytosis was expressed as the number of viable intracellular *B. anthracis* CFUs (both dormant and vegetative) recovered per 5×10^5 MØs.

Additionally, the Vybrant Phagocytosis assay (Molecular Probes) was used and performed according to the manufacturer's instructions. MØs (1×10^5 /well) were seeded in 96-well plates (quadruplicate wells per condition) and pre-treated with EdTx for 3, 6, and 24 h. Controls of untreated cells and Cytochalasin B treated MØs were also included. Further, some wells received 6-Bnz-cAMP (300 μ M), mPKI (25 μ M), or 8-CPT-2Me (100 μ M) for 1 h. Next, fluorescein isothiocyanate (FITC)-conjugated *E. coli* Bioparticles (Molecular Probes; 100 μ l) were added to each well and incubated for 1 h at 37°C. After removal of the Bioparticles, trypan blue was added to quench extracellular fluorescence, and the plate was read with a SpectraMax M5^e plate reader (Molecular Probes) with settings of 480 nm excitation and 520 nm emission.

3.2.6 *F-actin content*

Similar to Hu et al. (2005), 2.5×10^5 MØs were seeded in quadruplicate wells of 96-well plates and left untreated or treated with EdTx for indicated time points, Cytochalasin B (10 μ g/ml) for 2 h, or 6-Bnz-cAMP (300 μ M), mPKI (25 μ M), or 8-CPT-2Me (100 μ M) for 1 h. Some wells received a combination of EdTx with mPKI simultaneously for 6 h, while rescue wells were treated with EdTx for 5 h, then cells were washed and replaced with fresh media containing mPKI for an additional hour. FITC-

labeled *E. coli*-conjugated particles were then added to each well for 1 h to elicit cellular motility and phagocytosis. Cells were subsequently washed, fixed with 3.7% paraformaldehyde, and permeabilized with 0.1% Triton-X 100. After washing again, Alexa Fluor 594 phalloidin was added to cells for 30 min before several final washes. A small volume of PBS was left in each well and the plate was read on a plate reader with settings of 590 nm excitation and 617 nm emission. This experiment was repeated three times for each MØ type and the graph depicts one representative experiment.

3.2.7 Immunofluorescence and cell spreading

This experiment followed the protocol of Lasunskaja *et al.* (2006). HL-60 MØs were seeded on glass coverslips and pre-treated with EdTx (2, 6, 12, and 24 h), Cytochalasin B (1 h), or EF or PA alone (24 h). Next, FITC-conjugated *E. coli* particles were added as a phagocytic stimulus for an additional hour. Coverslips were washed in PBS and then permeabilized with 0.1% Triton-X 100 for 5 min. Following another PBS wash, cells were fixed with 3.7% paraformaldehyde for 30 min at room temperature. Finally, cells were washed and labeled with Alexa Fluor 594-conjugated phalloidin for 30 min before being mounted with SlowFade Gold with DAPI mounting solution (Molecular Probes). Coverslips were viewed with an Axioplan II fluorescent microscope, and images were recorded using the Axiophot 2 dual camera. For quantification of MØ spreading, the ImageJ v1.37 software (NIH, Bethesda, MD, <http://rsb.info.nih.gov/ij/>) was employed to measure cellular dimensions. The perimeter of cells in at least five fields of view per slide was manually traced and the software calculated the area, perimeter, length, and width of

each individual cell. The spreading index was expressed as a relation of a mean cell area of EdTx-treated cells compared to control untreated cells. At least 100 randomly selected cells of each slide were examined by the ImageJ software.

3.2.8 PKA activity assay

For the PKA activity assay, following EdTx pre-treatment, HL-60 cultures grown in 10 cm plates were lysed with the lysis buffer provided with the Omnia PKA Assay (Invitrogen, Carlsbad, CA), along with phosphatase and protease inhibitors. After clarification of the extracts by centrifugation, the lysates were stored at -80°C until analysis. The BCA protein assay (Bio-rad, Hercules, CA) was performed in order to quantitate protein levels of each sample, and the PKA Assay kit protocol was adhered to for subsequent assessment of kinase activity. Briefly, the reaction was initiated by adding the master mix, i.e., appropriate buffers, ATP, the PKA substrate, and a non-PKA inhibitor cocktail, to 1 µg total protein of the lysates. Fluorescence intensity readings were collected every 2 min for 20 min (360 nm excitation, 485 nm emission). For graphing purposes, the data were expressed as a cell lysate PKA activity curve (relative fluorescence units versus time). This experiment was performed independently three times and all showed the same trend. The figure is representative of one particular experiment.

3.2.9 Rap1 pulldown assay and Western blot analysis

To assess Rap1 activation, a pulldown assay followed by Western blot analysis was performed. Heavily seeded HL-60 cultures were grown in 10 cm plates, treated with EdTx for appropriate times, washed once with PBS, and then lysed with small volumes of lysis buffer included in the EZ Detect Rap1 kit (Pierce, Rockford, IL). Following a high-speed spin to pellet cell debris, supernatants were collected and protein quantitation was performed on each sample. Following the manufacturer's instructions, samples were incubated with glutathione *S*-transferase (GST)-fusion protein RNA binding domain (RDB) of RalGDS immobilized to glutathione beads for 1 h at 4°C with gentle agitation to specifically isolate active (GTP-bound) Rap1. The resin was washed several times with wash buffer before the final collection of sample by centrifugation. Proteins were resolved by SDS-PAGE (25 µg protein/lane) and transferred to a nitrocellulose membrane. Finally, the membrane was probed with a rabbit anti-Rap1 antibody (Pierce; 1:1,000 dilution) overnight at 4°C, followed by the appropriate HRP-conjugated secondary antibody for 1 h at room temperature. Finally, SuperSignal chemiluminescence detection reagent (Pierce) was applied. Densitometry (Quantity One, Bio-Rad) was utilized to quantitate each band, and data were expressed as fold-change compared to untreated controls. To ensure equal protein amounts were loaded, in each lane, cell lysates were also immunoblotted with anti-GAPDH antibodies. This experiment was performed two times and the graph shown is an average of both experiments.

To examine PKA RII α and Epac levels, Western blot analysis was performed similarly as described above. However, treated cells were instead lysed with RIPA buffer containing phosphatase and protease inhibitors for 1 h on ice. Similarly, samples were subjected to SDS-PAGE (20 µg protein/lane) and transferred to nitrocellulose membranes. Next, membranes were probed with primary antibody for 1 h (1:500 dilution

of PKA RII α or Epac), followed by incubation with the appropriate HRP-conjugated secondary antibodies (Santa Cruz Biotech) for 1 h. Membranes were developed as mentioned above, densitometry was performed, and data expressed as fold-change compared to untreated controls. Again, GAPDH levels were examined to ensure equal protein loading. This experiment was performed three times for each antibody and the graphs show the average of all three experiments.

3.2.10 MTT assay

Differentiated HL-60 cells or primary cells were seeded in 96-well plates (2.5 x 10⁵/well) and treated with EdTx (1.25 μ g/ml EF + 5 μ g/ml PA) for 2, 6, and 24 h. Controls of untreated cells and those receiving EF or PA alone were included. Next, 10 μ l of the MTT reagent (3-(4, 5-dimethylthiazoyl-2)-2, 5-diphenyltetrazolium bromide), included in the MTT Cell Proliferation Assay (ATCC), was added to each well and the plate was incubated for 2 h at 37°C. Subsequently, 100 μ l of the detergent reagent was added per well and the plate incubated at room temperature overnight in the dark. Finally, the absorbance was read at 570 nm. Internal controls included wells with no cells (only media plus MTT reagent and detergent) to detect background absorbance levels. A decrease in absorbance indicated a decrease in cell viability, and the experiment was performed independently three times.

3.2.11 Statistics

As indicated, experimental conditions were performed in either triplicate or quadruplicate and repeated at least three times to ensure reproducibility. Data were expressed as mean \pm SD of the replicates. Differences were considered statistically significant when the p value was <0.05 as determined by one-way analysis of variance (ANOVA), using SigmaStat software, followed by the Dunnett test, Student-Newman-Keub, or Dunn's test, where indicated.

3.3 RESULTS

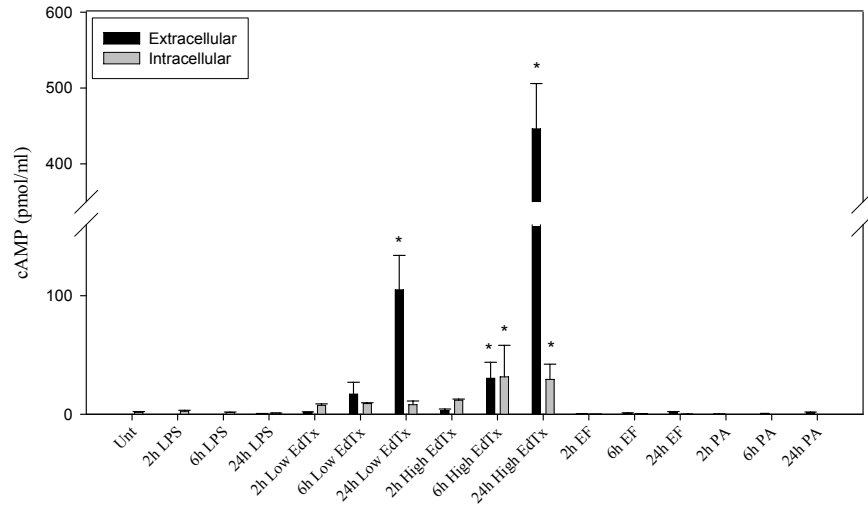
3.3.1 EdTx increases cAMP levels in HL-60 MØs

Experiments in this study were performed with both human primary alveolar-like MØs and the human promyelocytic cell line HL-60. Human monocytes cultured with GM-CSF differentiate into cells closely resembling alveolar MØs, with respect to morphology (Nakata *et al.*, 1991), expression of cell surface antigens (Akagawa *et al.*, 1994; Andressen *et al.*, 1990), and function (Komuro *et al.*, 2001; Matsuda *et al.*, 1995; Nakata *et al.*, 1995). Alternatively, HL-60 cells can be differentiated into various cell types depending on the treatment (Collins *et al.*, 1987). Phorbol 12-myristate 13-acetate (PMA) was added for 24 h to differentiate the nonadherent HL-60 cells into adherent, MØ-like cells capable of phagocytosis and bacterial killing (Collins *et al.*, 1987; Fontana *et al.*, 1981).

To verify that both MØ types were susceptible to the activity of EdTx, a cAMP ELISA was performed. HL-60 cells and primary MØs were exposed to EdTx at two

concentrations (either 0.625 µg/ml EF + 2.5 µg/ml PA or 1.25 µg/ml EF + 5 µg/ml PA) for 2, 6, and 24 h before extracellular supernatants and intracellular lysates were collected. Both pools were evaluated in order to determine whether the majority of cAMP evoked by EdTx treatment was secreted or contained intracellularly. IBMX (phosphodiesterase inhibitor 3-isobutyl-1-methylxanthine; 50 µM) was applied during the incubations to prevent intrinsic phosphodiesterase activity from degrading cAMP. **Figure 3.1** shows that the higher concentration of EdTx significantly increased total cAMP production in both cell types at 6 h, and this effect was further enhanced at 24 h. Therefore, this concentration of EdTx was chosen for all subsequent studies presented here. Controls of EF and PA alone did not evoke significant cAMP production. *E. coli* LPS (1 ng/ml) was also applied to mimic the low levels of LPS contamination found in the toxin; however, it did not elicit cAMP production.

A) HL-60



B) Primary

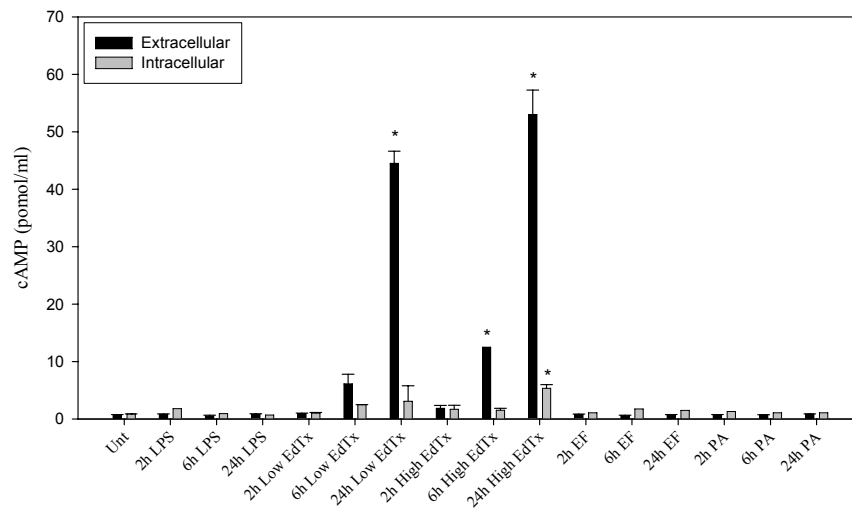


Figure 3.1. cAMP production by EdTx-treated human MØs. HL-60 (A) and primary (B) MØs in triplicate wells per condition were treated with EdTx at two concentrations (Low = 0.625 µg/ml EF + 2.5 µg/ml PA; High = 1.25 µg/ml EF + 5 µg/ml PA), LPS, EF, PA, or left untreated. At each time point, extracellular and intracellular samples were collected and analyzed with a cAMP ELISA. EF and PA treatment did not elicit significant cAMP production in either cell type. * indicates statistical significance of $p < 0.05$ versus unt using ANOVA and Dunnett's tests.

To determine whether EdTx was cytotoxic to the HL-60 and primary MØs, the MTT assay was used to monitor cell viability following toxin treatment for 2, 6, and 24 h. Results showed that EdTx (1.25 µg/ml EF + 5 µg/ml PA), EF, and PA treatment did not decrease MØ survival at any of the tested time points (**Figure 3.2**). Additionally, protein levels were measured in MØs treated with EdTx for 0, 2, 6, and 24 h. Protein levels did not change despite exposure to EdTx, further verifying that cell viability was not altered and thus allowing for subsequent investigation of MØ functions without having to correct for a reduction in cell concentration over time (data not shown).

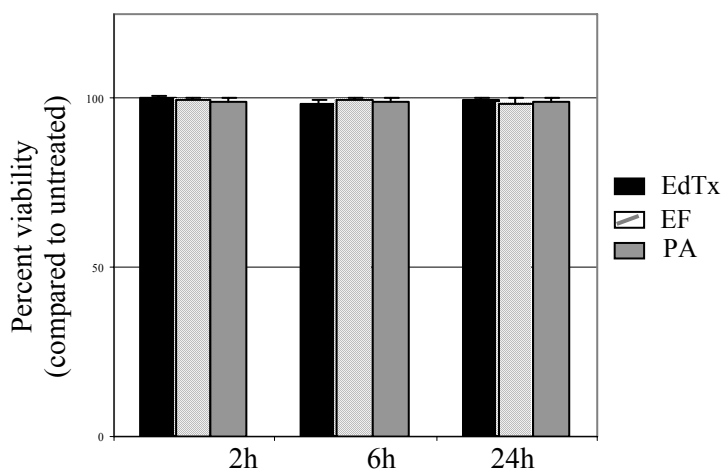


Figure 3.2. Effects of EdTx on human MØ viability. Primary MØs were treated with EdTx, EF, or PA. The MTT assay was used to assess viability at each time point. Absorbance was read at 570 nm, and the graph is an average of three independent experiments.

3.3.2 EdTx reduces the phagocytic capacity of human MØs

When encountering microorganisms, MØs undergo a rapid course of action consisting of chemotaxis, phagocytosis, and intracellular killing *via* oxygen-independent and oxygen-dependent (oxidative burst) mechanisms. The effect of EdTx on MØ phagocytosis of virulent *B. anthracis* Ames spores was investigated. Primary alveolar-like and HL-60 MØs were pre-treated with EdTx for 2, 6, or 24 h before co-culturing with spores at a MOI of 5 for 1 h. Control wells were left untreated, while other wells were treated with Cytochalasin B before the addition of spores. This agent is a fungal toxin that disrupts actin filaments and was used as a negative control in this experiment and others in this study. All MØs were then lysed and plated to quantify the number of organisms successfully phagocytosed in each well. **Figure 3.3** shows that uptake of spores by both MØ types was significantly inhibited following 6 and 24 h of EdTx exposure. Toxin treatment for 24 h exhibited a level of phagocytosis inhibition similar to that elicited by Cytochalasin B treatment. Furthermore, MØ phagocytosis of FITC-labeled *E. coli*-conjugated particles following EdTx treatment was analyzed. Similar to the spore uptake results, EdTx pre-treatment for 3, 6, and 24 h significantly lowered human primary and HL-60 MØ phagocytosis of the *E. coli* particles (**Figure 3.4**).

To explain the mechanism responsible for the decreased phagocytosis exhibited by MØs, it was hypothesized that two cAMP-binding signaling molecules, PKA and Epac, would likely be targeted by EdTx-generated cAMP. cAMP analogs with specificity in their activation toward Epac or PKA were included to determine if stimulation of one or both pathways would mimic results observed in response to EdTx treatment. 6-Bnz-cAMP is an activator of PKA, while 8-CPT-2Me is a selective Epac activator. The

concentrations of these compounds were chosen from previous publications (Aronoff *et al.*, 2005; Bryn *et al.*, 2006; Hong *et al.*, 2007) and their effectiveness at these concentrations were verified with HL-60 MØs (data not shown). Similar to the EdTx groups, both compounds significantly suppressed the phagocytic uptake of *E. coli* particles by primary alveolar-like and HL-60 MØs (**Figure 3.4**). Because PKA and Epac activation mimicked the EdTx-induced inhibition of uptake, it suggested that both pathways were potentially involved in the effects elicited by EdTx. We also pre-treated cells with the highly specific, myristoylated peptide PKA inhibitor mPKI₁₄₋₂₂ (mPKI). As shown in **Figure 3.4**, mPKI did not cause phagocytosis inhibition as that elicited by EdTx. A final group was exposed to EdTx and mPKI simultaneously for 6 h in order to prevent potential PKA activation by EdTx. In both MØ cell types, phagocytosis was still reduced, suggesting this was not a process solely dependent on PKA.

Overall, these experiments indicated that EdTx impairs human MØ phagocytosis of treated human MØs. Application of selective PKA and Epac activators caused a similar reduction in phagocytosis, implicating both of these pathways as potential mediators in EdTx-induced cAMP signaling. The suppressed phagocytosis, together with the previously reported impairment in MØ migration following EdTx treatment (Rossi *et al.*, 2007), raised the possibility that the actin cytoskeleton was involved. Because EdTx elicited similar levels of impairment of phagocytosis in both the primary and HL-60 MØs, the HL-60 cells were determined to be a suitable model of human MØs and used in all subsequent experiments.

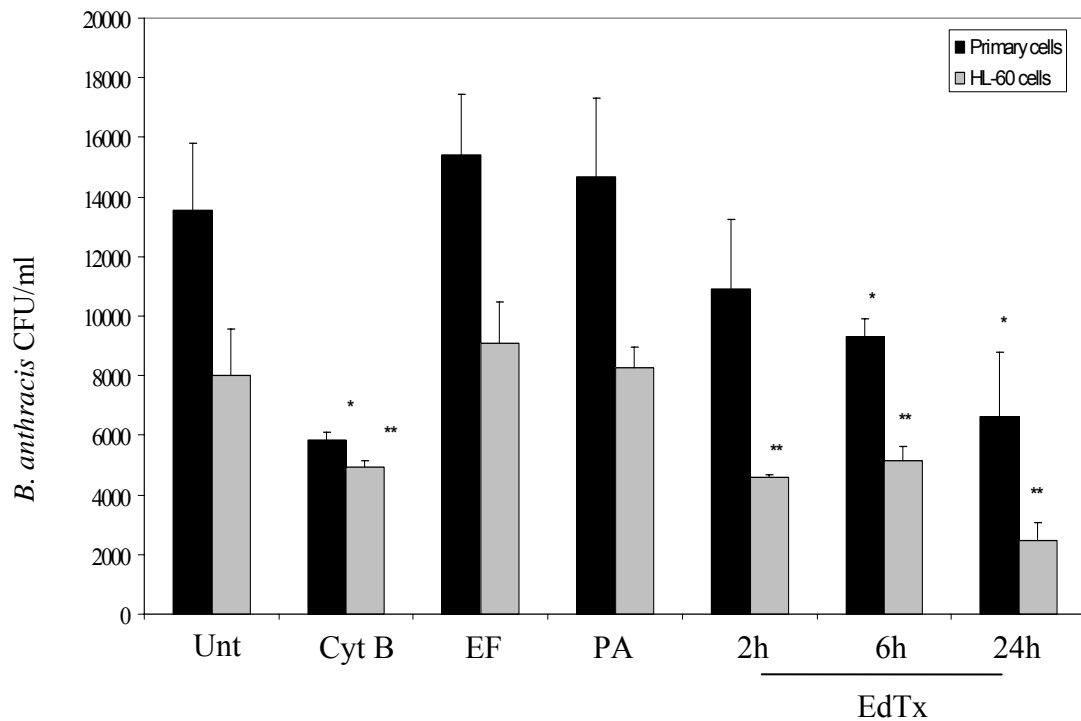


Figure 3.3. Effects of EdTx on phagocytic activity of human MØs. Primary alveolar-like and HL-60 MØs (5×10^5 /well) were seeded in triplicate and pre-treated with EdTx (1.25 μ g/ml EF + 5 μ g/ml PA), EF (1.25 μ g/ml), or PA (5 μ g/ml) for 2-24 h. Cells were then infected with Ames spores (MOI of 5) for 1 h. Following gentamicin treatment and PBS washes, cells were lysed and plated on blood agar plates. Colonies were counted and the graph shows the combined results of three experiments. *, $p < 0.05$ vs untreated primary cells; ** $p < 0.05$ vs untreated HL-60 cells (both using ANOVA and Dunnett's tests).

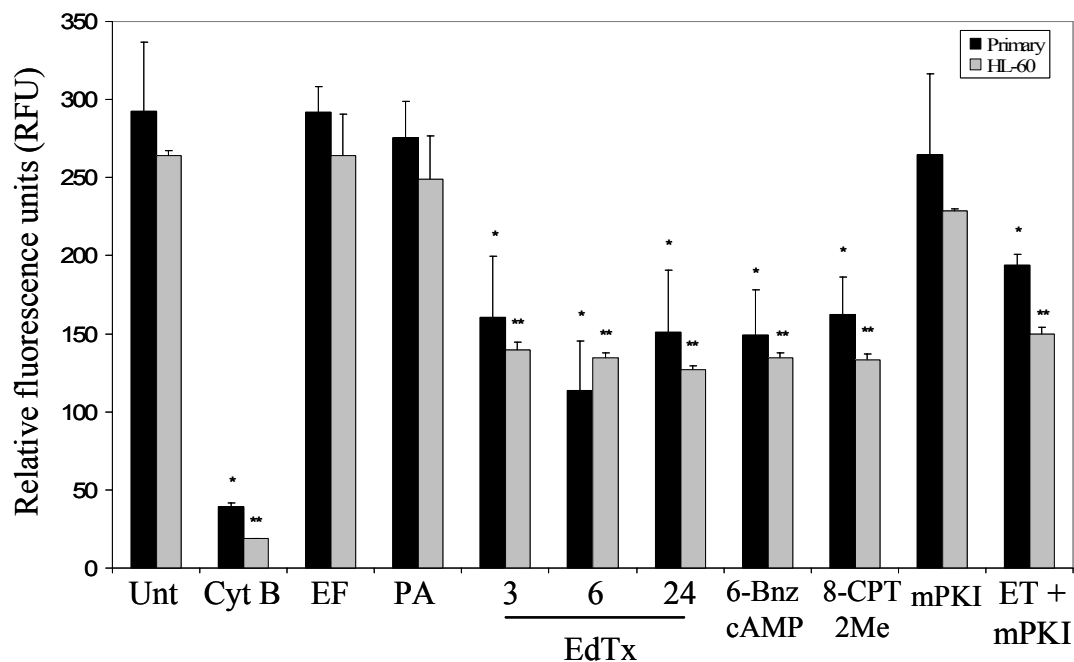


Figure 3.4. Phagocytosis of *E. coli* particles by EdTx-treated human MØs. Primary alveolar-like and HL-60 MØs (1×10^5 /well) were seeded in quadruplicate and exposed to EdTx (1.25 μ g/ml EF + 5 μ g/ml PA), EF (1.25 μ g/ml), PA (5 μ g/ml), cytochalasin B (10 μ g/ml), or the cAMP analogs alone (300 μ M 6-Bnz-cAMP, 25 μ M mPKI, 100 μ M 8-CPT-2Me). One group received a combination of EdTx plus the PKA inhibitor mPKI for 6 h (labeled ET + mPKI). An aliquot (100 μ l) of FITC-conjugated *E. coli* particles were then added for 1 h and the fluorescence was measured. *, $p < 0.05$ vs untreated primary cells; **, $p < 0.05$ vs untreated HL-60 cells (both using ANOVA and Dunnett's tests).

3.3.3 Treatment with EdTx reduces MØ cytoskeletal spreading and F-actin levels

To examine the possibility of EdTx-induced cytoskeletal changes, the effect on MØ cell spreading was next examined. MØs were exposed to EdTx for 2, 6, 12, and 24 h. FITC-labeled *E. coli* particles were then added for 1 h to stimulate cellular movement. Following staining with phalloidin, a fluorescence microscope was used to view and capture images of cells under each condition. In the untreated group exposed to the *E. coli* particles, the majority of MØs displayed a spread out morphology with numerous actin-rich membrane protrusions called filopodia (**Figure 3.5A**). EdTx treatment for 6 and 24 h caused reorganization of the actin cytoskeleton so that the cells appeared less spread out and displayed a reduced number of filopodia (**Figure 3.5C & D**). Cytochalasin B also altered the morphology of cells and reduced the number of filopodia, as shown in **Figure 3.5B**. Manually tracing the footprints of the cells with ImageJ software (see Methods) allowed calculation of the mean cellular area (**Figure 3.5E**), which was then converted to the spreading index. The spreading index of toxin pre-treated MØs dropped significantly at 6, 12, and 24 h compared to untreated cells (spreading index of 0.8, 0.6, and 0.6, respectively, compared to an untreated cell index of 1). The cell elongation index, defined as the length/width ratio, did not change among the groups (data not shown).

Similarly, the F-actin content of the MØs was significantly lowered in response to EdTx treatment, as determined with an immunofluorescence assay that labeled actin with phalloidin. Cells were treated with toxin for 2, 6, and 24 h before culturing with FITC-labeled *E. coli*-conjugated particles and labeling with phalloidin. Cells pre-treated for 6 and 24 h with EdTx contained approximately 1.6-fold less F-actin than untreated cells

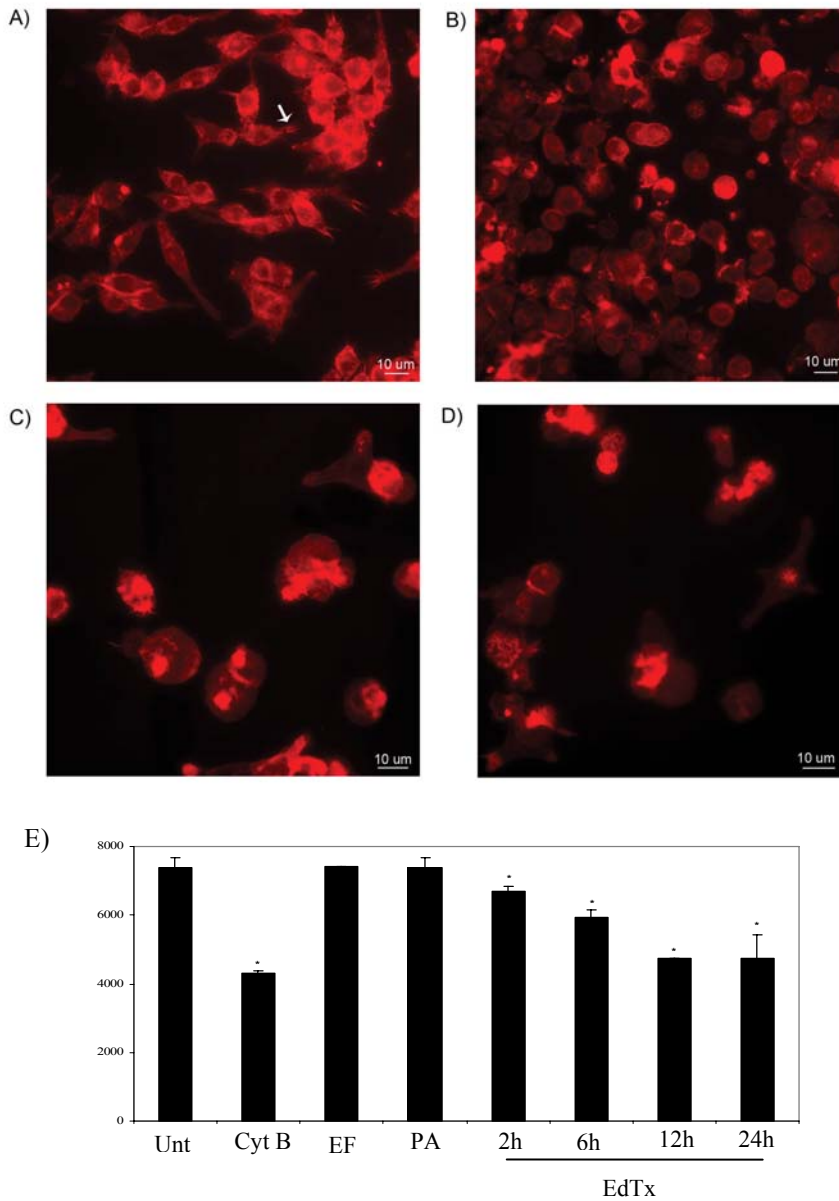


Figure 3.5. Assessment of morphological responses and spreading index of EdTx-treated MØs. HL-60 MØs on glass coverslips were treated with EdTx (1.25 µg/ml EF + 5 µg/ml PA), cytochalasin B, EF alone or PA alone (not shown here) for various times. FITC-labeled *E. coli* particles were added for 1 h, then the cells were permeabilized, fixed, and stained with phalloidin. **(A)** untreated cells (white arrow points to filopodia), **(B)** cytochalasin B treated for 2 h, **(C)** 6 h EdTx treatment, **(D)** 24 h EdTx treatment. Scale equals 10 µM. **(E)** Images containing at least 100 randomly selected cells in five fields of view were captured and ImageJ software was used to calculate the area of each cell. * indicates statistical significance of $p < 0.05$ versus untreated using ANOVA and Student-Newman-Keub method.

(Figure 3.6). This was almost as great a reduction in F-actin levels as that evoked by the positive control Cytochalasin B (1.7-fold drop). Treating groups with the 6-Bnz-cAMP and 8-CPT-2Me **(Figure 3.6)** revealed that activating both the PKA and Epac pathways mimicked the EdTx-induced effects. Inhibiting PKA with mPKI did not have an effect on F-actin levels compared to untreated cells. Similar to results in the phagocytosis experiment, wells that received a combination of PKA inhibitor and EdTx simultaneously in the same wells showed reduced F-actin content. Because the actin reduction was still seen, even when PKA was not allowed to become activated, it implied that another pathway in addition to PKA was involved. Further, we were interested to determine if inhibiting PKA, *via* mPKI, after EdTx treatment would rescue F-actin levels by preventing the EdTx-generated cAMP from modulating PKA to a further extent. Rescue wells were treated with EdTx for 5 h before cells were washed and replaced with fresh media containing mPKI for an additional 1 h. It must be noted that the majority of the EF and PA was likely internalized after the 5 h incubation (Abrami *et al.*, 2005), thus, the goal was not to remove the toxin from the cells, but only to prevent EdTx-generated cAMP from further manipulating PKA. As **Figure 3.6** shows, F-actin levels were not rescued because they remained significantly reduced in both cell types compared to untreated cells and those treated with mPKI alone for 1 h. This supports the hypothesis that PKA is not the only pathway responsible for the effects on the actin cytoskeleton initiated by EdTx.

Together, these experiments indicated that EdTx interfered with cytoskeletal rearrangements as detected by inhibition of the cell spreading response, reduced filopodia, and lowering of F-actin content. Results also provided further evidence to support a role for both pathways in downstream EdTx-generated cAMP signaling.

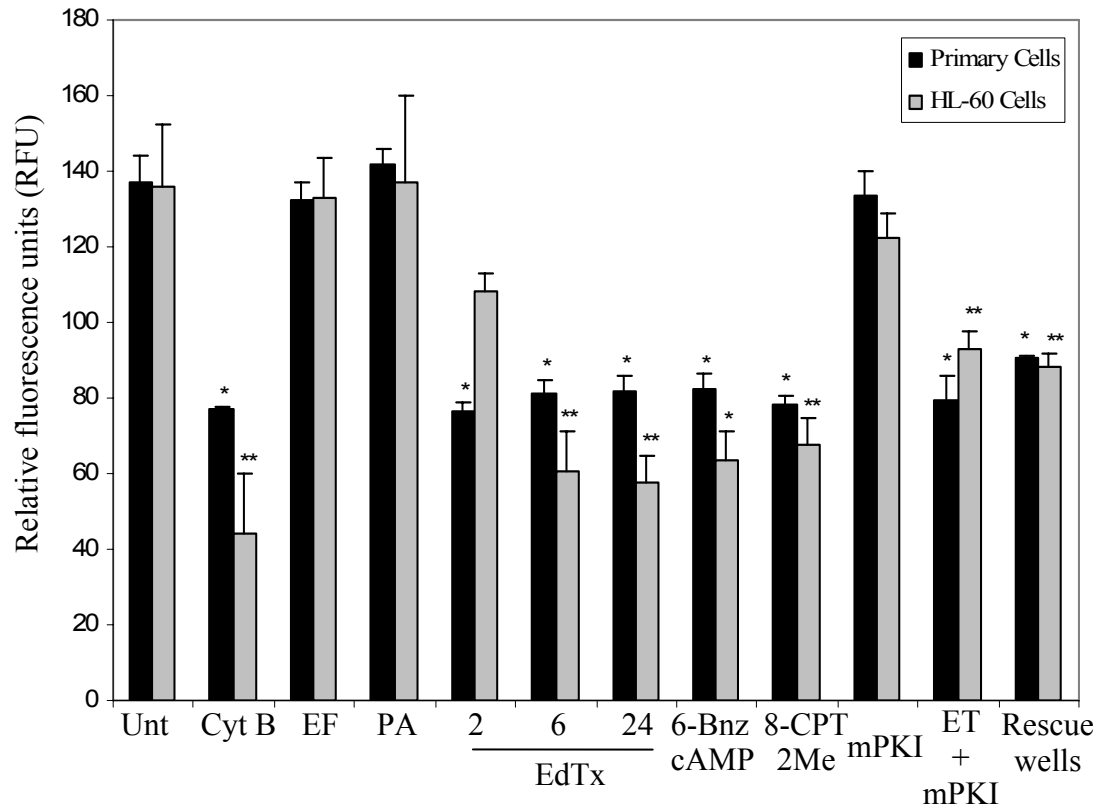


Figure 3.6. Effects of EdTx on the F-actin content of human MØs. Primary alveolar-like and HL-60 MØs (2.5×10^5 /well) in 96-well plates were pre-treated with EdTx (1.25 μ g/ml EF + 5 μ g/ml PA), EF (1.25 μ g/ml), PA (5 μ g/ml) or cytochalasin B (10 μ g/ml). Some groups were pretreated with 6-Bnz-cAMP (PKA activator; 300 μ M), mPKI (PKA inhibitor; 25 μ M) or 8-CPT-2Me (Epac activator; 100 μ M) alone for 1 h. Additionally, two treatment groups received a combination of EdTx with mPKI for 6 h (labeled ET + mPKI). Rescue wells indicates that cells were treated with EdTx for 5 h, then cells were washed and given fresh media containing mPKI for 1 h (labeled Rescue wells). FITC-labeled *E. coli*-conjugated particles were added for 1 h to provide phagocytic stimuli. Cells were then fixed, permeabilized, and actin labeled with Alexa Fluor-conjugated phalloidin. Fluorescence was measured with a plate reader. *, $p < 0.05$ vs untreated primary cells; **, $p < 0.05$ vs untreated HL-60 cells (both using ANOVA and Dunnett's tests).

3.3.4 Macrophage PKA/Epac-1 protein levels and activity are altered following EdTx treatment

Due to the targeting of the PKA and Epac pathways by EdTx-generated cAMP, the effect of EdTx on the production of these two molecules was next examined. Western blot analysis of PKA protein levels in toxin-treated MØ lysates revealed a time-dependent alteration of the regulatory Type II subunit of PKA (RII α). Compared to untreated MØs, PKA RII α levels initially increased after a 2 h treatment, but then dropped below normal levels after a 6-24 h toxin exposure (**Figure 3.7A**). Contrary to the depressed expression of PKA RII α observed at time points beyond 2 h, Epac-1 showed increased production at all tested time points. Protein levels were enhanced between 2.4-3.4 fold after 2-24 h of toxin treatment (**Figure 3.7B**). These data indicated that MØs were responding to the increased cAMP production induced by EdTx by altering production of the two signaling proteins that directly bind cAMP molecules.

Because PKA RII α levels were altered during the toxin treatment time course, the enzymatic activity of PKA as a whole was evaluated with a fluorescence-based kinase assay. Similar to the protein production results, the 1 and 2 h EdTx treatment significantly increased PKA activity compared to untreated cells (**Figure 3.8**). However, the 6 h pre-treatment resulted in activity very similar to that of untreated control cells, and PKA activity among the 24 h samples was significantly lower than samples of the untreated group.

To address the effect of EdTx on Epac-1 activity in HL-60 MØs, activity of Rap1, the small GTPase directly activated by Epac-1, was used as an indicator of Epac

activation. Detection of GTP-bound Rap1 after toxin treatment times of 2, 6, and 24 h were evaluated. As **Figure 3.9** shows, GTP-Rap1 levels were increased (approximately 2-fold) as compared to untreated cell lysate and levels remained elevated even 24 h post-toxin treatment.

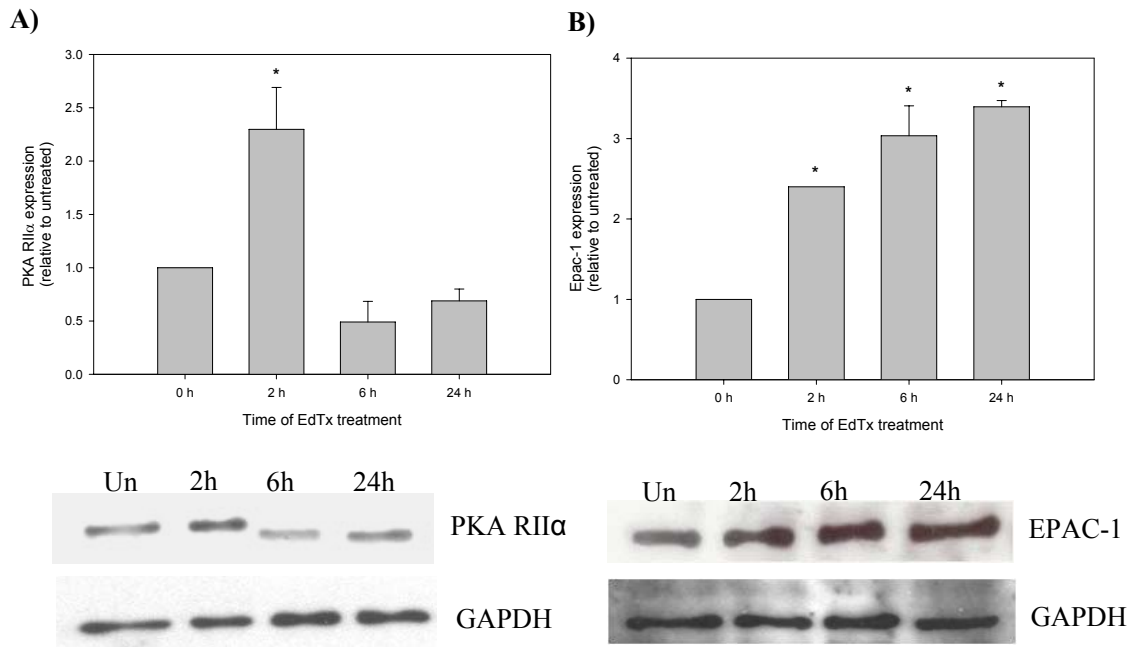


Figure 3.7 Western Blot analysis of PKA RIIα and Epac levels post-EdTx treatment. Following toxin treatment (1.25 $\mu\text{g/ml}$ EF + 5 $\mu\text{g/ml}$ PA), HL-60 MØs were lysed and samples were subjected to Western blot analysis with antibodies against PKA RIIα (panel **A**) and Epac-1 (panel **B**). Densitometry was performed for each band and data are expressed as fold-change difference compared to untreated control cells. Below each graph is an image of the Western Blot against PKA RIIα and Epac-1, along with the results of blotting against GAPDH to verify equal protein loading. * $p < 0.05$ versus 0 h, ANOVA and Dunn's test.

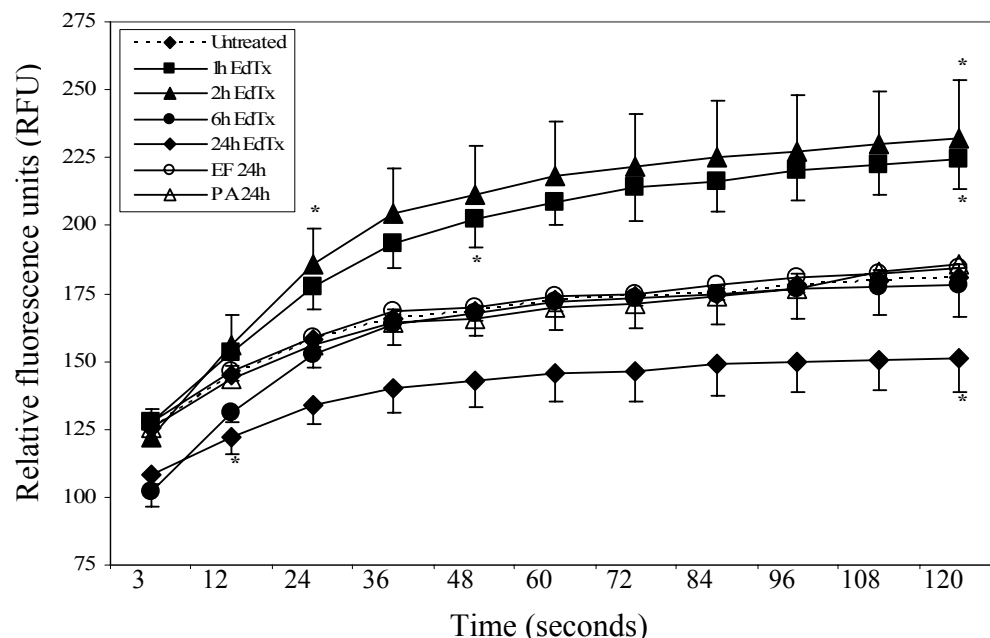


Figure 3.8 PKA activity assay of human MØs following exposure to EdTx. Following EdTx treatment, HL-60 MØs were lysed. Samples were then analyzed for PKA activity using a fluorescence-based assay every 2 min for 20 min. Controls of EF and PA alone did not influence PKA activity. * marks the beginning and ending of significance for each curve versus unt curve ($p < 0.05$ as determined by ANOVA and Dunnett's tests).

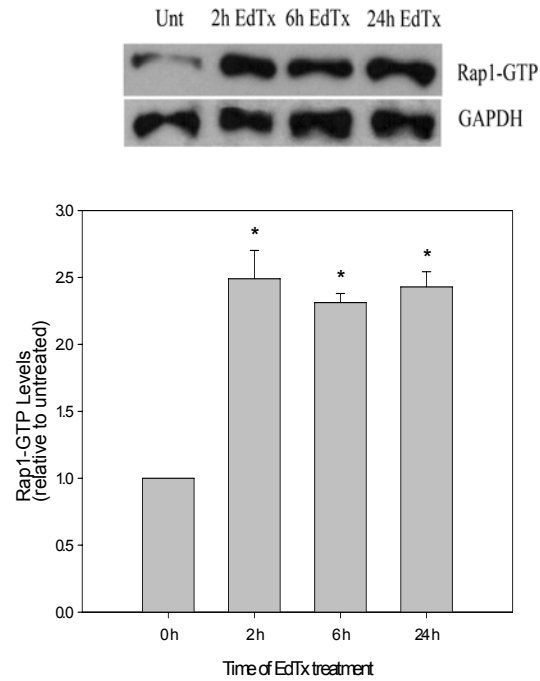


Figure 3.9 Pull-down assay to evaluate Epac activation of Rap1 in EdTx-treated MØs. Following EdTx treatment, HL-60 MØs were lysed and incubated with the GST-RDB of RalGDS immobilized to glutathione beads to specifically pull down the GTP-bound Rap1. Then samples were subjected to Western blot analysis using antibodies against Rap1 or GAPDH (loading control). The graph shows densitometry that was performed and data are expressed as fold-change difference compared to untreated control cells. * $p < 0.05$ versus 0 h, ANOVA and Dunn's test.

3.4 DISCUSSION

EdTx is one of several powerful weapons utilized by *B. anthracis* to thwart host immune defenses and establish a successful infection. It belongs to the same class of adenylate cyclases as Exo Y of *Pseudomonas aeruginosa*, adenylate cyclase of *Yersinia pestis*, and adenylate cyclase toxin of *Bordetella pertussis* (reviewed by Ahuja *et al.*, 2004). The intrinsic adenylate cyclase activity of EdTx upsets the delicate physiological equilibrium inside a wide variety of cells. For years it was speculated that this would lead to a suppressed immune response, but only recently has this prospect started to be explored. It is now known that EdTx disrupts cytokine networks in monocytes (Hoover *et al.*, 1994), inhibits platelet aggregation (Alam *et al.*, 2005), reduces MØ and T-cell migration (Rossi *et al.*, 2007), and disrupts T-cell functions (Comer *et al.*, 2005; Paccani *et al.*, 2005) just to list a few examples.

The MØ actin cytoskeleton is a highly dynamic structure that rapidly adapts to the cells' demands in order to successfully utilize two of its powerful weapons: motility and phagocytosis. Each of these processes is highly complex, but continuous feedback from the extracellular milieu and surrounding cells allows the MØ to be a quick responder during a microbial invasion. During *B. anthracis* infection, human monocytes and murine MØs are subject to the adenylate cyclase activity of EdTx (Hoover *et al.*, 1994; Kumar *et al.*, 2002). As predicted, EdTx generated a strong surge of cAMP in the human HL-60 and primary MØs in a dose- and time-dependent manner. For instance, after a 6 h exposure of HL-60 cells to EdTx, combined intracellular and extracellular cAMP levels were 38-fold greater than untreated HL-60 MØs. Levels of cAMP secreted by EdTx-

treated HL-60 MØs were much higher than that produced by EdTx-treated primary MØs. This may be due to the differing methods of MØ differentiation used to prepare these two cell types (PMA treatment versus GM-CSF). Also, the amount of cAMP evoked by EdTx appears to be highly dependent upon the cell type. For example, human neutrophils and RAW 264.7 cells are not particularly sensitive to EdTx, while Chinese hamster ovary (CHO) cells and human lymphocytes are extremely sensitive (Kumar *et al.*, 2002). It has been demonstrated that injecting mice intravenously with EdTx resulted in organ lesions and murine death (Firoved *et al.*, 2005). Although we cannot directly compare the toxin doses administered *in vivo* (100 µg EF + 100 µg PA) with the concentration used in these *in vitro* experiments (1.25 µg/ml EF + 5 µg/ml PA), it is important to note that neither the primary or HL-60 MØs were susceptible to killing following exposure to EdTx. It appears that cells vary in their susceptibility to EdTx-induced lethality, as CHO cells are not killed by the toxin, while RAW 264.7 cells are susceptible to the effect of the toxin (Voth *et al.*, 2005).

The ability of EdTx, as well as LeTx, to inhibit migration of human MØs by down-regulating chemokine receptor signaling was recently discovered (Rossi *et al.*, 2007). However, the effect of EdTx on MØ phagocytosis remained unknown. This study was the first to report the ability of EdTx to reduce phagocytosis of both virulent Ames spores and *E. coli* particles by human primary cells and a human cell line. Uptake inhibition was observed after all toxin pre-treatment times, ranging from 3 to 24 h. The reduction in phagocytosis was not an artifact due to depletion of the MØ population, as MØ survival was not affected by EdTx exposure. Although MØs are considered a favorable site for spore germination and as a mechanism of transportation to the lymph nodes, it has been shown that MØs kill the majority of intracellular spores and vegetative

cells (Hu *et al.*, 2006; Kang *et al.*, 2005; Welkos *et al.*, 2002). These data also correlated with our observation that human monoclonal antibody to PA blocked dissemination of *B. anthracis* Ames to the bloodstream from the lungs (Peterson *et al.*, 2007). The ability of EdTx to reduce the likelihood of spore/bacilli phagocytosis by MØs is likely important during later stages of the infection, particularly when large volumes of EdTx are being secreted by rapidly multiplying, extracellular vegetative cells. At this time, EdTx-induced suppression of MØ phagocytosis would be of tremendous benefit to the survival of the bacteria and any viable dormant spores, and would likely increase the host's susceptibility to fulminant anthrax disease. Similar to our findings, a previous publication showed EdTx-treated human neutrophils exhibited impaired uptake of Sterne spores (O'Brien *et al.*, 1985). Thus, the ability of EdTx to lower phagocytic uptake of two types of the host's professional phagocytes, MØs and neutrophils, may explain how quickly the organism begins to multiply systemically and infiltrate numerous host tissues.

To explain the lowered phagocytic activity, we hypothesized that impairment of the actin cytoskeleton may be a downstream effect elicited by such high production of EdTx-generated cAMP. Indeed, our studies demonstrated that EdTx treatment brought about morphological changes in the actin cytoskeleton of HL-60 MØs. Cells contained less filopodia than untreated cells, even in the presence of FITC-conjugated *E. coli* particles, and although the cytoskeleton appeared intact and complete, EdTx exposure reduced the cell spreading index of MØs in a time-dependent manner. Formation of pseudopodia and filopodia during phagocytosis requires actin nucleation, which is formation of new actin filaments, along with an increase in the length of existing filaments (May *et al.*, 2001). Accompanied with the reduced filopodia response observed

in this study, the F-actin content of both MØ types was also significantly impaired as early as 6 h post-toxin treatment and was sustained even at 24 h.

The observed defects in actin rearrangement and F-actin content are supported and possibly explained by the striking down-regulation of multiple genes related to the cytoskeleton that was published previously from our laboratory (Comer *et al.*, 2006). Microarray analysis revealed, for instance, that the gene encoding PDZ and LIM domain protein 2 (PDLIM2) was down-regulated 6.8-fold in murine MØs after 6 h of EdTx treatment. This adaptor protein located on the actin cytoskeleton promotes cell attachment by interacting with extracellular matrix proteins (Loughran *et al.*, 2005). Formin-binding protein-1 like (FNBP1L) is a microtubule-associated protein that is predicted to function as scaffolding proteins for microtubules, Rho family GTPases, and WASP family proteins (Katoh *et al.*, 2004). FNBP1L can also promote actin nucleation (Ho *et al.*, 2004), and the gene encoding this protein was down-regulated 8.9-fold in EdTx-treated RAW cells. Additionally, switch associated protein 70 (SWAP-70) interacts with Rac and mediates signaling leading to membrane ruffling (Shinohara *et al.*, 2002). This protein can also bind F-actin directly, and mutant cells exhibited abnormal actin rearrangement and migration deficiencies (Ihara *et al.*, 2006). The gene for SWAP-70 was down-regulated 3.6-fold post-toxin treatment (Comer *et al.*, 2006).

Due to their ability to directly bind cAMP and participate in cAMP signaling cascades, we determined whether the PKA pathway alone, the Epac pathway alone, or a combination of both pathways was responsible for translating the high accumulation of intracellular cAMP to the altered MØ phenotypes and inhibited functions described in this work. MØs treated with EdTx for 2 h exhibited increased expression of PKA RII α , corresponding to the beginning of the increase in intracellular cAMP caused by the

adenylate cyclase activity of EdTx. This early time point of toxin treatment also led to significantly greater PKA activity than samples collected from untreated MØs. PKA activation at 2 h has previously been observed in EdTx-treated rabbit platelets (Alam *et al.*, 2005). After 6-24 h of EdTx treatment, however, PKA RII α expression levels were down-regulated. These data corresponded to time points when cAMP levels were significantly higher in toxin-treated cells versus untreated cells. Similar to the protein expression trends, it was determined that at 6 h, EdTx-treated MØs showed a PKA activity curve very similar to that of untreated cells and the 24 h toxin treatment produced an activity curve significantly lower than that of untreated MØs. Down-regulation of the regulatory subunit of PKA, which contains cAMP-binding sites, at the later time points, as well as impaired PKA activity may represent the target cell's strategy to compensate for the flood of cAMP produced by EdTx and attempt to return the cell to a basal state.

Epac-1 protein levels, on the other hand, remained elevated throughout the time course of toxin exposure. The activity pattern of Epac, assessed by examining levels of activated Rap1, also resembled the expression data, as the amount of GTP-bound Rap1 became elevated 2 h post-toxin exposure and remained high for as long as 24 h. Because the effects of EdTx on MØ function are stronger at 6 h and beyond, when PKA expression/activity are down-regulated and Epac expression/activity are up-regulated, perhaps Epac is principally responsible for the effects of EdTx at the later time points. It was next considered that the disruption in the balance of PKA/Epac protein production and activity initiated by EdTx was ultimately responsible for the reduced phagocytosis, F-actin content, and cell spreading observed in toxin-treated cells.

Phosphodiesterase-resistant cAMP analogs that are highly specific in their activation of either PKA or Epac have been developed in recent years (Christensen *et al.*,

2003). We incorporated the best characterized of these compounds (6-Bnz-cAMP, mPKI and 8-CPT-2Me) to determine which pathway the EdTx-generated cAMP was targeted in order to cause the observed inhibition of phagocytosis and cell spreading.

Pre-treatment of cells with 6-Bnz-cAMP and 8-CPT-2Me, activators of PKA and Epac, respectively, during phagocytosis of FITC-conjugated *E. coli* particles resulted in inhibition of uptake by both types of MØs. The inhibition mimicked conditions of toxin-treated cells, suggesting that EdTx-generated cAMP likely targets both the PKA and Epac-1 pathways in order to cause such a decline in phagocytosis. These results are in agreement with a previous report showing that activation of the PKA and Epac pathways is capable of reducing phagocytic activity of human monocyte-derived MØs (Bryn *et al.*, 2006) and rat alveolar MØs (Aronoff *et al.*, 2005).

These compounds were also included in the F-actin content experiments. Similar to the phagocytosis experiments, pre-treatment with 6-Bnz-cAMP and mPKI revealed that activation of PKA was likely involved in EdTx-related events. In addition, two other treatment groups suggested that another pathway was participating in the cAMP signaling events, and pre-treatment with 8-CPT-2Me implicated the Epac-1 pathway as a likely candidate. It is important to note that although PKA and Epac seem to play major roles with regard to EdTx signaling in MØs, participation by other signaling proteins cannot be excluded.

Though once believed to play only a moderate role during anthrax infection, mounting evidence of sporicidal and bactericidal behavior exhibited by MØs is shifting the view (Chakrabarty *et al.*, 2006; Kang *et al.*, 2005; Welkos *et al.*, 2002). Mice depleted of MØs before challenge with Ames spores were more susceptible to infection and present with higher bacterial loads compared to saline-treated mice (Cote *et al.*, 2006).

Once only speculated, it has become clear, through this work and others, that the high quantity of cAMP produced by the intrinsic adenylate cyclase nature of EdTx does indeed allow it to disrupt key functions of MØs, thus crippling an important arm of the host's innate immune system. In addition to EdTx impairing MØ chemotaxis (Rossi *et al.*, 2007) and disturbing monocyte cytokine signaling (Hoover *et al.*, 1994), decreasing the phagocytic activity and cell spreading response of human MØs through targeting the PKA and Epac pathways provides further evidence of the powerful activity of EdTx.

CHAPTER 4: Transcriptional profiling of murine lung genes in response to infection with *Bacillus anthracis*

4.1 INTRODUCTION

Due to inhalation of particles containing bacteria and LPS from the environment and commensal flora in the nasopharynx, the lung is continuously exposed to potentially inflammatory components. Thus, the lung has evolved ingenious methods to fight off foreign invaders, while simultaneously avoiding a relentless inflammatory response. Road-blocks such as mucus, cilia, and resident alveolar MØs and DCs aid the lung in maintaining a state of homeostasis.

The lung is the primary route of infection in cases of inhalational anthrax. This form of anthrax infection progresses rapidly and the mortality rate often approaches 100% (Inglesby *et al.*, 2002). When *B. anthracis* spores of the 1-5 µM size are inhaled deep into the alveolar space, a series of events are triggered. MØs and DCs are not the only means of spore dissemination because spores are also phagocytosed by and survive within human lung epithelial cells (Russell *et al.*, 2007). Both alveolar epithelial cells (Radyuk *et al.*, 2003) and alveolar MØs (Chakrabarty *et al.*, 2006) secrete inflammatory cytokines when exposed to spores, indicating that the lung recognizes *B. anthracis* as a foreign invader.

Following the intentional release of *B. anthracis* in the United States in 2001, significant anthrax-related research ensued and substantial progress was made regarding

the understanding of how this organism elicits disease. There is no data to-date, however, regarding the overall transcriptional responses of genes in different organ systems of animals after *B. anthracis* infection. As a result, it is still unclear how animals and humans succumb to infection without exhibiting serious symptoms (Mock *et al.*, 2003). Furthermore, few studies have utilized the Ames strain, a virulent form similar to what was used in the 2001 attacks in the U.S., for studying *B. anthracis* and host interactions. Finally, the precise cause of lethality incurred by anthrax has yet to be described. To test the hypothesis that *B. anthracis* infection results in severe modulation of host genes in the lung, the transcriptional profiles of the lungs of mice exposed to anthrax via respiratory challenge were examined.

4.2 METHODS

4.2.1 Mouse nasal inoculation

Specific pathogen-free (SPF) female Swiss Webster 7-8 week old mice were purchased from Taconic Farms (Georgetown, NY) and housed in the Association for Assessment and Accreditation of Laboratory Animal Care-accredited Animal Resources Center at UTMB. Mice were anesthetized with an intraperitoneal (i.p.) injection of ketamine-HCl (90 mg/kg) and xylazine-HCl (10 mg/kg). After anesthesia, the mice were suspended by their front incisors to facilitate nasal inoculation. Mice were given 5 LD₅₀ (approximately 5.6×10^4 colony forming units [cfu]) of *B. anthracis* Ames strain spores in 40 μ l of PBS, after which the mice remained suspended for an additional 1-2 min to

ensure a complete lung inoculation. Subsequently, the mice were returned to their cages for the appropriate incubation time.

*4.2.2 Determining *B. anthracis* levels in mouse organs*

At 8, 24, and 48 h post-infection, infected mice were anesthetized, followed by euthanasia by CO₂ narcosis. Cervical dislocation was subsequently performed to ensure death. Lungs were aseptically removed from 3 mice and placed in 1 ml of PBS in 50 ml Kendall tissue homogenizers (Kendall, Mansfield, MA). Following homogenization of the tissues, serial dilutions of the samples were made in PBS and 100 µl of each dilution was plated on 5% sheep blood agar plates (BD Biosciences, Franklin Lakes, NJ); which were incubated overnight at 37°C. In total, 3 independent experiments representing 3 biological replicates each were performed, and data were statistically analyzed using one-way ANOVA.

4.2.3 Tissue fixation and slide preparation

At 48 h post-infection, aseptic collection of lungs was performed as described above. The tissues were fixed in 4% paraformaldehyde for 48 h and tested for viable bacteria by plating on blood agar plates. Tissue sections were routinely processed, embedded in paraffin, mounted on slides, and stained with hematoxylin and eosin (H&E), as well as the gram stain at the University of Texas, M.D. Anderson Cancer Center

(Bastrop, Texas). Bacterial load and tissue architecture was evaluated and compared to that of control mice that were given only PBS.

4.2.4 Cytokine profiling

Infected mice were sacrificed at 8, 24, 36, or 48 h post infection. A 22-gauge needle was used to perform a cardiac puncture and approximately 1 ml of blood was removed and placed in Microtainer serum separator tubes (BD Biosciences) at 4°C overnight. Blood was centrifuged at 1,000 x g for 10 min and the serum transferred to a new tube, filtered with a 0.22 µm syringe filter, plated overnight to ensure sterility, and stored at -20°C until assayed. The sera of three mice from the control, 8, 24, 36, and 48 h experimental groups were analyzed using a 23-plex Bioplex kit (Bio-RAD, Hercules, CA). Three replicates were performed and statistically parsed by one-way ANOVA. Whole blood from the aforementioned groups was used in conjunction with the ProChem V analyzer and a panel of biochemistry cuvettes (Drew Scientific Inc., Dallas, TX) to assess biochemical profiles. Analysis was performed as recommended by the manufacturer to measure the serum levels of amylase, alkaline phosphatase (AKP), alanine aminotransferase (ALT), aspartate aminotransferase (AST), bicarbonate, calcium, and glucose.

4.2.5 Affymetrix GeneChip analysis

Lungs were aseptically removed from 3 anesthetized mice at 8 and 48 h post-infection and placed in 50 ml tissue homogenizers with 1 ml RNALater (Ambion, Austin Inc., TX) on ice and immediately transferred to -80°C for storage. The RNAqueous kit (Ambion) was used to purify RNA from the tissue homogenates. The RNA was allowed to precipitate overnight and then resuspended in a volume of 20 µl diethylpyrocarbonate-treated water. Pellets were stored at -80°C. Subsequently, RNA samples were tested for sterility by streaking on 5% sheep blood agar plates. An Agilent chip was then used to analyze the purity of RNA samples, and the corresponding cDNA was applied to Affymetrix murine GeneChips (430 Plus 2; Affymetrix, Santa Clara, CA) for transcriptional profiling of genes in different organs.

Briefly, total RNA (25 µg) was processed and hybridized to GeneChip arrays in the Molecular Genomics Core at UTMB. The cDNA synthesis, *in vitro* transcription, and labeling and fragmentation to produce the oligonucleotide probes were performed as instructed by the GeneChip manufacturer (Affymetrix). The probes were first hybridized to a test array (Affymetrix) and then to the 430 Plus 2 GeneChip, both performed using the GeneChip Hybridization Oven 640. The chips were washed in a GeneChip Fluidics Station 400 (Affymetrix) and the results visualized with a Gene Array scanner using the Affymetrix software. These experiments were performed in triplicate, and the data were analyzed separately using three different softwares: GeneSifter (VizX Labs, Seattle, WA), Significance Analysis of Microarrays (SAM; Stanford, CA) and Spotfire DecisionSite 9.0 (Spotfire Inc., Somerville MA). Changes in gene expression were considered significantly altered if the *p* value was less than 0.05, the fold-change value was at least 1.5, and alteration in gene expression occurred in all 3 experiments.

Additionally, genes that were altered between any two uninfected control samples were disregarded, as these alterations most likely represented normal variations among mice.

4.2.6 Real-time reverse transcriptase-polymerase chain reaction (RT-PCR)

Real-time quantitative RT-PCR was performed in the Prism 7000 Sequence Detection System (Applied Biosystems, Foster City, CA) using SYBR Green PCR Master Mix (Applied Biosystems). RNA samples were first quantified using a Nanodrop Spectrophotometer (Nanodrop Technologies Inc., Wilmington, DE) and qualified by analysis on an RNA Nano chip using the Agilent 2100 Bioanalyzer (Agilent Technologies Inc, Santa Clara, CA). Synthesis of cDNA was performed using 1 µg of RNA in a 20-µL-reaction volume containing reagents from the Taqman Reverse Transcription Reagents kit (Applied Biosystems). Q-PCR amplifications were performed in triplicate, using 2 µl of cDNA in a total volume of 25 µl containing SYBR Green and 900 nM primers. Custom-designed primers used for real-time PCR amplification are listed in Table 4.1.

A typical protocol included reverse transcription at 50°C for 2 min and a denaturation step at 95°C for 10 min followed by 40 cycles with 95°C denaturation for 15 s and 60°C annealing/extension step for 1 min. To confirm amplification specificity, the PCR products were subjected to a melting curve analysis. Negative controls containing water instead of RNA were concomitantly assayed to confirm that the samples were not cross-contaminated. Targets were normalized to reactions performed using 18S rRNA

amplimers, and fold change was determined using the comparative threshold method (Livak *et al.*, 2001).

Gene	Forward Primer	Reverse Primer
Angpt14	CCCCCAATGGCCTTTCC	AAACCACCAGCCACCAGAGA
Clu	ATGAAGTTCTATGCACGTGTCTGC	GTCGCCGTTTCATCCAGAAGT
Retnla	TCCAGCTAACTATCCCTCCACTGTA	AGTCATCCCAGCAGGGCAG

Table 4.1 Custom-designed primers used for RT-PCR confirmation of gene alterations induced by anthrax infection.

4.3 RESULTS

4.3.1 Monitoring *B. anthracis* levels in the lungs during infection

First, the quantity of *B. anthracis* organisms within each mouse lung at various times during infection was evaluated. The animals were infected by the intranasal route with a 5 LD₅₀ dose of Ames spores (5.6×10^4 cfu), and the lungs were extracted 8, 24, and 48 h later. The organs of three animals were pooled at each time point, homogenized, serial diluted, and then inoculated onto blood agar plates. **Figure 4.1** shows the number of anthrax organisms (cfu) in the lung resulting from 3 separate experiments. At 8 h post-infection, the lungs contained approximately 1.8×10^4 cfu *B. anthracis* organisms. By 24 h, the bacterial load decreased to 1×10^2 cfu. Forty-eight hours into infection, however,

the number of organisms dramatically increased. After confirming the presence of *B. anthracis* in the lungs, we evaluated the pathological consequences of infection in these tissues.

4.3.2 Histopathological analysis of B. anthracis-infected lungs

The lungs were removed from both uninfected mice and those infected with Ames spores for 48 h, and processed for H&E and Gram staining. **Figure 4.2** illustrates the presence of *B. anthracis* in the lungs of infected animals. Bacilli were present within alveoli, alveolar walls, and small and large vascular lumens. Focally, small areas of perivascular/peribronchiolar edema were observed with numerous bacilli. Hemorrhage was also detected in some alveoli.

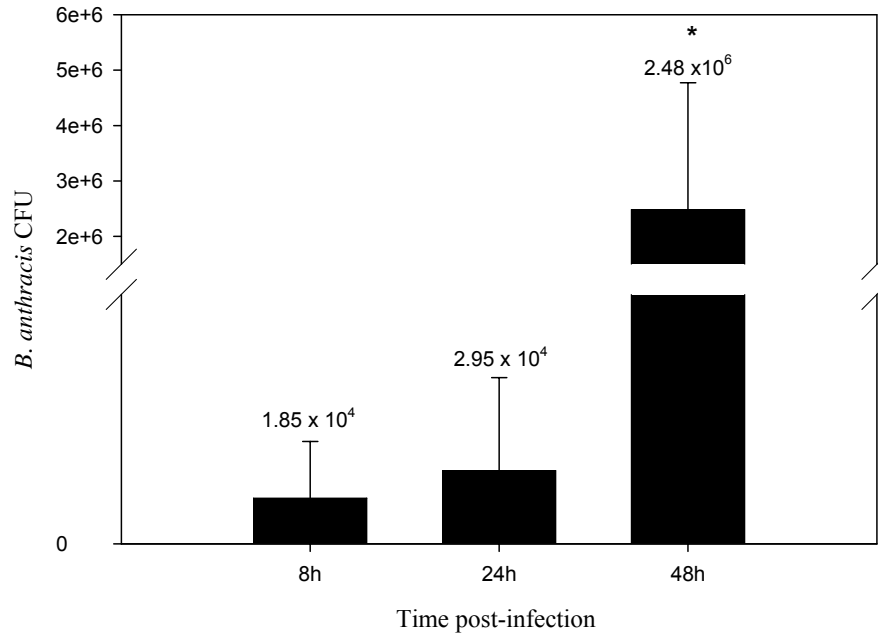


Figure 4.1. *B. anthracis* infection in murine lungs at 8, 24, and 48 h post-infection. Mice (n= 3/time point) were intranasally infected with 5 LD₅₀ Ames spores. Lungs were aseptically removed and homogenized in PBS. Serial dilutions of the samples were performed and plated on 5% sheep blood agar plates. Colonies were counted and data is expressed as total recovered *B. anthracis* organisms. In total, 3 independent experiments representing 3 biological replicates each were performed, and data were statistically analyzed using one-way ANOVA (p<0.05).

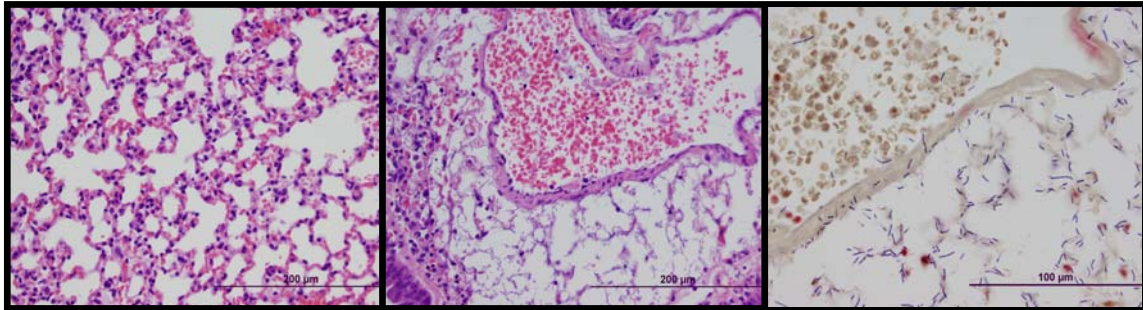


Figure 4.2 Histopathological analysis of anthrax-infected lungs. At 48 h post-infection, aseptic collection of lungs was performed and tissues were fixed in 4% paraformaldehyde for 48 h. Tissue sections were routinely processed, embedded in paraffin, mounted on slides, and stained with hematoxylin and eosin (H&E), as well as the gram stain. Bacterial load and tissue architecture was evaluated and compared to that of control mice that were given only PBS. Magnification 20x for left and middle panel, and 40x for right panel.

4.3.3 *B. anthracis* infection elicits a biphasic pattern of cytokine secretion in the serum of mice

To further characterize the host response to *B. anthracis* infection, the systemic cytokine response of infected mice was evaluated. Blood samples were collected at 0, 8, 24, 36, and 48 h post-infection, and the cytokine levels in sera were measured using a multiplex assay system. Pooled sera from three animals at each time point were assayed in duplicate.

Figure 4.3 shows that a biphasic response pattern was observed for IL-4, IL-6, G-CSF, KC, RANTES, and MCP-1 in sera of the *B. anthracis*-infected mice. In these terminally ill animals, anthrax infection induced an initial spike (8 h), followed by a decline and then a second spike at 48 h post-infection. IL-12 (p40) levels were the highest among the bacteria-induced cytokines at all time points except 36 h, with levels reaching statistical significance ranging from 175-275 pg/ml. TNF- α remained only slightly elevated except for a large increase to 450 pg/ml at 36 h, making it the cytokine with the greatest concentration at this point. IFN- γ showed relatively similar levels compared to uninfected controls throughout infection. G-CSF showed a significant increase at 8 h compared to basal levels, while KC significantly increased at 48 h. No appreciable induction was noticed for IL-2, IL-3, and IL-1 β (data not shown).

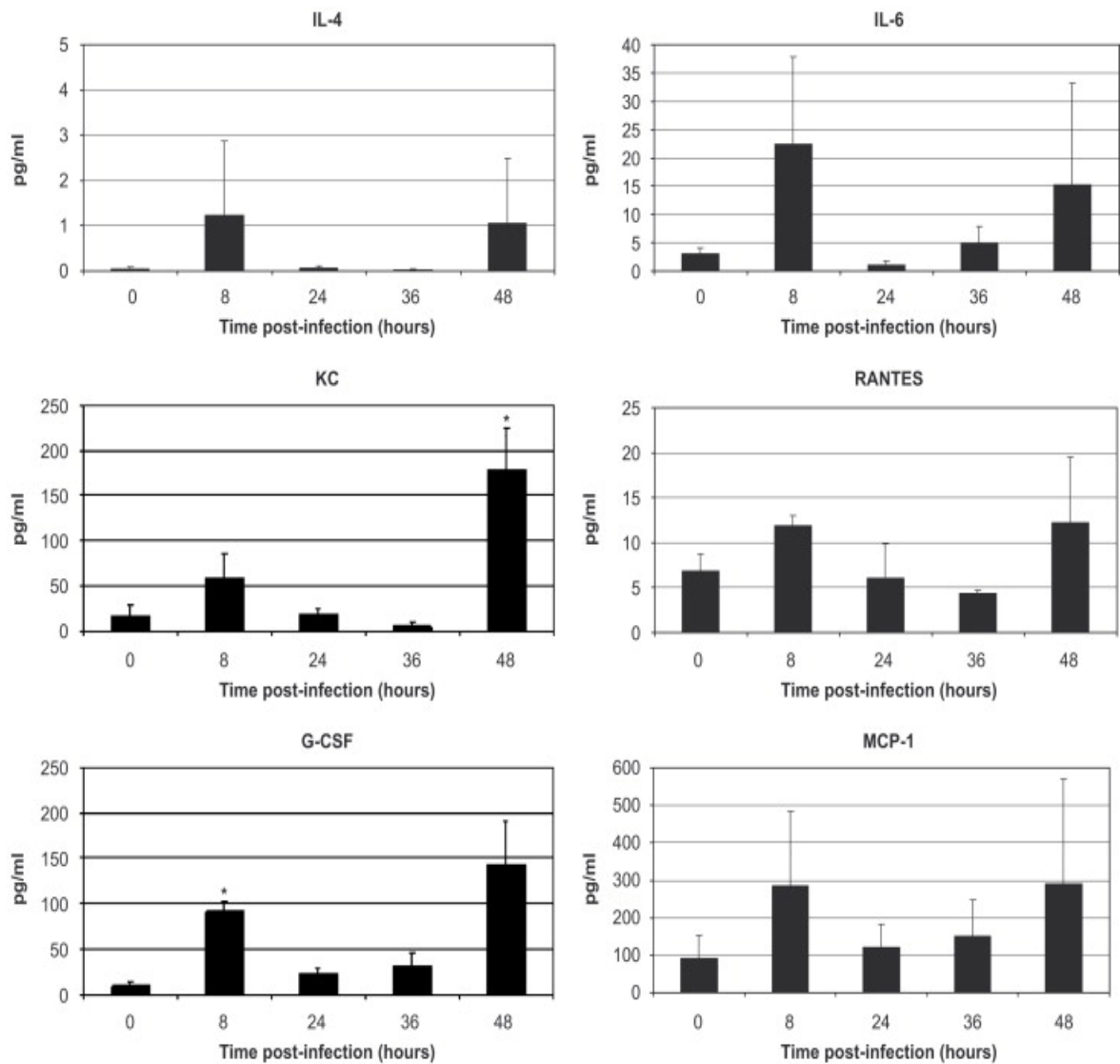


Figure 4.3 Cytokine array analysis of murine serum post-infection with Ames spores. Infected mice (n= 3/time point) were sacrificed at 8, 24, 36, or 48 h post infection and approximately 1 ml of blood was removed via cardiac puncture. Sera was extracted from the blood samples and cytokine levels analyzed using a 23-plex Bioplex kit. Three replicates were performed and statistically parsed by one-way ANOVA ($p < 0.05$).

4.3.4 Inhalational anthrax alters the expression of numerous murine genes in the lung at both early and late time points

After demonstrating anthrax bacilli infiltration and examining pathological consequences of infection in the lungs, the host transcriptional response within this organ was investigated. RNA was isolated from the lungs at 8 or 48 h following intranasal inoculation and subjected to Affymetrix GeneChip analysis.

Alterations in gene expression profiles found to be significant were compiled into lists by function and are summarized in **Table 4.2**. Specific examples of altered gene expression at 8 and 48 h are shown in **Tables 4.3, 4.4, and 4.5**.

Although the list of altered genes for the lung at 8 h post-infection was not large, several genes related to inflammation were up-regulated (i.e., clusterin and oxidized low density lipoprotein; **Table 4.3**). Examples of genes that were down-regulated included MHC class I receptor (H2-K1), surfactant associated protein C (Sftpc), and several genes encoding proteins related to cell proliferation. By 48 h, the lung displayed more dramatic signs of response to infection, including up-regulation of genes involved in hypoxia or inflammation (**Table 4.4**). Down-regulated genes included those involved in cell growth, differentiation, and various other cellular processes (**Table 4.5**).

*4.3.5 Confirmation of *B. anthracis*-induced gene expression alterations in mice*

In order to confirm the GeneChip findings, real-time RT-PCR was performed on three genes that were chosen based on their involvement in inflammation, signaling, or

physiological processes related to the lung (**Table 4.6**). RT-PCR experiments were performed in parallel, and fold-change values were determined after normalization of each gene to glyceraldehyde-3-phosphate dehydrogenase (GAPDH). The expression of genes encoding clusterin (Clu), angiopoietin-like 4 (Angptl4), and Retnl was increased in the lung 2.1-, 3.7-, and 3.3-fold, respectively, as determined by GeneChip analysis. Similarly, RT-PCR of lung tissue samples revealed that these genes were up-regulated 3.98-, 2.81-, and 6.35-fold (**Table 4.6**).

Category	Lung 8 h		Lung 48 h	
	Up	Down	Up	Down
Adhesion and Migration	–	–	–	1
Cytoskeleton Reorganization	–	–	–	2
Growth, Differentiation, and Development	–	2	–	4
Immune and Stress Response	2	2	8	1
Metabolism	1	–	2	–
Protein and RNA Processing	–	–	4	–
Signal Transduction	–	–	2	–
Transcriptional Regulation	–	2	–	2
Transport	1	–	–	2

Table 4.2 Functional categories of genes up- or down-regulated in murine lungs post-intranasal infection with Ames spores. This table was adapted with permission from Moen, S., Yeager, L., Lawrence, W., *et al.* (2008). *Microb Path* 44: 293-310.

Table 4.3 Significant genes up- or down-regulated in murine lungs 8 h post infection with Ames spores.

GenBank ID	Gene Name	Function	FC
Up-regulated in Response to <i>B. anthracis</i> Infection			
AV075715	Clusterin (Clu)	Stress response	2.1
NM_138648	Oxidized low density lipoprotein (lectin-like) receptor 1 (Olr1)	Inflammation; cell adhesion	1.9
Down-regulated in Response to <i>B. anthracis</i> Infection			
U96752	Major histocompatibility complex Q1b (H2-K1)	Antigen presentation	-2.5
BB428671	Platelet-derived growth factor, D polypeptide (Pdgfd)	Regulation of progression through cell cycle; proliferation	-2.1
AV169310	Surfactant associated protein C (Sftpc)	Regulation of liquid surface tension; regulatory gas exchange	-2.0

Note: FC indicates fold-change. Negative sign (-) before fold-change value indicates down-regulation. Genes shown more than once were represented by more than one probe set on the array, and each was determined separately to be significantly altered in response to *Bacillus anthracis* treatment. This table was adapted with permission from Moen, S., Yeager, L., Lawrence, W., *et al.* (2008). *Microb Path* 44: 293-310.

Table 4.4 Significant genes up-regulated in murine lungs 48 h post-infection with Ames spores, grouped by function.

GenBank ID	Gene Name	Function	FC
<i>Inflammation and stress response</i>			
NM_020581	Angiopoietin-like 4 (Angptl4)	Response to hypoxia or starvation; negative regulation of apoptosis; positive regulation of angiogenesis	3.7
NM_009841	CD14 antigen (Cd14)	Inflammatory response; Immune response to LPS	3.5
AA796766	Metallothionein 2 (Mt2)	Nitric oxide mediated signal transduction	6.0
NM_011082	Polymeric immunoglobulin receptor (Pigr)	Secretion of IgA and IgM (apical surface of epithelial cells)	1.9
<i>Metabolism</i>			
C85932	Crystallin, lamda 1 (Cryl1)	Fatty acid metabolism	2.6
<i>Other</i>			
NM_020509	Resistin like alpha (Retnla)	Hormone signaling	3.3

Note: FC indicates fold-change. Negative sign (-) before fold-change value indicates down-regulation. Genes shown more than once were represented by more than one probe set on the array, and each was determined separately to be significantly altered in response to *Bacillus anthracis* treatment. This table was adapted with permission from Moen, S., Yeager, L., Lawrence, W., *et al.* (2008). *Microb Path* 44: 293-310.

Table 4.5 Significant genes down-regulated in murine lungs 48 h post-infection with Ames spores, grouped by function.

GenBank ID	Gene Name	Function	FC
<i>Adhesion</i>			
BB477150	Protein tyrosine phosphatase, receptor type D (Ptpd)	Cell adhesion	-3.2
<i>Cytoskeletal organization</i>			
BM900139	Actin binding LIM protein family, member 3 (Ablim3)	Cytoskeleton organization and biogenesis	-1.8
<i>Growth and differentiation</i>			
BB428671	Platelet-derived growth factor, D polypeptide (Pdgfd)	Cell cycle regulation; proliferation	-2.1
NM_016686	Vascular endothelial zinc finger 1 (Vezf1)	Angiogenesis; endothelial cell development/differentiation; blood vessel morphogenesis	-2.5
<i>Signal transduction</i>			
BB216074	Protein kinase, cAMP dependent regulatory, type II beta (Prkar2b)	Inhibition of PKA catalytic subunits	-1.7
<i>Stress response</i>			
AB031049	REV3-like, catalytic subunit of DNA polymerase zeta RAD54 like (Rev3l)	DNA replication; DNA repair; response to DNA damage	-1.6
<i>Transcription regulation</i>			
AI639846	Transcription factor 4 (Tcf4)	Regulation of transcription, DNA-dependent; development	-1.7

Note: FC indicates fold-change. Negative sign (-) before fold-change value indicates down-regulation. Genes shown more than once were represented by more than one probe set on the array, and each was determined separately to be significantly altered in response to *Bacillus anthracis* treatment. This table was adapted with permission from Moen, S., Yeager, L., Lawrence, W., *et al.* (2008). *Microb Path* 44: 293-310.

Gene	Tissue	Time	Affy-metrix FC	RT-PCR FC	Function
Clusterin	Lung	8 hr	2.1	3.98	Molecular chaperone during stress-induced injury.
Angiopoietin-like Protein 4	Lung	48 hr	3.67	2.8	Protects vascularity during inflammation; maintains EC matrix.
Resistin-like Alpha	Lung	48 hr	3.32	6.34	Regulator of apoptosis and glucose uptake in adipose cells.

Table 4.6 Real-time RT-PCR confirmation of altered expression levels of selected genes from Ames-infected murine lungs. FC indicates fold-change. This table was adapted with permission from Moen, S., Yeager, L., Lawrence, W., *et al.* (2008). *Microb Path* 44: 293-310.

4.4 DISCUSSION

Past publications have examined the global transcriptional responses of host cells to treatment with the anthrax toxins. For instance, GeneChip analysis of EdTx-treated murine MØs revealed significant gene alterations that culminated in the modulation of various MØ functions (Comer *et al.*, 2006). Similarly, transcriptional analysis of murine MØ treated with LeTx (Comer *et al.*, 2005) or infected with Sterne spores (Bergman *et al.*, 2005) has been previously reported. Although these studies exposed abundant MØ genes seemingly important during interaction with spores or toxins, studies to date have neglected to examine the *in vivo* host response to *B. anthracis* spores. Here, for the first time, the *in vivo* global transcriptional responses of genes in the lungs of mice intranasally infected with fully virulent *B. anthracis* Ames spores is reported.

The infectious inoculum chosen was 5 LD₅₀ (56,000) Ames spores in order to ensure significant disease progression and pathological changes within the examined time frame. Preliminary experiments involved isolating RNA from mice infected 8, 24, 36, 48, and 60 h post-infection and performing GeneChip analysis. Upon examination of the data, however, the time points showing the most striking gene expression changes occurred at earliest time point examined (8 h) and at 48 h post-infection.

The lungs were analyzed because they are the primary route of infection for these experiments and in natural cases of inhalational anthrax. As expected, *B. anthracis* organisms were recovered from the lungs at all time points tested (8, 24, and 48 h). Similar to previously reported findings (Berdjais *et al.*, 1962; Bergman *et al.*, 2005; Kobiler *et al.*, 2006), the number of organisms significantly increased over time. This

supports the proposed model of anthrax infection, whereby spores engulfed by alveolar macrophages travel to the mediastinal lymph nodes, enter the bloodstream, and then disseminate to multiple tissue sites, including the return to the lungs (Lincoln *et al.*, 1965; Lyons *et al.*, 2004). Histopathological analysis of the lungs at 48 h post-infection confirmed the presence of bacilli within the alveoli, alveolar walls, and small and large vascular lumens. Focally, small areas of edema and hemorrhage were observed with fibrin. Additionally, some, but not all, infected mice showed mixed cellular infiltrates of neutrophils and mononuclear cells. These findings are consistent with previous microscopic observations in the lungs of mice (Duong *et al.*, 2006) and non-human primates (Friedlander *et al.*, 1993; Stearns-Kurosawa *et al.*, 2006) infected with *B. anthracis* Sterne spores.

Eight hours subsequent to intranasal inoculation of Ames spores, few transcriptional alterations were detected in the lungs. However, the genes that were up-regulated indicated that the lung recognized the onset of an infection. One of the genes that responded with the greatest fold-change encodes clusterin, a molecule known to be elevated following inflammatory stress and localized lung damage (Carneavali *et al.*, 2006). Clusterin protects the lung against apoptotic signals, reactive oxygen species (ROS), and complement factors (Heller *et al.*, 2003). Likewise, lectin-like oxidized LDL receptor (Olr1), which was up-regulated 1.9-fold, is associated with inflammatory and endotoxin-induced stress and functions as a vascular tethering ligand for rolling leukocytes (Hamilton *et al.*, 1995; Honjo *et al.*, 2003;). Alternatively, several genes involved in the immune response were down-regulated. The gene encoding MHC class I receptor (H2-K1) was down-regulated (2.5-fold) in the lung at 8 h, which may represent a

bacterial mechanism of immune evasion by which the bacteria interfere with antigen presentation to host immune effector cells. Notably, the gene encoding surfactant protein C (Sftpc) was down-regulated (2.0-fold) by 8 h. Sftpc, which normally functions to regulate lung surface tension and gas exchange, has been shown to be decreased in various animal models of inflammation and in response to TNF- α (Mulugeta *et al.*, 2006). Sftpc and other surfactant proteins play a role in the innate host defense system of the lung by binding to pattern recognition molecules, such as CD14 (Chaby *et al.*, 2005). Thus, lower Sftpc levels during anthrax infection may disrupt certain respiratory processes, as well as dampen innate immune defenses.

By 48 h, the lung showed increased expression of genes related to inflammation, suggesting a more active participation of the immune response against infection. This included CD14 antigen (3.5-fold increase), which is a receptor for the lipopolysaccharide (LPS)-binding protein/LPS complex. CD14 is also a cell-activating receptor for peptidoglycan (Muhvic *et al.*, 2001), possibly explaining its alteration during infection with *B. anthracis*. Also, the expressions of the multi-functional metallothionein 2 (Mt2) and polymeric immunoglobulin receptor (pIgR) genes were up-regulated. Besides their ability to bind metal ions, metallothioneins become acute phase proteins during inflammation (Min *et al.*, 1991) and possess antioxidant properties that may protect tissues against destructive inflammatory conditions (Coyle *et al.*, 2002; Penkowa *et al.*, 2005;). Further, the Mt2 protein has been shown to be elevated during hyperoxia (Piedboeuf *et al.*, 1994). pIgR proteins are responsible for mediating the continuous delivery of polymeric immunoglobulins (IgA and IgM) to the mucosal epithelial surface and external secretions. Expression of pIgR is regulated by microbial products through toll-like receptor (TLR) signaling and by host factors, such as cytokines (Kaetzel *et al.*,

2005). The elevation of CD14, Mt2, and pIGR gene expression likely assists the lungs in combating the infection and protecting itself from excessive damage resulting from inflammation.

An interesting pattern was observed in the levels of IL-4, IL-6, G-CSF, KC, RANTES, and MCP-1 measured in the sera of anthrax-infected animals. A bimodal response (i.e., an increase at 8 h, drop at 24 and 36 h, and spike at 48 h) was observed. Similarly, this trend was reported for two of these particular cytokines, IL-6 and MCP-1, by Firoved *et al.* (2005) following administration of EdTx to mice. Excluding IL-4, the affected cytokines are pro-inflammatory and mediate recruitment of various immune cells such as neutrophils, basophils, T-cells, and monocytes. The spike at 8 h may be indicative of the immediate immune response to inhalation of a foreign pathogen. For instance, murine cells are capable of recognizing dormant spores via the MyD88 receptor, and they respond with production of inflammatory cytokines (Glomski *et al.*, 2007).

Additionally, because alveolar MØs rapidly engulf spores, by 8 h these phagocytic cells are likely contributing with their own cytokine secretion. However, at later time points of 24 and 36 h, large amounts of LeTx and EdTx are likely released into the bloodstream. Each of these toxins has unique immunomodulatory properties, including cytokine abrogation. In both the mouse model and tissue culture systems, EdTx results in increased IL-6 secretion concomitant with impairment of the TNF- α response (Firoved *et al.*, 2005; Hoover *et al.*, 1994). *In vivo*, LeTx decreases IFN- γ , IL-2, and IL-4 production in rats. Additionally, LeTx has been shown to suppress the production of TNF- α and IL-1 β in murine macrophage cell lines (Erwin *et al.*, 2001). Thus, the combined action of these two toxins may contribute to the observed drop in cytokine levels at 24 and 36 h post-infection.

By 48 h following inoculation with Ames spores, the mice were terminally ill. High titers of *B. anthracis* bacilli plagued the bloodstream and infiltrated multiple tissues as confirmed with histopathology. The second jump in certain cytokine levels may result from host cells recognizing pattern-associated molecular products being shed by the bacteria, such as anthrolysin O (Park *et al.*, 2004) and peptidoglycan (Remer *et al.*, 2005). Perhaps this was the last attempt by the immune system to call in professional immune cells to try and control the infection. Analysis of the levels of selected biochemical components in the blood of infected mice was also performed. Although levels of three hepatic transaminases (alkaline phosphate, alanine aminotransferase, and aspartate aminotransferase) increased (2-3 fold) at 48 h compared to normal mice, which is often indicative of liver injury or dysfunction (Abboud *et al.*, 2007; Muftuoglu *et al.*, 2006), the increases were not statistically significant (data not shown).

In summary, the use of virulent *B. anthracis* Ames spores and an intranasal infection route in mice allowed conditions resembling the intentional release of weaponized, aerosolized anthrax spores to be mimicked. Stringent GeneChip analysis data revealed that the lungs of the infected mice underwent drastic transcriptional changes during early and late stages of the disease. Many of the upregulated genes play important roles in the inflammatory process, even as late as 48 h post-infection, confirming that the lung is an active player during anthrax pathogenesis at all stages of infection. Further, the identification of affected genes provides new opportunities to develop novel therapeutic strategies against this deadly disease.

CHAPTER 5: Conclusions and future directions

Although *B. anthracis* is a microorganism mainly afflicting herbivores, anthrax spores represent an infectious agent with significant potential for biowarfare and bioterrorism. Inhalational anthrax is a rapidly progressing disease with mortality rates approaching 100% (Inglesby *et al.*, 2002). Anthrax has a long history in biological warfare, with occurrences in World Wars I and II and even as recent as 2001; thus, it is not unreasonable to predict that this agent will be used again in the future.

Following the intentional release of *B. anthracis* spores in the mail supply of the U.S. Postal Service in 2001, a frenzy of research ensued to provide further insight into anthrax pathogenesis. The result has revealed an extremely complex story involving two forms of the organism (the spore and the bacilli) and powerful virulence factors such as two exotoxins, a unique capsule, and a cytolysin molecule. However, despite the flood of research, many questions concerning anthrax pathogenesis still remain. For instance, conflicting reports concerning the fate of spores phagocytosed by murine MØs ignored the important issue of what occurs inside the *human* MØs. Further, most researchers have focused on the mechanism of action and effects of LeTx on host cell types, consequently leaving the role of EdTx overlooked. Finally, previous studies examined transcriptional alterations of genes in MØs infected with spores or treated with the toxins, but transcriptional effects of infection *in vivo* had not been pursued. The work described in detail in the preceding chapters provided new insight into the interaction between virulent spores and human MØs, identified a novel immunosuppressive role for EdTx, and evaluated transcriptional changes in the lungs of anthrax-infected mice.

The *B. anthracis* spore is a metabolically inactive particle that germinates into a true bacterium only when exposed to favorable conditions. Development of an antispore immune response early in infection could feasibly offer protection against fatal infection. Therefore, understanding the interaction between spores and host MØs is vital for the creation of new therapeutic options. Though once considered immunologically inert, this work and previous publications have shown that the spore itself can trigger an immune response. For instance, we have shown that human MØs recognize virulent spores and respond with an oxidative burst. Two other groups reported that spores alone elicit early production of several important inflammatory cytokines by murine splenocytes (Glomski *et al.*, 2007) and human alveolar MØs (Chakrabarty *et al.*, 2006).

The current paradigm in the anthrax literature labels the MØ as the primary cell type utilized by anthrax spores as a safe site for germination and quick transport to the lymphatics. However, this work and several very recent reports has provided new evidence that is shifting the role of the MØ in anthrax pathogenesis. For instance, Cleret *et al* showed that interstitial lung dendritic cells, not alveolar MØs, were responsible for transporting spores into the thoracic lymph nodes from 30 min to 72 hours after intranasal infection of mice (Cleret *et al.*, 2007). Alveolar MØs were the first responding sentinels in their model, and rapidly phagocytosed spores but did not transport them. Additionally, spores have been found to be internalized by human lung epithelial cells and then translocate them through epithelial cell monolayers as a method of dissemination (Russell *et al.*, 2007). Data from this study support this new model because Ames spore infection actually reduced the level of basal migration of human MØs, and did not alter directed MØ chemotaxis.

This work was the first to report that instead of serving as a safe haven for spore survival, human MØs mediate the killing of the majority of internalized virulent *B. anthracis*. This included the dormant spore form of the organism, as well as newly germinated cells and outgrown vegetative cells. However, approximately 23% of dormant spores remained viable at 24 h post-infection. It is not clear how the surviving spores are able to resist the antimicrobial defenses of the human MØ, and more work is necessary to determine this. The “persistence” of some spores may allow the microbe to hide from the host long enough to avoid the first wave of the immune response and germinate at a later date. This likely occurs *in vivo* as well because humans may not develop systemic disease until 43 days after exposure (Meselson *et al.*, 1994). Several germinants for *B. anthracis* spores have been identified in recent years. For instance, the addition of inosine and alanine induces complete germination of Sterne spores *in vitro* (Akoachere *et al.*, 2007). Perhaps treatment strategies designed to force all inhaled spores to germinate into vegetative cells would result in 100% pathogen killing by the MØ and increase the survival of human patients. Additionally, eliminating the spore form of *B. anthracis* would likely be more beneficial when administering antibiotics such as ciprofloxacin because only vegetative cells are susceptible to the mechanism of action of antibiotics. Future *in vivo* studies are necessary to test this hypothesis.

It was also unknown whether human MØs were susceptible to killing following spore infection. This is an important issue when uncovering the secrets of anthrax pathogenesis. We found that in contrast to murine MØs, most human MØs survived spore infection. Determining the reason why human MØs are resistant to spore-induced death may reveal unique strategies that can be exploited for treatment. Bergman *et al* performed Microarray analysis of Sterne-infected RAW 264.7 cells and discovered that the gene

encoding the enzyme ornithine decarboxylase was up-regulated 15-fold 6 h post-infection. Over expression of this enzyme is sufficient to protect cells from apoptosis induced by several agents (Park *et al.*, 2002), and ornithine decarboxylase was discovered to be a key suppressor of apoptosis in spore-infected RAW 264.7 cells (Bergman *et al.*, 2005). Future microarray analysis of infected human MØs is pertinent for the identification of genes possibly responsible for the observed resistance to spore-evoked death.

The human MØs that did succumb to infection in this study died via the apoptosis route. Apoptosis as a response to intracellular infection has been shown for a wide range of pathogens (Chen *et al.*, 1994). In contrast to necrosis, a cell undergoing apoptosis is actively taking part in its own death. The suicide of a microbe-infected cell may be a proactive strategy to eliminate the production of pathogenic organisms in order to guarantee survival of the host. Because not all infected human MØs underwent apoptosis in this study, perhaps the cells that died sacrificed themselves due to phagocytosis of too many spores; thus, they were not able to efficiently destroy the pathogen.

While there are many published reports describing the suppressive effect of LeTx on various cell types, there is limited data regarding the role of EdTx during anthrax disease. The EF component of EdTx is an extremely active adenylate cyclase that converts ATP to cAMP, a ubiquitous second messenger in mammalian cells (Leppa, 1982). Perturbation of intracellular levels of cAMP disturbs a multitude of cellular signaling pathways, and other substances that increase cAMP levels have previously been shown to inhibit certain functions of immune cells (Cantarow *et al.*, 1978; Popov *et al.*, 2002; Scobie *et al.*, 2003).

In this study, we defined a new role for EdTx with respect to human MØs. The powerful wave of EdTx-generated cAMP resulted in a reduction of the actin content and cell spreading of human MØs, as well as reduced phagocytosis of Ames spores. The ability of EdTx to reduce spore/bacilli phagocytosis by MØs is likely important during later stages of the infection, particularly when large volumes of EdTx are being secreted by rapidly multiplying, extracellular vegetative cells. At this time, EdTx-induced suppression of MØ phagocytosis would be of tremendous benefit to the survival of the bacteria and any viable dormant spores, and would likely increase the host's susceptibility to fulminant anthrax disease.

PKA and Epac are two molecules that bind cAMP and initiate two independent signaling cascades that are involved in multiple pathways. Many of these pathways deal with processes related to the actin cytoskeleton. EdTx treatment elicited an early increase in protein levels of cAMP-dependent PKA, followed by decreased production over time. This was supported by enhanced PKA activity at early time points, and inhibited activity later. Down-regulation of the regulatory subunit of PKA, which contains cAMP-binding sites, as well as impaired PKA activity may represent the target cell's strategy to compensate for the flood of cAMP produced by EdTx and attempt to return the cell to a basal state. Alternatively, expression and activity of Epac remained up-regulated at all time points tested. This indicates that Epac may be primarily responsible for the observed phagocytosis inhibition that occurs at the later time points, as PKA had become down-regulated by this time.

The use of chemical analogues with specificity toward either PKA or Epac showed that the suppressed phagocytosis and accompanied reduction in F-actin content induced by EdTx exposure was mediated by both PKA and Epac-1 pathways. EdTx-

treated human endothelial cells underwent cytoskeletal changes and exhibited impaired chemotaxis, however this was solely due to activation of the Epac pathway and not PKA (Hong *et al.*, 2007). This shows that the signaling pathways utilized by EdTx-generated cAMP are cell type specific. This study was limited to examination of only these two molecules, and participation by other signaling proteins cannot be excluded. Experiments involving siRNA approaches with PKA and Epac are currently underway in our laboratory to provide further evidence of the role of these two molecules following EdTx-treatment.

When four of the eleven victims of the U.S. Post Office attacks died despite antibiotic therapy, it became clear that current anthrax treatments were not effective enough. This called for the development of novel treatments to better combat the infection. Microarray analysis is an invaluable tool that can potentially reveal new targets for treating diseases by providing a comprehensive list of all genes significantly altered as a consequence of infection. Until this point, only specific cell types had undergone microarray analysis following exposure to spores or anthrax toxins. Thus, the global transcriptional response *in vivo* remained unknown. To address this issue, GeneChip analysis of Ames-infected murine lungs was performed in this work.

Results confirmed that the lung plays a very important role in anthrax pathogenesis, not only as the primary route of entry, but also during the late stages of infection. *B. anthracis* Ames organisms were recovered from the lungs at all time points tested (8, 24, and 48 h), and the number of organisms increased significantly over time. This pattern is similar to previously reported findings (Berdjis *et al.*, 1962; Bergman *et al.*, 2005; Kobilier *et al.*, 2006). Eight hours post-infection, a total of 15 genes were found to be altered. The gene with the greatest fold-change was clusterin, a molecule commonly

elevated following inflammatory stress (Carneavali *et al.*, 2006) and is important for protecting the lung against apoptotic signals and reactive oxygen species (Heller *et al.*, 2003). Interestingly, the gene encoding MHC class I receptor was down-regulated 2.5-fold, possibly the result of an anthrax immune evasion strategy. Peptide presentation by MHC molecules is an essential component of the adaptive immune response, so it is not surprising that some pathogens have evolved a method of interfering with MHC antigen-presentation. For instance, *Salmonella* is able to reduce MHC class II surface expression of infected cells (Mitchell *et al.*, 2004) and enterobacteria down-regulate MHC class I expression of cells in human patients (Kirveskari *et al.*, 1999). The ability of *B. anthracis* to interfere with MHC expression and/or signaling has not been previously reported and warrants further investigation.

Another gene down-regulated 8 h post-infection encoded surfactant protein C. This likely has a devastating impact on the lung, as surfactant is vital for regulating lung surface tension and gas exchange. Further, surfactant protein C (SP-C) has been implicated in antimicrobial defense by binding to pattern recognition molecules, such as CD14 (Chaby *et al.*, 2005). Inhaled spores will inevitably encounter the thin layer of surfactant that coats alveolar epithelial cells, and the spore protein BclA has been shown to bind SP-C (Rety *et al.*, 2005). However, the exact role of surfactant in anthrax pathogenesis is not known and more knowledge may reveal potential therapeutic strategies to alleviate respiratory distress associated with the disease.

By 48 h, significant transcription changes in a total of 46 genes occurred in the lung. Particularly, there was increased expression of genes related to inflammation, suggesting a more active participation of the immune system against infection. Many of the elevated genes have significant protective roles and likely assist the lungs in

combating microbial infection while simultaneously shielding itself from excessive damage resulting from inflammation. Examples of elevated genes included CD14 antigen (3.5-fold increase), multi-functional metallothionein 2 (Mt2; 6-fold increase), and polymeric immunoglobulin receptor (pIgR; 1.9-fold increase). Important genes involved in cell cycle regulation, cell adhesion, angiogenesis, and protein kinase A were down-regulated, indicating the anthrax toxins were likely at work.

Although many aspects of anthrax pathogenesis continue to remain mysterious, the research presented in this report provided new insight into the role human MØs play during the initial stages of anthrax infection, revealed a new inhibitory effect of EdTx, and illustrated the way in which lungs responded to spore infection at the transcriptional level. Studies like these provide the members of the anthrax field with new information, with the ultimate goal of developing innovative and effective treatments to protect the human population against the imminent threat of the intentional release of weaponized anthrax spores.

References

- Abboud, G., Kaplowitz, N.** 2007. Drug-induced liver injury. *Drug Saf* **30**: 277–294.
- Abrami, L., Fivaz, M., van der Goot, F.** 2000. Adventures of a pore-forming toxin at the target cell surface. *Trends Microbiol* **8**: 168-172.
- Abrami, L., Reig, N., van der Goot, F.** 2005. Anthrax toxin: the long and winding road that leads to the kill. *Trends Microbiol* **13**: 72-78.
- Abramova, F., Grinberg, L., Yampolskaya, O., Walker, D.** 1993. Pathology of inhalational anthrax in 42 cases from the Sverdlovsk outbreak of 1979. *Proc Nat Acad Sci* **90**: 2291-2294.
- Agrawal, A., Lingappa, J., Leppla, S., Agrawal, S., Jabbar, A., Quinn, C., Pulendran, B.** 2003. Impairment of dendritic cells and adaptive immunity by anthrax lethal toxin. *Nature* **424**: 329-334.
- Ahuja, N., Kumar, P., Bhatnagar, R.** 2004. The adenylate cyclase toxins. *Crit Rev Microbiol* **30**: 187-196.
- Akagawa, K.** 1994. Differentiation and function of human monocytes. *Hum Cell* **7**: 116-120.
- Akagawa, K.** 2002. Functional heterogeneity of colony-stimulating factor-induced human monocyte-derived macrophages. *Int J Hematol* **76**: 27-34.
- Akoachere, M., Squires, R., Nour, A., Angelov, L., Brojatsch, J., Abel-Santos, E.** 2007. Identification of an in vivo inhibitor of *Bacillus anthracis* spore germination. *J Biol Chem* **282**: 12112-12118.
- Alam, S., Gupta, M., Bhatnagar, R.** 2005. Inhibition of platelet aggregation by anthrax edema toxin. *Biochem Biophys Res Commun* **339**: 107-114.
- Albrink, W.** 1961. Pathogenesis of inhalational anthrax. *Bacteriol Rev* **25**: 268-273.
- Albrink, W., Brooks, B., Biron, R., Kopel, M.** 1960. Human inhalational anthrax: A report of three fatal cases. *Am J Pathol* **36**: 147-171.
- Alileche, A., Serfass, E., Muehlbauer, S., Porcelli, S., Brojatsch, J.** 2005. Anthrax lethal toxin-mediated killing of human and murine dendritic cells impairs the adaptive immune response. *PLOS Path* **1**: 150-158.

- Andressen, R., Brugger, W., Scheibenbogen, C., Kreutz, M., Leser, H., Rehm, A., Lohr, G.** 1990. Surface phenotype analysis of human monocyte to macrophage maturation. *J Leuk Biol* **47**: 490-497.
- Aronoff, D., Canetti, C., Serezani, C., Luo, M., Peters-Golden, M.** 2005. Cutting edge: Macrophage inhibition by cyclic AMP (cAMP): differential roles of protein kinase A and exchange protein directly activated by cAMP-1. *J Immunol* **174**: 595-599.
- Baillie, L., Hibbs, S., Tsai, P., Cao, G., Rosen, G.** 2005. Role of superoxide in the germination of *Bacillus anthracis* endospores. *FEMS Microbiol Lett* **245**: 33-38.
- Banks, D., Barnajian, B., Maldonado-Arocho, F., Sanchez, A., Bradley, K.** 2005. Anthrax toxin receptor 2 mediates *Bacillus anthracis* killing of macrophages following spore challenge. *Cell Microbiol* **7**: 1173-1185.
- Barnard, J., Friedlander, A.** 1999. Vaccination against anthrax with attenuated recombinant strains of *Bacillus anthracis* that produce protective antigen. *Infect Immun* **67**: 562-567.
- Basu, S., Kang, T., Chen, W., Fenton, M., Baillie, L., Hibbs, S., Cross, A.** 2007. Role of *Bacillus anthracis* spore structures in macrophage cytokine responses. *Infect Immun* **75**: 2351-2358.
- Ben Nasr, A., Haithcoat, J., Masterson, J., Gunn, J., Eaves-Pyles, T., Klimpel, G.** 2007. Critical role for serum opsonins and complement receptors CR3 (CD11b/CD18) and CR4 (CD11c/CD18) in phagocytosis of *Francisella tularensis* by human dendritic cells (DC): uptake of *Francisella* leads to activation of immature DC and intracellular survival of the bacteria. *J Leuk Biol* **80**: 774-786.
- Berdjis, C., Gleiser, C., Hartmen, H., Kuehne, R., Gochenour, W.** 1962. Pathogenesis of respiratory anthrax in *Macaca mulatta*. *Br J Exp Pathol* **43**: 515-524.
- Bergman, N., Passalacqua, K., Gaspard, R., Shetron-Rama, L., Quackenbush, J., Hanna, P.** 2005. Murine macrophage transcriptional response to *Bacillus anthracis* infection and intoxication. *Infect Immun* **73**: 1069-1080.
- Bradley, K., Mogridge, J., Mourez, M., Collier, R., Young, J.** 2001. Identification of the cellular receptor for anthrax toxin. *Nature* **414**: 225-229.

- Brittingham, K., Ruthel, G., Panchal, R., Futter, C., Ribot, W., Hoover, T., Young, H., Anderson, A., Bavari, S.** 2005. Dendritic cells endocytose *Bacillus anthracis* spores: implications for anthrax pathogenesis. *J Immunol* **174**: 5545-5552.
- Bryn, T., Mahic, M., Enserink, J., Schwedem F., Aandahl, E., Tasken, K.** 2006. The cyclic AMP-Epac1-Rap1 pathway is dissociated from regulation of effector functions in monocytes but acquires immunoregulatory function in mature macrophages. *J Immunol* **176**: 7361-7370.
- Cantarow, W., Cheung, H., Sundharads, G.** 1978. Effects of prostaglandins on the spreading, adhesion, and migration of mouse peritoneal macrophages. *Prostaglandins* **16**: 39-42.
- Carnevali, S., Luppi, F., D'Arca, D., Caporali, A., Ruggieri, M., Vettori, M., Caglieri, A., Astancolle, S., Panico, F., Davalli, P., Mutti, A., Fabbri, L., Corti, A.** 2006. Clusterin decreases oxidative stress in lung fibroblasts exposed to cigarette smoke. *Am J Respir Crit Care Med* **174**: 393-399.
- Chaby, R., Garcia-Verdugo, I., Espinassous, Q., Augusto, L.** 2005. Interactions between LPS and lung surfactant proteins. *J Endotoxin Res* **11**: 181-185.
- Chakrabarty, K., Wu, W., Booth, J., Duggan, E., Coggeshall, K., Metcalf, J.** 2006. *Bacillus anthracis* spores stimulate cytokine and chemokine innate immune responses in human alveolar macrophages through multiple mitogen-activated protein kinase pathways. *Infect Immun* **74**: 4430-4438.
- Chen, Y., Zychlinsky, A.** 1994. Apoptosis induced by bacterial pathogens. *Microb Pathog* **17**: 203-212.
- Christensen, A., Selheim, J., de Rooj, S., Dremier, F., Schwede, F., Dao, K., Martinez, A., Maenhaut, C., Bos, J., Genieser, H., Dorskland, S.** 2003. cAMP analog mapping of Epac1 and cAMP kinase: discriminating analogs demonstrate that Epac and cAMP kinase act synergistically to promote PC-12 cell neurite extension. *J Biol Chem* **278**: 35394-35402.
- Cleret, A., Quesnel-Hellmann, Vallon-Eberhard, A., Verrier, B., Jung, S., Vidal, D., Mathieu, J., Tournier, J.** 2007. Lung dendritic cells rapidly mediate anthrax spore entry through the pulmonary route. *J Immunol* **178**: 7994-8001.
- Collins, S.** 1987. The HL-60 promyelocytic leukemia cell line: proliferation, differentiation, and cellular oncogene expression. *Blood* **70**: 1233-1244.

- Comer, J., Chopra, A., Peterson, J., Konig, R.** 2005 Direct inhibition of T-lymphocyte activation of anthrax toxins in vivo. *Infect Immun* **73**: 8275-8281.
- Comer, J., Galindo, C., Chopra, A., Peterson, J.** 2005. GeneChip analyses of global transcriptional responses of murine macrophages to lethal toxin of *Bacillus anthracis*. *Infect Immun* **73**: 1897-1885.
- Comer, J., Galindo, C., Zhang, F., Wenglikowski, A., Bush, K., Garner, H., Peterson, J., Chopra, A.** 2006. Murine macrophage transcriptional and functional responses to *Bacillus anthracis* edema toxin. *Microb Pathog* **41**: 96-110.
- Cote, C., Van Rooijen, N., Welkos, S.** 2006. Roles of macrophages and neutrophils in the early host response to *Bacillus anthracis* spores in a mouse model of infection. *Infect Immun* **74**: 469-480.
- Cote, C., DiMezzo, T., Banks, D., France, B., Bradley, K., Welkos, S.** 2008. Early interactions between fully virulent *Bacillus anthracis* and macrophages that influence the balance between spore clearance and development of a lethal infection. *Microb Infect* **10**: 613-619.
- Coyle, P., Philcox, J., Carey, L., Rofe, A.** 2002. Metallothionein: the multipurpose protein. *Cell Mol Life Sci* **59**: 627-647.
- Crawford, M., Aylott, C., Bourdeau, R., Bokoch, G.** 2006. *Bacillus anthracis* toxins inhibit human neutrophil NADPH oxidase activity. *J Immunol* **176**: 7557-7565.
- de Rooij, J., Zwartkruis, F. J., Verheijen, M. H., Cool, R. H., Nijman, S. M., Wittinghofer, A., Bos, J. L.** 1998. Epac is a Rap1 guanine-nucleotide-exchange factor directly activated by cyclic AMP. *Nature* **396**: 474-477.
- Dixon, T., Meselson, M., Guillemin, J., Hanna, P.** 1999. Anthrax. *N Engl J Med* **341**: 815-826.
- Drum CL, Yan SZ, Bard J, Shen YQ, Lu D, Soelaiman S, Grabarek Z, Bohm A, Tang WJ.** 2002. Structural basis for the activation of anthrax adenyl cyclase exotoxin by calmodulin. *Nature* **415**: 396-402.
- Drysdale, M., Heninger, S., Hutt, J., Chen, Y., Lyons, R., Koehler, T.** 2005. Capsule synthesis by *Bacillus anthracis* is required for dissemination in murine inhalation anthrax. *Eur Mol Biol Org J.* **24**: 221-227.
- Duong, S., Chiaraviglio, L., Kirby, J.** 2006. Histopathology in a murine model of anthrax. *Int J Exp Path* **87**: 131-137.

- Erwin, J., DaSilva, L., Bavari, S., Little, S., Friedlander, A., Chanh, T.** 2001. Macrophage-derived cell lines do not express proinflammatory cytokines after exposure to *Bacillus anthracis* lethal toxin. *Infect Immun* **69**: 1175–1187.
- Etienne-Toumlin, I., Sirard, J., Dufлот, E., Mock, M., Fouet, A.** 1995. Characterization of the *Bacillus anthracis* S-layer: cloning and sequencing of the structural gene. *J Bacteriol* **177**: 614-620.
- Firoved, A., Miller, G., Moayeri, M., Kakkar, R., Shen, Y., Wiggins, J., McNally, E., Tang, W., Leppla, S.** 2005. *Bacillus anthracis* edema toxin causes extensive tissue lesions and rapid lethality in mice. *Am J Pathol* **167**: 1309-1320.
- Fontana, J., Colbert, D., Deisseroth, A.** 1981. Identification of a population of bipotent stem cells in the HL60 human promyelocytic leukemia cell line. *Proc Nat Acad Sci* **78**: 3863-3866.
- Franz, D., Jahrling, P., Friedlander, A., McClain, D., Hoover, D., Bryne, W., Pavlin, J., Christopher, G., Eitzen, E.** 1997. Clinical recognition and management of patients exposed to biological warfare patients. *J Amer Med Assoc* **278**: 399-411.
- Friedlander, A., Bhatnagar, R., Leppla, S., Johnson, L., Singh, Y.** 1993. Characterization of macrophage sensitivity and resistance to anthrax lethal toxin. *Infect Immun* **61**: 245-252.
- Friedlander, A., Welkos, S., Pitt, M.L., Ezzell, J., Worsham, P., Rose, K., Ivins, B., Lowe, J., Howe, G., Mikesell, P., et al.** 1993. Post-exposure prophylaxis against experimental inhalational anthrax. *J Infect Dis* **167**: 1239-1242.
- Friedlander, A.** 1999. Clinical aspects, diagnosis, and treatment of anthrax. *J Appl Microbiol* **87**: 303-311.
- Glomski, I., Fritz, J., Keppler, S., Balloy, V., Chignard, M., Mock, M., Goossens, P.** 2007. Murine splenocytes produce inflammatory cytokines in a MyD88-dependent response to *Bacillus anthracis* spores. *Cell Microbiol* **9**: 502-513.
- Gold, J., Hoshino, Y., Hoshino, S., Jones, M., Nolan, A., Weiden, M.** 2004. Exogenous gamma and alpha/beta interferon rescues human macrophages from cell death induced by *Bacillus anthracis*. *Infect Immun* **72**: 1291-1297.
- Grinberg, L., Abramova, F., Yampolskaya, O., Walker, D., Smith, J.** 2001. Quantitative pathology of inhalational anthrax I: quantitative microscopic findings. *Mod Pathol* **14**: 482-495.

- Guidi-Rontani, C., Weber-Levy, M., Labruyere, E., Mock, M.** 1999. Germination of *Bacillus anthracis* spores within alveolar macrophages. *Mol Microbiol* **31**: 9-17.
- Guidi-Rontani, C., Levy, M., Ohayon, H., Mock, M.** 2001. Fate of germinated *Bacillus anthracis* spores in primary murine macrophages. *Mol Microbiol* **42**: 931-938.
- Gutting, B., Gaske, K., Schilling, A., Slaterbeck, A., Sobota, L., Mackie, R., Buhr, T.** 2005. Differential susceptibility of macrophage cell lines to *Bacillus anthracis*-Vollum 1B. *Toxicology in Vitro* **19**: 221-229.
- Hamilton, T., Major, J., Chisolm, G.** 1995. The effects of oxidized low density lipoproteins on inducible mouse macrophage gene expression are gene and stimulus dependent. *J Clin Invest* **95**: 2020-2027.
- Heller, A., Fiedler, A., Braun, P., Stehr, S., Bodeker, H., Koch, T.** 2003. Clusterin protects the lung from leukocyte-induced injury. *Shock* **20**: 166-170.
- Ho, H., Rohatgi, R., Lebensohn, A., Ma, L., Li, J., Gygi, S., Kirschner, M.** 2004. Toca-1 mediates Cdc42-dependent actin nucleation by activating the N-WASP-WIP complex. *Cell* **118**: 203-216.
- Hoffmaster, A., Koehler, T.** 1997. Control of virulence gene expression in *Bacillus anthracis*. *J Appl Microbiol* **87**: 279-281.
- Hong, J., Doebele, R., Lingen, M., Quilliam, L., Tang, W., Rosner, M.** 2007. Anthrax edema toxin inhibits endothelial cell chemotaxis via Epac and Rap1. *J Biol Chem* **282**: 19781-19787.
- Honjo, M., Nakamura, K., Yamashiro, K., Kiryu, J., Tanihara, H., McEvoy, L., Honda, Y., Butcher, E., Masaki, T., Sawamura, T.** 2003. Lectin-like oxidized LDL receptor-1 is a cell adhesion molecule involved in endotoxin-induced inflammation. *Proc Nat Acad Sci* **100**: 1274-1279.
- Hoover, D., Firedlander, A., Rogers, L., Yoon, I.** 1994. Anthrax edema toxin differentially regulates LPS-induced monocyte production of tumor necrosis factor alpha and interleukin-6 by increasing intracellular cAMP. *Infect Immun* **62**: 4432-4439.
- Howe, A.** 2004. Regulation of actin-based cell migration by cAMP/PKA. *Biochem Biophys Act* **1692**: 159-174.
- Howe, A., Baldor, L., Hogan B.** 2005. Spatial regulation of the cAMP-dependent protein kinase during chemotactic cell migration. *Proc Nat Acad Sci* **102**: 14320-14325.

- Hu, T., RamachandraRao, S., Siva, S., Valancius, C., Zhu, Y., Mahadev, K, Toh, I., Goldstein, B., Woolkalis, M., Sharma, K.** 2005. Reactive oxygen species production via NADPH oxidase mediates TGF- β -induced cytoskeletal alterations in endothelial cells. *Am J Physiol Renal Physiol* **289**: F816-842.
- Hu, H., Sa, Q., Koehler, T., Aronson, A., Zhou, D.** 2006. Inactivation of *Bacillus anthracis* spores in murine primary macrophages. *Cell Microbiol* **8**: 1634-1642.
- Hu, H., Emerson, J., Aronson, A.** 2007. Factors involved in the germination and inactivation of *Bacillus anthracis* spores in murine primary macrophages. *FEMS Microbiol Lett* **272**: 1-6.
- Inglesby, T., O'Toole, T., Henderson, D. et al.** 2002. Anthrax as a biological weapon, 2002: updated recommendations for management. *J Amer Med Assoc* **287**: 2236-2252.
- Ihara, S., Oka, T., Fukui, Y.** 2006. Direct binding of SWAP-70 to non-muscle actin is required for membrane ruffling. *J Cell Sci* **119**: 500-507.
- Jernigan D., Raghunathan P., Bell B. et al.** 2002. Investigation of bioterrorism-related anthrax, United States, 2001: epidemiologic findings. *Emerg Infect Dis* **8**: 1019–1028.
- Joellenbeck, L., Zwanziger, L., Durch, J., Storm, B., eds.** The Anthrax Vaccine. New York, NY: National Academy Press, 2002.
- Jones, S., Shareif, Y.** 2005. Asymmetrical protein kinase A activity establishes neutrophil cytoskeletal polarity and enables chemotaxis. *J Leuk Biol* **78**: 248-258.
- Kaetzel, C.** 2005. The polymeric immunoglobulin receptor: bridging innate and adaptive immune responses at mucosal surfaces. *Immunol Rev* **206**:83–99.
- Kang, T., Fenton, M., Weiner, M., Hibbs, S., Basu, S., Baillie, L., Cross, A.** 2005. Murine macrophages kill the vegetative form of *Bacillus anthracis*. *Infect Immun* **73**: 7495-7501.
- Kassam, A., Der, S., Mogridge, J.** 2005. Differentiation of human monocytic cell lines confers susceptibility to *Bacillus anthracis* lethal toxin. *Cell Microbiol* **7**: 281-292.
- Katoh, M. and Katoh, M.** 2004. Identification and characterization of human FNBP1L gene in silico. *Int J Mol Med* **13**: 157-162.

- Kawasaki, H., Springett, G. M., Mochizuki, N., Toki, S., Nakaya, M., Matsuda, M., Housman, D. E., Graybiel, A. M.** 1998. A family of cAMP-binding proteins that directly activate Rap1. *Science* **282**: 2275–2279.
- Kelly, D., Chulay, J., Mikesell, P., Friedlander, A.** 1992. Serum concentrations of penicillin, doxycycline, and ciprofloxacin during prolonged therapy in rhesus monkeys. *J Infect Dis* **166**: 1184-1187.
- Kim, S., Jing, Q., Hoebe, K., Beutler, B., Duesbery, N., Han, J.** 2003. Sensitizing anthrax lethal toxin-resistant macrophages to lethal toxin-induced killing by tumor necrosis factor- α . *J Biol Chem* **278**: 7413-7421.
- King, M., Radicchi-Mastroianni, M.** 2002. Effects of caspase inhibition on camptothecin-induced apoptosis of HL-60 cells. *Cytometry* **49**: 28-35.
- Kirby, J.** 2004. Anthrax lethal toxin induces human endothelial cell apoptosis. *Infect. Immun.* **72**: 430-439.
- Kirveskari, J., He, Q., Leirisalo-Repo, M., Maki-Ikola, O., Wuorela, M., Putto-Laurila, A., Granfors, K.** 1999. Enterobacterial infection modulates major histocompatibility complex class I expression on mononuclear cells. *Immunol* **97**: 420-428.
- Kobiler, D., Weiss, S., Levy, H., Fisher, M., Mechaly, A., Pass, A., Altboum, Z.** 2006. Protective antigen as a correlative marker for anthrax in animal models. *Infect Immun* **74**:5871–5876.
- Komuro, I., Keicho, N., Iwamoto, A., Akagawa, K.** 2001. Human alveolar macrophages and granulocyte-macrophage colony-stimulating factor-induced monocyte-derived macrophages are resistant to H₂O₂ via their high basal and inducible levels of catalase activity. *J Biol Chem* **276**: 24360-24364.
- Kumar, P., Ahuja, N., Bhatnagar, R.** 2002. Anthrax edema toxin requires influx of calcium for inducing cyclic AMP toxicity in target cells. *Infect Immun* **70**: 4997-5007.
- Lasunskaja, E., Campos, M., de Andrade, M., Damatta, R., Kipnis, T., Einicker-Lamas, M., Da Silva, W.** 2006. Mycobacteria directly induce cytoskeletal rearrangements for macrophage spreading and polarization through TLR2-dependent PI3K signaling. *J Leuk Biol* **80**: 1480-1490.
- Lebowich, R., McKillip, B., Conboy, J.** 1943. Cutaneous anthrax: A pathological correlation study with clinical correlation. *Am J Clin Pathol* **13**: 505-515.

- Leppa, S.** 1982. Anthrax toxin edema factor: a bacterial adenylate cyclase that increases cyclic AMP concentrations of eukaryotic cells. *Proc Nat Acad Sci* **79**: 3162-3166.
- Leppa, S.** 1984. *Bacillus anthracis* calmodulin-dependent adenylate cyclase: chemical and enzymatic properties and interactions with eukaryotic cells. In *Advances in Cyclic Nucleotide and Protein Phosphorylation Research*. Greengard, P., Robinson, B.A. (eds). New York, NY: Raven Press, pp. 189–198.
- Lin, C., Kao, Y., Liu, W., Huang, H., Chen, K., Wang, T., Lin, H.** 1996. Cytotoxic effects of anthrax lethal toxin on macrophage-like cell lines J774A.1 *Curr Microbiol* **33**: 224-227.
- Little, S., Ivins, B., Fellows, P., Friedlander, A.** 1997. Passive protection by polyclonal antibodies against *Bacillus anthracis* infection in guinea pigs. *Infect Immun* **65**: 5171-5175.
- Lincoln, R., Hodges, D., Klein, F., Mahlandt, B., Jones, W., Haines, B., Rhian, M., Walker, J.** 1965. Role of the lymphatics in the pathogenesis of anthrax. *J Infect Dis* **115**: 481–494.
- Livak, K., Schmittgen, T.** 2001. Analysis of relative gene expression data using real-time quantitative PCR and the 2⁻(-Delta Delta C(T))Method. *Methods* **25**:402–408.
- Loughran, G., Healy, N., Kiely, P., Huigsloot, M., Kedersha, N., O'Connor, R.** 2005. Mystique is a new insulin-like growth factor-I-regulated PDZ-LIM domain protein that promotes cell attachment and migration and suppresses Anchorage-independent growth. *Mol Biol Cell* **16**: 1811-1822.
- Lyons C.R., Lovchik, J., Hutt, J., Lipscomb, M., Wang, E., Heninger, S., Berliba, L., Garrison, K.** 2004. Murine model of pulmonary anthrax: kinetics of dissemination, histopathology, and mouse strain susceptibility. *Infect Immun* **72**: 4801–4809.
- MacLean, J., Xia, W., Pinto, C., Zhao, L., Liu, H., Kradin, R.** 1996. Sequestration of inhaled particulate antigens by lung phagocytes. A mechanism for the effective inhibition of pulmonary cell-mediated immunity. *Am J Pathol* **148**: 657-666.
- Matsuda, S., Akagawa, K., Honda, M., Yokota, Y., Takebe, Y., Takemori, T.** 1995. Suppression of HIV replication in human monocyte-derived macrophages induced by granulocyte/macrophage colony-stimulating factor. *AIDS Res Hum Retroviruses* **11**: 1031-1038.

- May, R. and Machesky, L.** 2001. Phagocytosis and the actin cytoskeleton. *J Cell Sci* **114**: 1061-1077.
- Meselson, M., Guillemin, J., Hugh-Jones, M., Langmuir, A., Popova, I., Shelokov, A., Yampolskaya, O.** 1994. The Sverdlovsk anthrax outbreak of 1979. *Science* **266**: 1202-1208.
- Mesnager, S., Tosi-Couture, E., Mock, M., Gounon, P., Fouet, A.** 1997. Molecular characterization of the *Bacillus anthracis* main S-layer component: evidence that it is the major cell associated antigen. *Mol Microbiol* **23**: 1147-1155.
- Min, K., Terano, Y., Onosaka, S., Tanaka, K.** 1991. Induction of hepatic metallothionein by nonmetallic compounds associated with acute-phase response in inflammation. *Toxicol Appl Pharmacol* **111**: 152-162.
- Mitchell, E., Mastroeni, P., Kelly, A., Trowsdale, J.** 2004. Inhibition of cell surface MHC class II expression by *Salmonella*. *Eur J Immunol* **34**: 2559-2567.
- Mock M, Mignot T.** 2003. Anthrax toxins and the host: a story of intimacy. *Cell Microbiol* **5**:15-23.
- Moen, S., Yeager, L., Lawrence, W., Ponce, C., Galindo, C., Garner, H., Bazem W., Suarez, G., Peterson, J., Chopra, A.** 2008. Transcriptional profiling of murine organ genes in response to infection with *Bacillus anthracis* spores. *Microb Path* **44**: 293-310.
- Muftuoglu M., Aktekin, A., Ozdemir, N., Saglam, A.** 2006. Liver injury in sepsis and abdominal compartment syndrome in rats. *Surg Today* **36**: 519-524.
- Muhvic, D., El-Samalouti, V., Flad, H., Radosevic, B., Rukavena, D.** 2001. The involvement of CD14 in the activation of human monocytes by peptidoglycan monomers. *Mediators Inflamm* **10**: 155-162.
- Mulugeta S., Beers, M.** 2006. Surfactant protein C: its unique properties and emerging immunomodulatory role in the lung. *Microbe Infect* **8**:2317-2323.
- Nakata, K., Akagawa, K., Fukayama, M., Hayashi, Y., Kadokura, M., Tokunaga, T.** 1991. Granulocyte-macrophage colony-stimulating factor promotes the proliferation of human alveolar macrophages *in vitro*. *J Immunol* **147**: 1266-1272.
- Nakata, K., Weiden, M., Harkin, T., Ho, D., Rom, W.** 1995. Low copy number and limited variability of proviral DNA in alveolar macrophages from HIV-1-infected

- patients: evidence for genetic differences in HIV-1 between lung and blood macrophage populations. *Mol Med* **1**: 744-757.
- O'Brien, J., Friedlander, A., Dreier, T., Ezzell, J., Leppla, S.** 1985. Effects of anthrax toxin components on human neutrophils. *Infect Immun* **47**: 306-310.
- Oliva, C., Swiecki, M., Griguer, C., Lisanby, M., Bullard, D., Turnbough, C., Kearney, J.** 2008. The integrin Mac-1 (CR3) mediates internalization and directs *Bacillus anthracis* spores into professional phagocytes. *Proc Nat Acad Sci* **105**: 1261-1266.
- Paccani, S., Tonello, F., Ghittoni, R., Natale, M., Muraro, L., D'Elia, W., Montecucco, C., Balderi, C.** 2005. Anthrax toxins suppress T lymphocyte activation by disrupting antigen receptor signaling. *J Exp Med* **201**: 325-331.
- Park, J., Y. Chung, S. Kang, J. Kim, Y. Kim, H. Kim, Y. Kim, J. Kim, Yoo, Y.** 2002. c-Myc exerts a protective function through ornithine decarboxylase against cellular insults. *Mol Pharmacol* **62**:1400-1408.
- Park, J., Ng, V., Maeda, S., Rest, R., Karin, M.** 2004. Anthrolysin O and other gram-positive cytolysins are toll-like receptor 4 agonists. *J Exp Med* **200**: 1647-1655.
- Penkowa, M., Florit, S., Giralt, M., Quintana, A., Molinero, A., Carrasco, J., Hidalgo, J.** 2005. Metallothionein reduces central nervous system inflammation, neurodegeneration, and cell death following kainic acid-induced epileptic seizures. *J Neurosci Res* **79**: 522-534.
- Peterson, J., Comer, J., Baze, W., Noffsinger, D., Wenglikowskie, A., Walberg, K., Hardcastle, J., Pawlik, J., Bush, K., Taormina, J., Moen, S., Thomas, J., Chatuev, B., Sower, L., Chopra, A., Stanberry, L., Sawada, R., Scholz, W., Sircar, J.** 2007. Human monoclonal antibody AVP-21D9 to protective antigen reduces dissemination of the *Bacillus anthracis* Ames strain from the lungs in a rabbit model. *Infect Immun* **75**: 3414-3424.
- Piedboeuf B, Johnston, C., Watkins, R., Hudak, B., Lazo, J., Cherian, M., Horowitz, S.** 1994. Increased expression of tissue inhibitor of metalloproteinases (TIMP-I) and metallothionein in murine lungs after hyperoxic exposure. *Am J Respir Cell Mol Biol* **10**: 123-132.
- Pitt, M.L., Little, S., Ivins, B., Fellows, P., Barth, J., Hewetson, J., Gibbs, P., Dertzbaugh, M., Friedlander, A.** 2001. In vitro correlation of immunity in a rabbit model of inhalational anthrax. *Vaccine* **19**: 4768-4773.

- Popov, S., Villasmil, R., Bernardi, J., Grene, E., Cardwell, J., Wu, A., Alibek, D., Bailey, C., Alibek, K.** 2002. Lethal toxin of *Bacillus anthracis* causes apoptosis of macrophages. *Biochem Biophys Res Commun* **293**: 349-355.
- Preisz, H.** 1909. Experimentelle Studien Über Virulenz, Empfänglichkeit und 541 Immunität beim Milzbrand. *Zeitschr Immunität. -Forsch* **5**:341–452.
- Raines, K., Kang, T., Hibbs, S., Cao, G., Weaver, J., Tsai, P., Baillie, L., Cross, A., Rosen, G.** 2006. Importance of nitric oxide synthase in the control of infection by *Bacillus anthracis*. *Infect Immun* **75**: 2268-2276.
- Razin, E., Bauminger, S., Globerson, A.** 1978. Effects of prostaglandins on phagocytosis of sheep erythrocytes by mouse peritoneal macrophages. *J Reticuloendothel Soc* **23**: 237-242.
- Reissman D., Whitney E., Taylor T. et al.** 2004. One-year health assessment of adult survivors of *Bacillus anthracis* infection. *J Amer Med Assoc* **291**: 1994–1998.
- Remer, K., Reimer, T., Brcic, M., Jungi, T.** 2005. Evidence for involvement of peptidoglycan in the triggering of an oxidative burst by *Listeria monocytogenes* in phagocytes. *Clin Exp Immunol* **140**: 73–80.
- Rety, S., Salamitou, S., Garcia-Verdugo, I., Hulmes, D., Le Hegarat, F., Chaby, R., Lewit-Bentley, A.** 2005. The crystal structure of the *Bacillus anthracis* spore surface protein BclA shows remarkable similarity to mammalian proteins. *J Biol Chem* **280**: 43073-43078.
- Ribot, W., Panchal, R., Brittingham, K., Ruthel, G., Kenny, T., Lane, D., Curry, B., Hoover, T., Friedlander, A., Bavari, S.** 2006. Anthrax lethal toxin impairs innate immune functions of alveolar macrophages and facilitates *Bacillus anthracis* survival. *Infect Immun* **74**: 5029-5034.
- Ross, J.** 1957. The pathogenesis of anthrax following the administration of spores by the respiratory route. *J Pathol Bacteriol* **78**: 485-494.
- Rossi, S., Tonello, F., Patrussi, L., Capitani, N., Simonato, M., Montecucco, C., Baldari, C.** 2007. Anthrax toxins inhibit immune cell chemotaxis by perturbing chemokine receptor signaling. *Cell Microbiol* **9**: 924-929.
- Russell, B., Vasan, R., Keene, D., Koehler, T., Xu, Y.** 2007. Potential dissemination of *Bacillus anthracis* utilizing lung epithelial cells. *Cell Microbiol* **10**: 945-957.

- Ruthel, G., Ribot, W., Bavari, S., Hoover, T.** 2004. Time-lapse confocal imaging of development of *Bacillus anthracis* in macrophages. *Proc Nat Acad Sci* **100**: 12426-12431.
- Sherer, K., Li, Y., Cui, X., Eichacker, P.** 2007. Lethal and edema toxins in the pathogenesis of *Bacillus anthracis* septic shock. *Am J Respir Crit Care Med* **175**: 211–221.
- Scobie, H., Rainey, G., Bradley, K., Young, J.** 2003. Human capillary morphogenesis protein 2 functions as an anthrax toxin receptor. *Proc Nat Acad Sci* **100**: 5170-5174.
- Scorpio, A., Chabot, D., Day, W., O'Brien, D., Vietri, N., Itoh, Y.** 2007. Poly-gamma glutamate capsule-degrading enzyme treatment enhances phagocytosis and killing of encapsulated *Bacillus anthracis*. *Antimicrob Agents Chemother* **51**: 215-222.
- Shinohara, M., Terada, Y., Iwamatsu, A., Shinohara, A., Mochizuki, N., Higuchi, M., Gotoh, Y., Ihara, S., Nagata, S., Itoh, H., Fukui, Y., Jessberger, R.** 2002. SWAP-70 is a guanine-nucleotide-exchange factor that mediates signaling of membrane ruffling. *Nature* **416**: 759-763.
- Smith, H., Keppie, J.** 1954. Observations on experimental anthrax; demonstration of a specific lethal factor produced in vivo by *Bacillus anthracis*. *Nature* **173**: 869-871.
- Stearns-Kurosawa D., Lupu, F., Taylor, F., Kinasewitz., G., Kurosawa, S.** 2006. Sepsis and pathophysiology of anthrax in a nonhuman primate model. *Am J Pathol* **169**: 433–444.
- Swiderski, Richard.** Anthrax, a History. Jefferson, NC: McFarland & Company, Inc., 2004.
- Takei, K., Tokuyama, K., Kato, M., Morikawa, A.** 1998. Role of cAMP in reducing superoxide anion generation in guinea pig alveolar macrophages. *Pharmacol* **57**: 1-7.
- Tang, W., Krupinski, J., Gilman, A.** 1991. Expression and characterization of calmodulin-activated (type 1) adenylylcyclases. *J Biol Chem* **266**: 8595-8603.
- Titball, R., Turnbull, P., Hutson, R.** 1991. The monitoring and detection of *Bacillus anthracis* in the environment. *Soc Appl Bacteriol Ser* **20**: 9S-18S.
- Turnbull, P.** 2002. Introduction: anthrax history, disease, and ecology, *Curr Top Microbiol Immunol* **271**: 1-19.

- Vitale, G., Bernardi, L., Napolitano, G., Mock, M. Montecucco, C.** 2000. Susceptibility of mitogen-activated protein kinase family members to proteolysis by anthrax lethal factor. *Biochem J* **352**: 739-745.
- Voth, D., Hamm, E., Nguyen, L., Tucker, A., Salles, I., Ortiz-Leduc, O., Ballard, J.** 2005. *Bacillus anthracis* oedema toxin as a cause of tissue necrosis and cell type-specific cytotoxicity. *Cell Microbiol* **7**: 1139-1149.
- Welkos, S., Trotter, R., Becker, D., Nelson, G.** 1989. Resistance to the Sterne strain of *B. anthracis*: phagocytic cell responses of resistant and susceptible mice. *Microb Pathog* **7**: 15-35.
- Welkos, S., Friedlander, A., Weeks, S., Little, S., Mendelson, I.** 2002. *In vitro* characterization of the phagocytosis and fate of anthrax spores in macrophages and the effects of anti-PA antibody. *J Med Microbiol* **51**: 821-831.
- Wright, G., Mandell, G.** 1986. Anthrax toxin blocks priming of neutrophils by lipopolysaccharide and by muramyl dipeptide. *J Exp Med* **164**: 1700-1709.

VITA

Linsey Alison Yeager was born on April 12, 1981 in the small town of Denton, Texas to Keith and Julie Anderson. After graduating from West Brook High School in Beaumont, Texas in 1999, Linsey began working on her bachelor degree at the University of North Texas (UNT) in Denton, Texas. She was first introduced to the biodefense field through her involvement in a laboratory that was developing neuronal-based biosensors designed to detect the intentional release of chemical and biological weapons. Further, she intensively studied the field of microbiology and taught a Microbiology Laboratory course while in her senior year of college. After receiving her B.S. in Biology from UNT in 2003, she immediately joined the doctoral program at the University of Texas Medical Branch in Galveston, Texas to pursue a Ph.D. in the areas of microbiology and biodefense. While in Galveston, she met and married her husband, Zachary Yeager. They currently reside there.

Permanent address: 4720 Avenue Q ½ Galveston, TX, 77551

This dissertation was typed by Linsey A. Yeager.